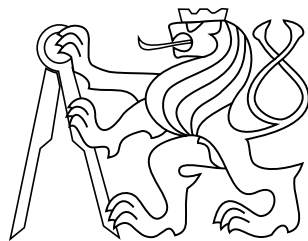


Master's thesis

The effects of climate or location change on functionality of a small modular house

Daniel Brýda, Ing. arch.



May 2018

Kopecký Pavel, Ing. Ph.D.

Czech Technical University in Prague
Faculty of Civil Engineering, Department of Building Structures



ZADÁNÍ DIPLOMOVÉ PRÁCE

I. OSOBNÍ A STUDIJNÍ ÚDAJE

Příjmení: Brýda	Jméno: Daniel	Osobní číslo: 369676
Zadávající katedra: K124 - Katedra konstrukcí pozemních staveb		
Studijní program: (N3649) Budovy a prostředí		
Studijní obor: (3608T006) Budovy a prostředí		

II. ÚDAJE K DIPLOMOVÉ PRÁCI

Název diplomové práce: Vliv rozdílného klimatického prostředí na fungování malého modulárního domu	
Název diplomové práce anglicky: The effects of climate or location change on functionality of a small modular house	
Pokyny pro vypracování:	
1) Provedení analýzy klimatických dat za různá časová období pro pět vybraných rozličných lokalit.	
2) Popis výchozí modelové budovy, pro kterou se budou zpracovávat jednotlivé simulační výpočty.	
3) Provedení výpočetních simulací a zhodnocení dopadů jednotlivých změn klimatu na fungování budovy.	
4) Stanovení možných dodatečných opatření (v již hotovém domě) reagujících na případnou změnu klimatu.	
5) Výpočtová optimalizace návrhu budovy stejných prostorových dimenzí jako výchozí budova, tak aby lépe odolávala změnám klimatu a prostředí.	
6) Bonus - Dílčí výpočtová studie: Lze budovu energeticky provozovat (vytápět a chladit) pouze z vlastních zdrojů tepla a energie za předpokladu, že se zásadně sníží její objem a optimalizuje její obálka a použité technologie?	
Seznam doporučené literatury:	
Jméno vedoucího diplomové práce: Kopecký Pavel, Ing. Ph.D.	
Datum zadání diplomové práce: 2.3.2018	Termín odevzdání diplomové práce: 20.5.2018
<i>Údaj uveďte v souladu s datem v časovém plánu příslušného ak. roku</i>	
Podpis vedoucího práce	Podpis vedoucího katedry

III. PŘEVZETÍ ZADÁNÍ

Beru na vědomí, že jsem povinen vypracovat diplomovou práci samostatně, bez cizí pomoci, s výjimkou poskytnutých konzultací. Seznam použité literatury, jiných pramenů a jmen konzultantů je nutné uvést v diplomové práci a při citování postupovat v souladu s metodickou příručkou ČVUT „Jak psát vysokoškolské závěrečné práce“ a metodickým pokynem ČVUT „O dodržování etických principů při přípravě vysokoškolských závěrečných prací“.

Datum převzetí zadání	Podpis studenta(ky)
-----------------------	---------------------

Acknowledgement

I would like to express my deep gratitude to my thesis supervisor, Ing. Pavel Kopecký, Ph.D. for his patient guidance, enthusiastic encouragement and useful critiques of this master thesis. Our friendly discussions have always recharged me with new energy and motivation. My grateful thanks are also extended to my girlfriend and my family for their support and encouragement throughout my studies.

Declaration

I declare that I worked out the presented thesis independently and I quoted all used sources of information in accord with Methodical instructions about ethical principles for writing academic thesis.

Abstract

Běžné domy jsou navrhovány pro danou oblast a veškeré výpočty a optimalizace návrhu jsou prováděny dle odpovídajícího klimatu. U malých modulárních domů je při výrobě předem počítáno s možností snadného transportu, a proto musí být schopny čelit různým podnebním podmínkám. Se vzrůstající kvalitou výroby a delší předpokládanou životností, mohou mobilní domy čelit proměnným podnebním podmínkám i na původním místě vlivem globálního oteplování. Velice podrobná data z klimatického modelu, předpovídajícího změnu podnebí v pěti různých lokalitách, byla nezbytná k vytvoření výpočetního modelu. K výpočtu průběhu vnitřní teploty a změn v potřebách energií na provoz domu byla použita hodinová simulace vnitřního prostředí domu. Zatímco analýza klimatických dat naznačovala značné budoucí změny podnebí a podstatné rozdíly mezi jednotlivými lokalitami, výsledky simulací dokázaly, že by modelový dům ve svém původním návrhu obstál ve všech modelových scénářích. Vysoce efektivní systém aktivního stínění oken a snižování teploty řízeným větráním, dokáže zabránit nadměrnému přehřívání i v teplejších lokalitách a i za předpokladu globálního oteplování.

Klíčová slova

malý modulární dům; změna klimatu; globální oteplování; výpočetní model; simulace vnitřního prostředí; chování domu; optimalizace; energeticky úsporné budovy; ostrovní dům; soběstačný dům

Abstract

The regular houses are usually built for one particular location and all the calculations and optimizations are done to fit its climate zone. But small modular houses are designed to be movable and therefore need to be able to face various climatic conditions. With the increased quality of production and longer life span of such buildings, change of the environment can occur even in the original location simply due to the inevitability of the climate change. High resolution data from a weather model that predicts climate change in five different locations were necessary to create a calculation model. Hourly simulations of the house behavior during typical years were used to calculate how the interior temperature and specific energy demands change in different scenarios. While the weather data analysis proposed large climate changes and significant differences between the location, the simulation results proved that the model house in its original design would manage to perform reasonably well in all described scenarios. Efficient systems of active window shading and ventilative cooling managed to prevent excessive overheating of the house even in the warmer locations and despite the effects of the climate change.

Keywords

small modular house; climate change; global warming; calculation model; simulation of interior environment; house performance; optimization; energy efficient buildings; off-grid house; sustainable house

Contents

1	Introduction	1
1.1	Problem statement	1
1.2	Motivation	2
1.3	Objectives	2
1.4	Thesis structure	3
2	Climatic data	4
2.1	Data description	4
2.2	Analysis	6
2.2.1	Ambient Temperature	8
2.2.2	Solar Irradiance	13
2.2.3	Rain and Humidity	14
2.2.4	Heating and cooling degree hours	17
2.2.5	Wind	20
2.3	Characteristic year generation	22
3	Case study	24
3.1	Case description	24
3.2	Model house	24
3.3	Calculation model	26
3.4	Simulation settings	33
3.4.1	Simulation scenarios	33
3.4.2	Parameter optimization	35
3.5	Results	37
3.6	Discussion	47
4	Conclusion	48
	Appendices	
	Bibliography	50
A	Weather Data Analysis - Additional Figures	51
B	Case Study Results - Additional Figures	75
C	Model House Documentation	87

Abbreviations

SMH	small modular house
BALTEX	baltic sea experiment
REMO	regional model
GERICS	climate service center germany
CTU	czech technical university
EU	european union
IPCC	intergovernmental panel on climate change
TA	ambient air temperature
HREL	relative humidity of ambient air
ISGH	global solar Irradiance on horizontal plane
ISD	diffuse solar irradiance on horizontal plane
PSTA	air pressure
RN	normal rain
WD	wind direction
WS	wind speed
CI	cloud cover
ILAH	atmospheric counter horizontal radiation
ILTH	terrestrial counter horizontal radiation
GT	ground surface temperature
GR	ground reflectance
ST	solar time
ISGT	global solar irradiance on tilted plane
HSP	specific humidity of ambient air
HDH	heating degree hour
CDH	cooling degree hour
WSH	wind speed hour
ACPH	air changes per hour
DoD	depth of discharge
SoC	state of charge
CoP	coefficient of performance
RES	renewable energy source

1 Introduction

The segment of small modular houses is fast growing. With the rising demand comes better offer in terms of quality, which makes them a viable option for permanent residency living. For purposes of this theses, under the term of a small modular house (SMH) is understood a building which is designed and produced more like a industrial product then a civil engineering construction. It is usually assembled in an industrial facility and then moved to the owner's location after it is finished. Due to its similarity to an industrial product, such small modular house is usually designed universally and for repetitive production, with little to none custom modifications for each customer. Therefore, the very same small modular house can end up in various very different locations.

Also, with higher construction quality and the design aim for permanent residency, the life expectancy of modular houses can in some cases be similar to traditional wood-frame homes, or even higher. Thus some of modular houses designed today might be expected to still function in hundred years from now. Considering that currently ninety seven percent of climate experts agree that global warming is a real thing and caused by humans [1], it is almost certain that conditions in year 2100 might be very different from year 2000. Consensus on how strong the effect of global warming would actually be still differs highly, because after accepting the fact that it is being caused by the people, it all depends on our current estimates of our future behavior.

Nevertheless, it can be certainly said, that due to its mobility and/or due to the global warming, the same small modular house should be able to deal with various very different climatic conditions during its life.

1.1 Problem statement

Traditional houses are usually designed and built for one specific location and its climate conditions. The design normally follows some best practices guidelines which ensure that house will perform as expected and will be relatively energy efficient to do so. If there is any issue in the future functionality of the house, it can be usually fixed, thanks to the robustness of the construction, during smaller or larger refurbishment.

But unlike regular "unmovable" buildings, small modular houses usually share one universal design which still follows the best practices guidelines for regular houses but are not customized for any specific climatic conditions. Also, due to the nature of its design being very lightweight and tailored for the transportation, possibilities of future modifications might be very limited. On the other hand, thanks to its small size, total energy needs in a small modular house might be low enough that different climatic condition might change the total energy balance but still be within its technical system capabilities.

1.2 Motivation

With increased pressure on energy efficiency, decreasing carbon dioxide emissions, renewable resources, producing less waste and so on, downsizing as a social trend is only going to get stronger. Rising demand of smaller, energy sustainable houses is a natural result of this movement in housing segment.

In nature, all animals are able to build their own homes and find perfect balance of their size. Their houses are always just large enough that all the inhabitants can easily fit in, but the total volume is still small enough that all heat energy need is covered solely by interior gains, usually from body warmth.

We humans, on the other hand, have developed all sorts of complicated things and technologies - from nonrenewable power plants, over sized energy transportation grids to powerful heating and cooling systems. All that to be able to waste with space and energy in our homes. Maybe it is time to try and use all the available technologies and materials we have discovered to make our houses similarly sustainable as in nature. To design them just large enough, and let them use mostly the energy they already get from their inhabitants or that can be produced through renewable technologies seamlessly integrated into the house design.

1.3 Objectives

The objective of this thesis is to take one particular small modular house, which has been designed by the author of this thesis as a completely off-grid and energy self sustainable house for one specific location in the Czech Republic and to figure out how it would perform if moved to another location in the Czech Republic or elsewhere in Europe. Other objective, of even higher importance, is to find out how the house would perform in these locations in a near and especially in a distant future.

In order to be able to make a precise enough calculation, it is primarily necessary to have a relevant weather data and to process them in a correct way to get a typical year data for each location and time period of interest. Secondly, it is vital to have granular enough simulation model which calculates energy balance of the house in each calculation step, according to the granularity of the climatic data. The aim is to use hourly weather data and one hour step simulation and to simulate over 8760 hours in a typical year. The third necessary component is to have precise house description in terms of its envelope construction and its physical characteristics as an input for the simulation.

To be able to make some valuable conclusions of the results, it is important to figure out the best way how to actually quantify and measure the house performance. That can be done via three aspects - interior house temperature (which affects thermal comfort), how much energy is needed to keep the temperature in optimal range (which correlates with house's design and energy efficiency) and lastly how much of that energy would need to come from a back-up or external source (which effects both ecological footprint and operating costs of the house).

The result of the calculation should provide necessarily information to discuss whether the original design is able to deal with various climatic conditions or how it could be optimized to be either more universal or to face certain weather in a specific location. Also, another objective of the calculation and discussion is to determine how can be future performance of the house improved by making changes that do not require complete reconstruction, for example using the mobility of the house to change the azimuth of the front facade or to provide additional external shading.

1.4 Thesis structure

The thesis is structured as follows:

Chapter 2 Climatic data contains *Section 2.1 Data description* with information about the dataset used in this work. Following *Section 2.2 Analysis* contains statistical analysis of some chosen variables from the dataset and compares differences between five locations and the effects of the climate change.

Chapter 3 Case Study contains the description of the *Model house* in *Section 3.2*. The structure of the *Calculation model* and the simulation process are explained in *Section 3.3*. The simulation and optimization scenarios are described in *Section 3.4 Simulation settings* while the next *Section 3.5* contains the *Results*.

At the end, the *Chapter 4 Conclusion* elaborates over the implications of the results and states proposals for future work.

2 Climatic data

2.1 Data description

Having precise weather data is of the utmost importance for any house behavior simulation. The climatic data used in this thesis are calculated by REMO model [2], which was originally developed in 1991 by Max Planck Institute for Meteorology in Hamburg, Germany, as an atmospheric component of the coupled atmosphere-hydrology model system in the German BALTEX (BALTIC Sea Experiment). In 1993, the model was redeveloped as a regional model suitable for climate modeling and weather forecast which subsequently was named REMO. The validation of REMO concentrated on the hydrological components of the water cycle. The simulation results of long runs, up to ten years, have been compared successfully with observations in [3].

The model is nowadays further developed and maintained by the Climate Service Center Germany (GERICS) also in Hamburg, Germany. Over the last two decades, REMO has been used for creating regional climate information data in many research projects. The whole list of finished and ongoing projects can be found in [4]. The data for this thesis were obtained through the partnership of the Czech Technical University in Prague in EU funded project Climate for Culture [5]. The project tries to evaluate possible damages to the structure and stability of historic buildings and cultural heritage they present. To be able to use high-resolution simulation models for the near and far future, new climate models were necessary to be developed during the project using the REMO model.

The provided data were calculated as an A1B scenario based on the 4th report from the Intergovernmental Panel on Climate Change (IPCC) predicting a greater CO₂ emission increase assumed until 2050 and a decrease afterwards [6]. In order to successfully reproduce global climate features on a regional scale, a reliable source of climate change information is required. For that purpose the REMO model allows to obtain data from a spatial resolution of up to 10x10 km grid size by dynamical downscaling [6].

The content of climatic data used:

1. Three time periods

- 1960 - 1990 ... the recent past
- 2020 - 2050 ... the near future
- 2070 - 2100 ... the far future

2. Five locations

- Fichtelberg
 - Longitude - 12.950 ° East
 - Latitude - 50.430 ° North

- Altitude - 716.146 *m* above sea level
- Helsinki
 - Longitude - 24.967 ° East
 - Latitude - 60.317 ° North
 - Altitude - 45.405 *m* above sea level
- Hradec Kralove
 - Longitude - 15.833 ° East
 - Latitude - 50.183 ° North
 - Altitude - 242.634 *m* above sea level
- Marseille
 - Longitude - 5.217 ° East
 - Latitude - 43.433 ° North
 - Altitude - 105.376 *m* above sea level
- Prague
 - Longitude - 14.283 ° East
 - Latitude - 50.100 ° North
 - Altitude - 295.325 *m* above sea level

3. Thirteen climate variables

- Ambient Air Temperature (TA) - [$^{\circ}C$]
- Relative Humidity of Ambient Air (HREL) - [0 – 1]
- Global Solar Irradiance on horizontal plane, short wave (ISGH) - [W/m^2]
- Diffuse Solar Irradiance on horizontal plane, short wave (ISD) - [W/m^2]
- Air Pressure (PSTA) - [hPa]
- Normal Rain (RN) - [mm/h]
- Wind Direction (WD) - [$^{\circ}$]
- Wind Speed (WS) - [m/s]
- Cloud Cover (CI) - [0 – 1]
- Atm. Counter Horizontal Radiation, long-wave (ILAH) - [W/m^2]
- Terr. Counter Horizontal Radiation, long-wave (ILTH) - [W/m^2]
- Ground Surface Temperature (GT) - [$^{\circ}C$]
- Ground Reflectance (GR) - [0 – 1]

Each dataset contains 31 years with 8760 hourly values for each variable in each year. All years are of the same length, leap years do not include 29th of February. All times are GMT, regardless of the real time zone of the location, but transformation into a solar time is not actually the same for all the location as will be mentioned later in *Section 2.2*.

2.2 Analysis

The dataset includes thirteen climate variables, but not all of them are actually directly needed for the calculation model in *Chapter 3, Section 3.3*. There are, on the other hand, some variables that are needed and not present in the dataset, but can be calculated from the given variables.

Variables that are going to be used directly as input to the simulation:

- Ambient Air Temperature (TA) - [$^{\circ}C$]
 - Exterior temperature
 - TA is used to calculate the amount of energy transmitted and ventilated

- Diffuse Solar Irradiance on horizontal plane, short wave (ISD) - [W/m^2]
 - ISD is used as a simplification to indicate when the lights in the house might be needed to turn on
 - When the house is inhabited, the people turn the lights on when ISD drops below certain level

- Normal Rain (RN) - [mm/h]
 - RN is used to calculate amount of water collected on the roof during the rain
 - It is important to properly design the dimensions of the rain watter tank and the diameter of the gutter outlet tube
 - RN is also used to simulate the behavior of the inhabitants as it can be set that they remain home when it is raining (when house serves for recreational purposes)

- Wind Speed (WS) - [m/s]
 - WS is used to calculate wind turbine's production

Variables that are going to be calculated from other variables:

- Solar time (ST)
 - ST is calculated from real time in minutes in year (525600 minutes) and days in year (365 days) and by using location's meridian and longitude

- ST is necessary to correctly calculate irradiance on tilted plane
- Global Irradiance on tilted plane (ISGT) - $[W/m^2]$
 - ISGT is calculated from ISGH by also using ST, GR, location's latitude and tilted plane's slope and azimuth
 - ISGT is used to calculate window solar gains and solar panels' production
- Specific humidity of ambient air (HSP) - $[g/kg]$
 - HSP is calculated from HREL, TA and PSTA
 - HSP would be necessary for calculating moisture transfer and content in construction as well as in ventilation and interior air
 - The simulation is not calculating moisture processes at this point of development
 - HSP is used for the analysis of the climate change

Variables that are going to be analyzed:

- Ambient Air Temperature (TA) - $[^{\circ}C]$
 - See *Subsection 2.2.1*
- Global Solar Irradiance on horizontal plane, short wave (ISGH) - $[W/m^2]$
 - See *Subsection 2.2.2*
- Normal Rain (RN) - $[mm/h]$
- Specific humidity of ambient air (HSP) - $[g/kg]$
 - See *Subsection 2.2.3*
- Heating degree hours (HDH) - $[^{\circ}C * h]$
- Cooling degree hours (CDH) - $[^{\circ}C * h]$
 - See *Subsection 2.2.4*
- Wind speed hours (WSH) - $[(m/s) * h]$
 - See *subsection 2.2.5*

The purpose of the analysis is to determine what are the actual effects of the climate change in the scenario A1B that the data represent and also to recognize the differences between the five locations. For each variable analyzed, several types of values and plots were chosen to show the data as demonstratively as possible. Usually for each value

type there is one plot for each location and then a similar plot that brings comparison between all the location. From the single location plots, only Prague will be displayed, the other locations can be found in *Appendix A*.

2.2.1 Ambient Temperature

As many people already like to mix the terms climate change and global warming, Ambient Air Temperature (TA) is expected to change the most. It is also a variable that probably effects the house behavior the most. In order to get clear idea about what the dataset contains, a heat map plot in *Figure 1* was generated to depict a daily average temperature of every day in Prague from 1960 to 2100.

The heat map is basically a pixelated image where each line of 365 pixels represents one year and therefore each pixel represents one day in that year. The color of each pixel stands for the average daily temperature. The color scale is shown on the color bar below the heat map. The years that are missing in the dataset (data in between the time periods) are shown in gray color.

In Prague heat map, as well as in all other locations (*Figures 36 to 39 in Appendix A*) can be clearly seen two things. Primarily, how the pixels gradually change the color from recent past to distant future. While the purple and blue pixels representing the very cold days disappear almost entirely, the yellow, orange and red pixels representing warm days become even more numerous. Secondly, it is easily visible how the temperature changes with the seasons throughout the year. Especially interesting is the heat map in Marseille (*Figure 39 in Appendix A*) where the heat map is very asymmetrical and the summer comes later in the year. This is most probably caused by the close proximity to the sea, because the water takes longer time to heat than the land.

Similarly to the heat map of daily average temperatures, the heat map of atypically hot and cold days was created. It also has one pixel for each day in the dataset, but the color scale of the heat map only has five colors, representing five categories. All the pixels are sorted into the following categories based on the temperatures throughout the day the pixel stands for:

- Freezing cold day
 - a day when the TA's maximum value is below 0 °C
 - depicted in dark blue

- Ice cold day
 - a day when the TA's minimum value is below 0 °C
 - depicted in light blue

- Average day
 - a day when the TA's values are between 0 °C and 30 °C

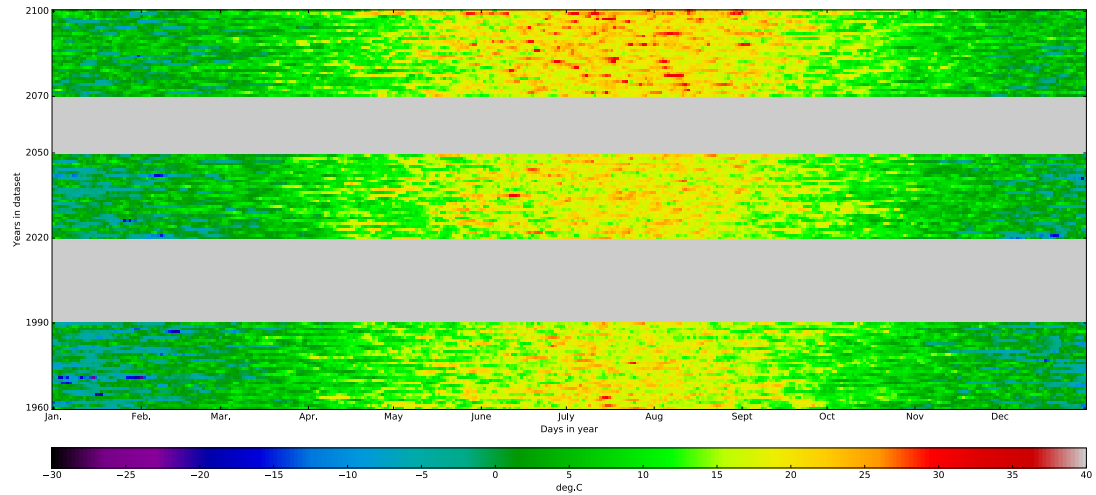


Figure 1 Daily average temperatures in Prague

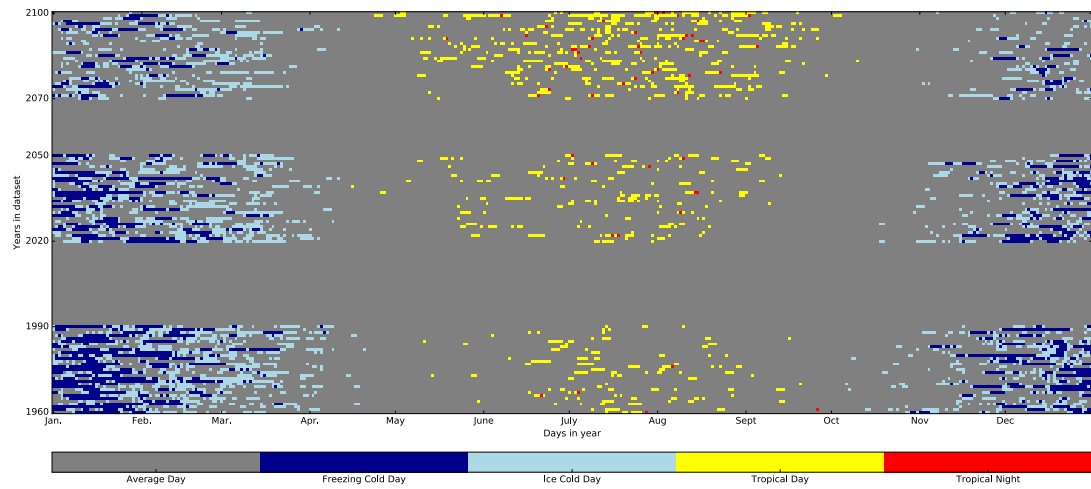


Figure 2 Atypically hot and cold days in Prague

– depicted in dark gray

- Tropical day
 - a day when the TA's maximum value is above $30\text{ }^{\circ}\text{C}$
 - depicted in yellow
- Tropical night
 - a day when the TA's minimum value is above $20\text{ }^{\circ}\text{C}$
 - depicted in red

2 Climatic data

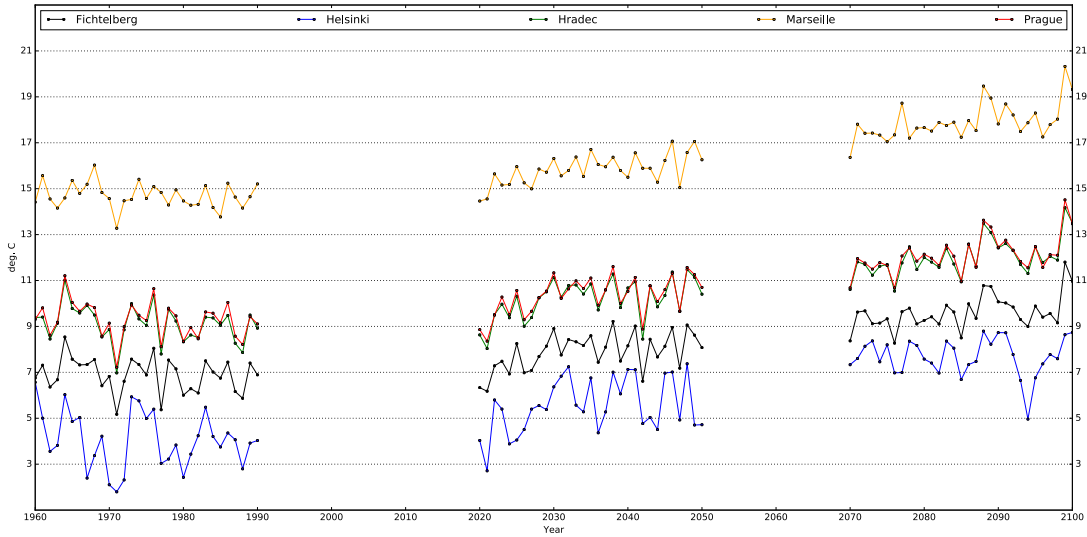


Figure 3 Annual average temperatures, all locations

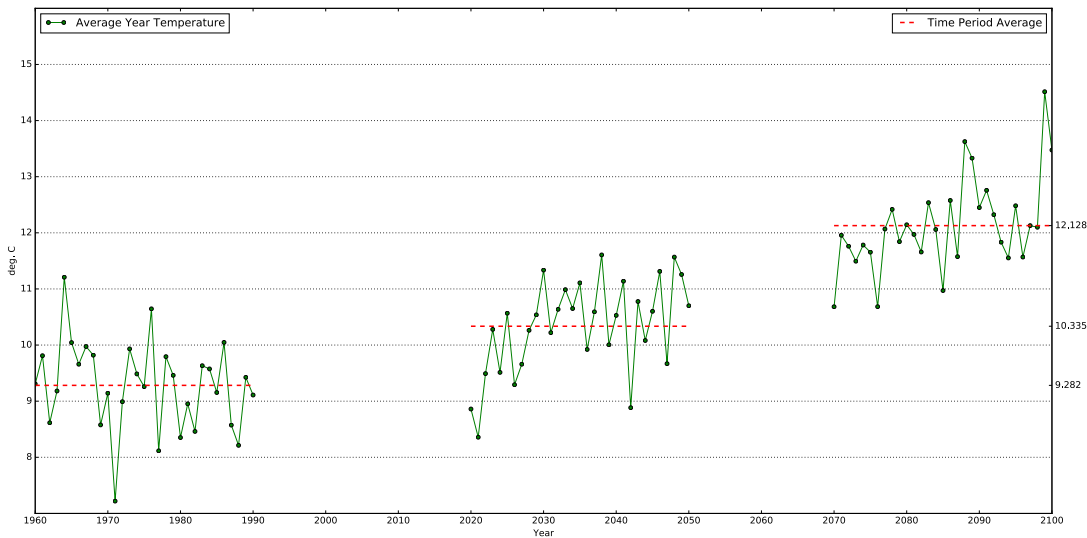


Figure 4 Annual average temperatures in Prague

This second heat map in *Figure 2* for Prague even more clearly shows how the cold days disappear and the tropical days and nights "multiply". It needs to be though that the the freezing cold days do not reduce in their number more than the ice cold day and that they are still similarly present even in distant future. The heat maps for the other locations can be found in *Figures 40 to 43* in *Appendix A*. It is interesting to note, that while Helsinki would experience the first tropical night around the year 2080, Marseille would be having the last ice cold day around the same time.

The five locations in the dataset were chosen for their expected differences in climate and that is most apparent on TA. *Figure 3* shows annual average temperatures throughout all the time periods for all the locations. It is apparent that with the exception of Prague and Hradec Kralove which are very similar, all the locations are in their average temperature zone, with Helsinki being the coldest, Marseille being the warmest. Prague and Hradec Kralove represent almost the average between Helsinki and Marseille, while

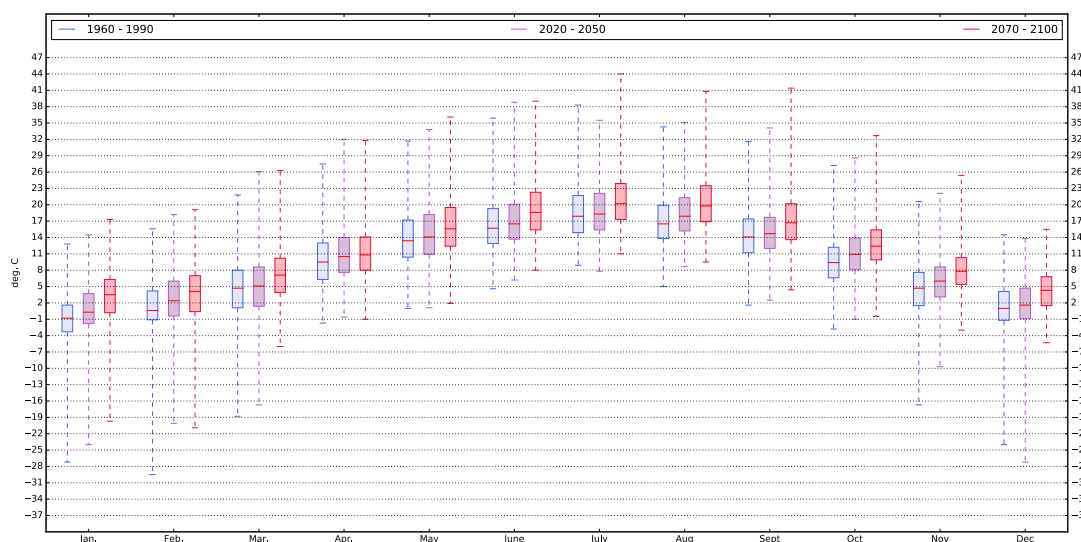


Figure 5 Monthly box-plot for temperatures in all time periods in Prague

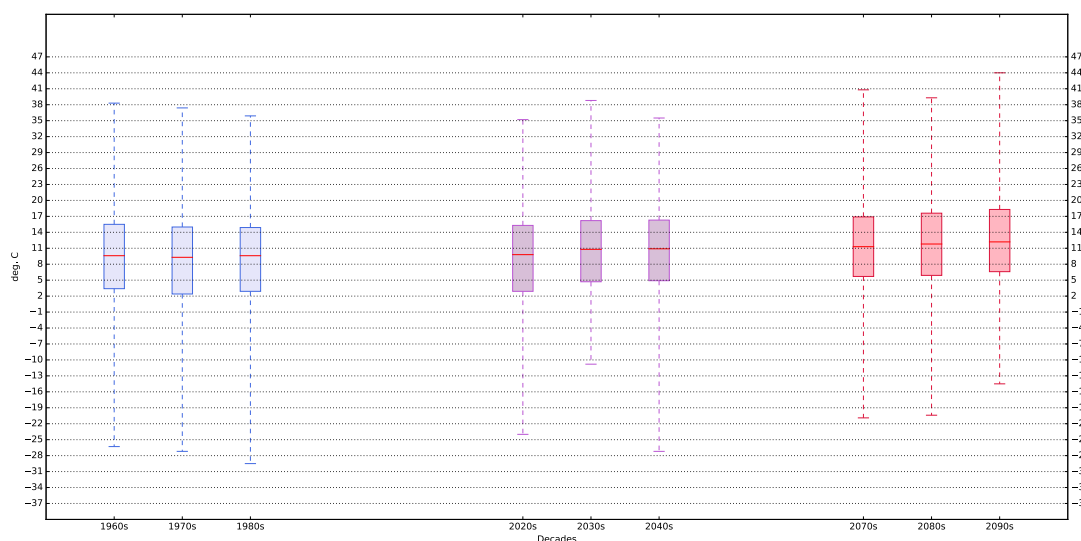


Figure 6 Box-plot for temperatures in decades in Prague

Fichtelberg sits in between Helsinki and Prague. It can be observed, that the warmest years of one location are almost similar in terms of annual average temperature as the coldest years of the next warmer location in the dataset.

Actual effect of the climate change can be most simply depicted on the time period average temperature. The total result of global warming - between recent past and far future is almost constant and same for all the locations. As can be seen in *Figure 4* which displays annual average temperatures as well as the time period averages only for Prague, average ambient temperature rises from 9.3 [$^{\circ}C$] between 1960 and 1990 to 12.1 [$^{\circ}C$] between 2070 and 2100. Similar value rises can be observed in every location as confirmed on *Figures 44 to 47 in Appendix A*. It is also noticeable that the effect of the global warming is not linear. While the average temperature in Prague rises by 2.9 degrees, it only rises by 1.1 degree between recent past and near future, but by 1.8 degree between near and far future. And that's despite the fact that seconds change

2 Climatic data

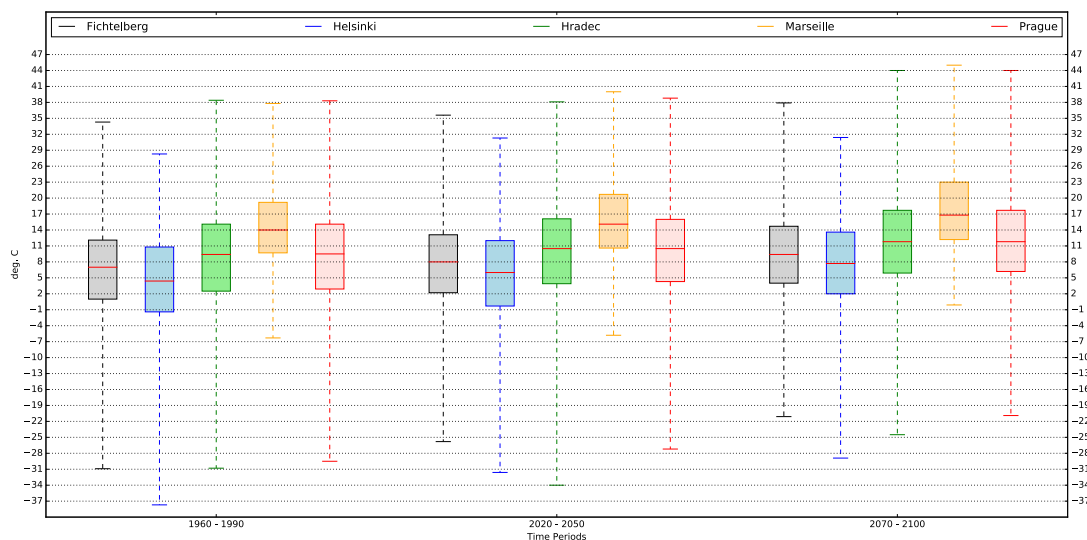


Figure 7 Box-plot for temperatures in each time period and location

happens over ten less years.

To be able to further analyze differences between the locations, it is important not to focus only on average temperatures but also on the extremes. To that purpose best serves box plot which depicts the ambient air temperature in its quartiles. The bottom of the box is the first quartile while the top of the box is the third quartile. Box is then completed with whiskers from minimum to maximum value and the red band inside the box that is the second quartile (the median).

Figure 5 shows all the TA values for Prague separated by months and within each month by time periods. It then allows to easily assess two information at once, how the temperature moves during the year and how the behavior changes with the climate change. In Prague, it can be noted that the global warming raises the TA's minimums in winter months significantly (especially in November and December) while the maximums do not change that much. In summer months, the effect is reversed with TA's maximums raising (especially from July to September), while the minimums change only slightly. Similar thing can be found in Fichtelberg and Hradec Kralove (*Figure 49 and 50 in Appendix A*). In Helsinki (*Figure 48 in Appendix A*), mainly the minimum temperatures go up in each month while, on the other hand, in Marseille (*Figure 51 in Appendix A*), the maximum values rise even higher.

If the box plot is generated chronologically with the data separated by decades, like in *Figure 6* that represents Prague, the previously mentioned fact, that the effect of global warming is not linear and that the effects are much more prevailing in the last time period, can be observed again. This box plot confirms that the median growth is about three degrees but it also shows that while the lowest temperatures rise by approximately 5 degrees, the highest values rise only by one or two degrees on average. The similar thing applies for Helsinki, Fichtelberg and Hradec Kralove in *Figures 52 to 54 in Appendix A*. In Marseille (*Figure 55 in Appendix A*), the opposite occurs. It is also important to note, that in last two decades of the dataset, there are no freezing temperatures in Marseille.

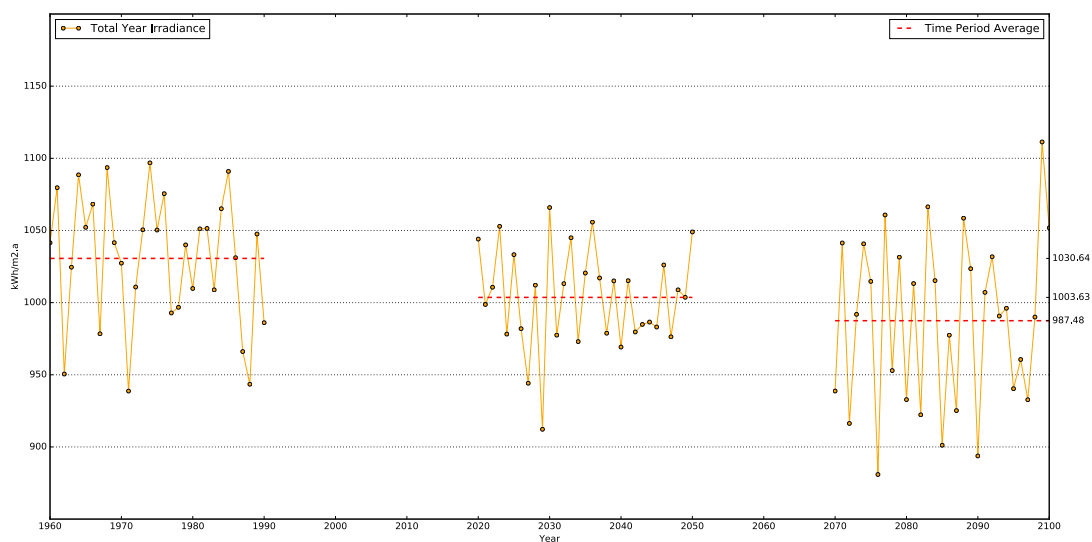


Figure 8 Annual summary of global irradiance in Prague

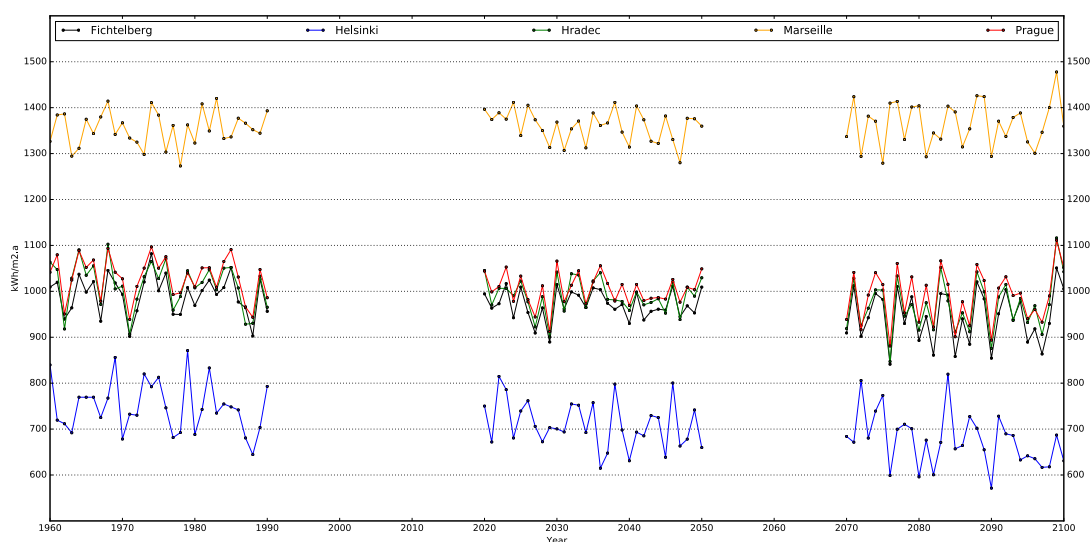


Figure 9 Annual summary of global irradiance, all locations

The last box plot (*Figure 7*) shows all the locations with the data split into the three time periods. Based on the graph, it can be said that while the median and minimum temperatures in Marseille are much higher, Prague and Hradec Kralove share the same maximum values. This characteristic remains unchanged by the climate change.

2.2.2 Solar Irradiance

While the raise of the average temperatures caused by global climate change was confirmed by the data analysis, it might have been expected that the solar irradiance would similarly increase. But while all the energy on earth comes from the solar energy, the global warming is not actually caused by increased sun radiation. The main factor responsible for the climate change is the alteration of the gases' concentrations

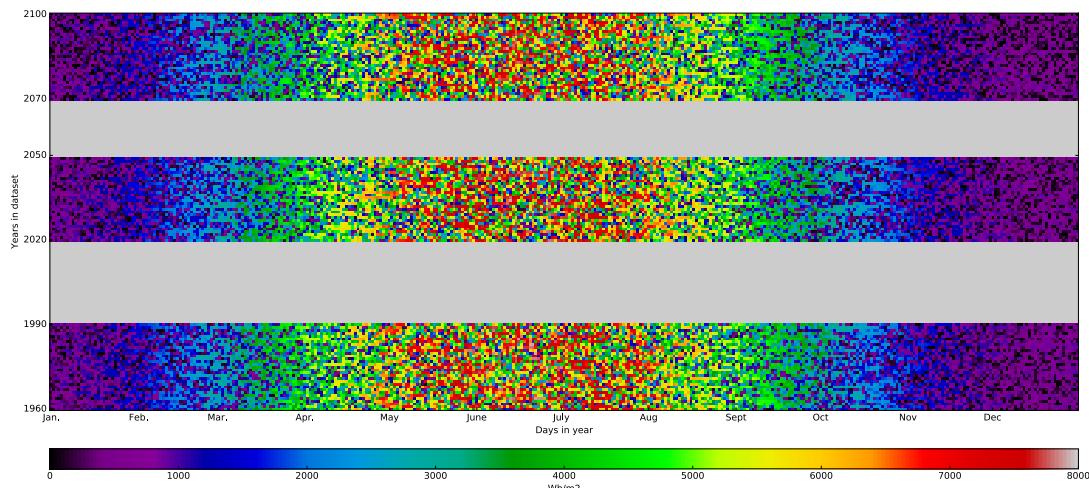


Figure 10 Daily summary of global irradiance in Prague

in the atmosphere, especially huge release of CO₂ emissions caused by human activity since industrial revolution. This atmosphere alteration actually causes slight decrease in global irradiance on horizontal plane by approximately 4% which can be seen in *Figure 8* that depicts annual summary of ISGH in Prague. While in Fichtelberg and Hradec Kralove (*Figures 57 and 58* in Appendix A) the decrease is also between 4 and 5%, in Helsinki (*Figure 56* in Appendix A) the decrease in ISGH is almost 10%. In Marseille though (*Figure 59* in Appendix A), there is even very small increase (less than 1%).

In *Figure 9* that compares annual total irradiance among all locations, it is depicted that while Prague, Hradec Kralove and Fichtelberg have average ISGH's values, irradiance in Helsinki is much lower and in Marseille much higher. The difference only gets larger with climate change. This affects mainly the importance of the passive window shading and the potential of the solar panels' production.

Similar heat map, as the one that was generated for daily average temperature, was made for global solar irradiance. *Figure 10* shows daily summary values of ISGH in Prague. *Figures 60 to 63* in Appendix A display other locations, but in none of the heat maps the climate change is apparent. Similarly to the temperature heat maps, it very well points out the vast difference between summer and winter irradiance.

2.2.3 Rain and Humidity

While rain and specific humidity are not important at all for building energy calculation, they might be interesting variables for the climate change analysis. Like with the irradiance, many people might also believe that the global warming might also cause the climate to become drier and the annual precipitation lower. That has also not been proven by the values in the dataset and as the *Figure 11* shows, the annual precipitation in Prague even goes up by almost exactly 10 %. It is good to note, that it is actually the first significant difference between Prague and Hradec, which stagnates on the same average values as can be seen in *Figure 66* in Appendix A.

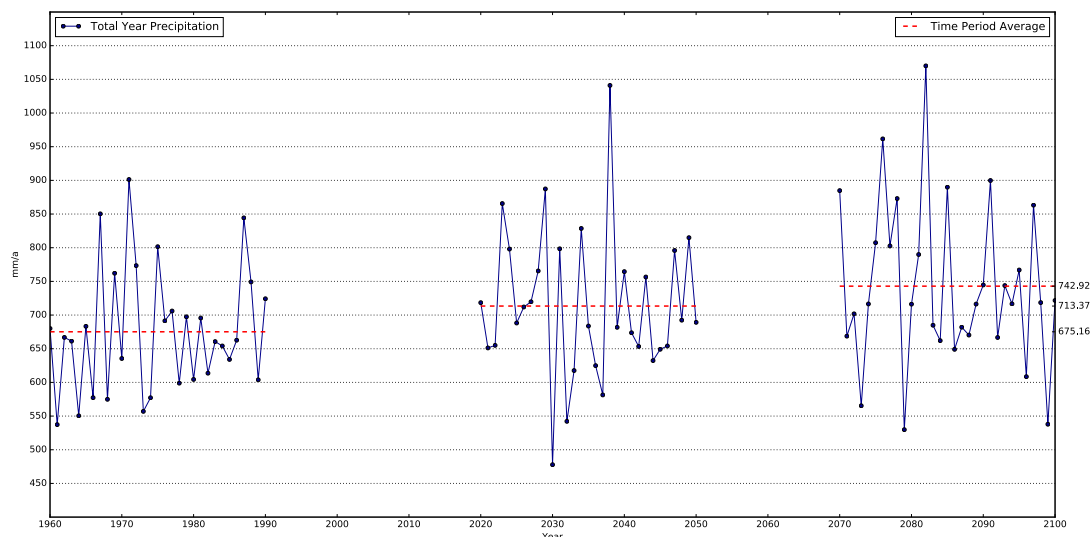


Figure 11 Annual precipitation in Prague

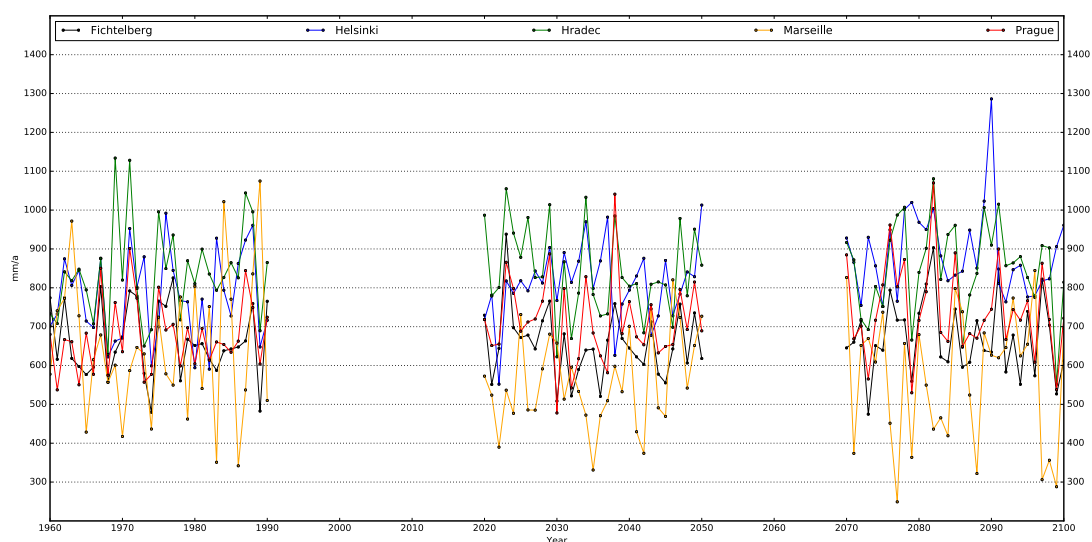


Figure 12 Annual precipitation, all locations

Fichtelberg (*Figure 65 in Appendix A*) also experiences little to no change, but annual precipitation in Helsinki (*Figure 64 in Appendix A*) is almost 15 % higher, which is even greater increase than in Prague. The only city that would actually suffer from fewer rain is Marseille (*Figure 67 in Appendix A*) with roughly 12 % decrease. The *Figure 12* compares all the locations in one plot and while it might not be easiest to read, it shows that all other location are balanced around 700 to 800 mm/a , Marseille can get as low as 200 mm/a during the drier years.

Specific humidity is a variable that is not originally included in the REMO dataset, but was calculated using the following formula:

$$w = 0.622 \cdot \frac{\varphi \cdot p_{vs}}{p - \varphi \cdot p_{vs}} \quad (1)$$

2 Climatic data

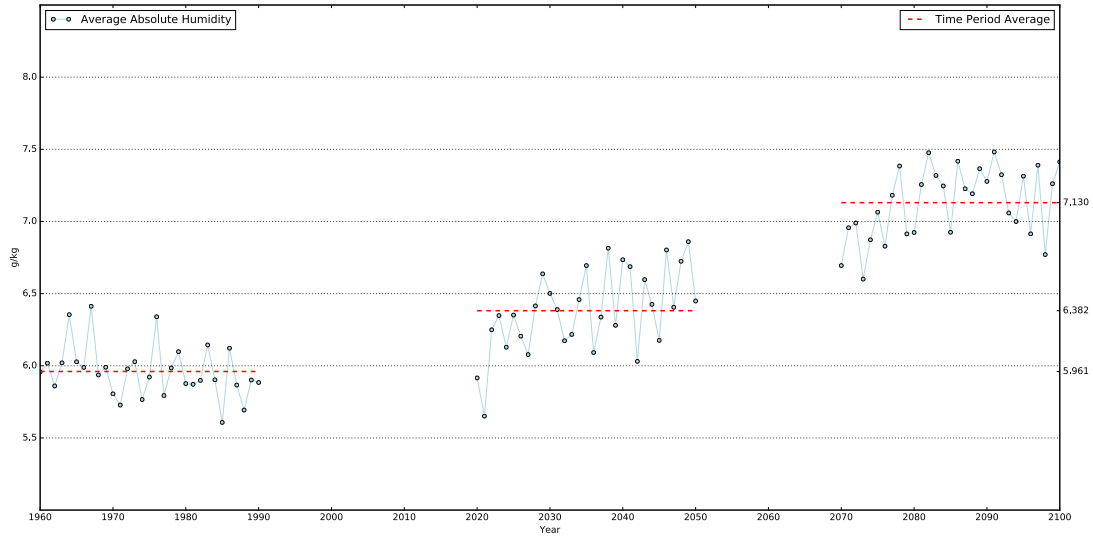


Figure 13 Annual average specific humidity in Prague

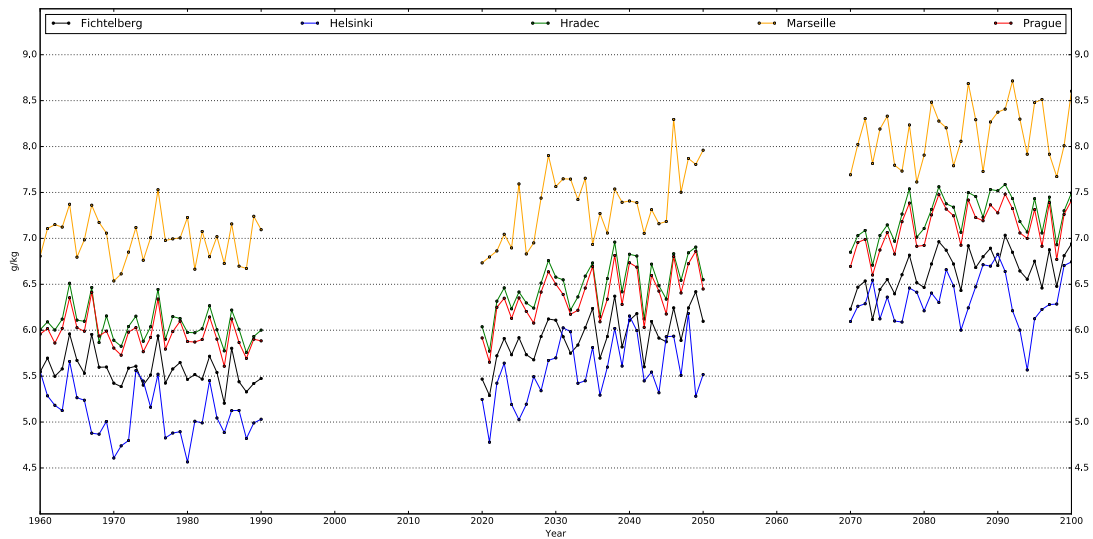


Figure 14 Annual average specific humidity, all locations

where:

- w ... specific humidity of ambient air (HSP) - $[g/kg]$
- φ ... relative Humidity of ambient air (HREL) - $[0 - 1]$
- p ... air pressure (PSTA) - $[Pa]$
- p_{vs} ... saturation vapor pressure - $[Pa]$

The saturation vapor pressure depends only on the temperature of the ambient air and it can be calculated by the following formulas with an error smaller than 1‰:

- for temperatures bellow $0^{\circ}C$:

$$\ln(p_{vs}) = 28.926 - \frac{6148}{273.15 + t_{ae}} \quad (2)$$

- for temperatures above 0 °C:

$$\ln(p_{vs}) = 23.58 - \frac{4044.2}{235.6 + t_{ae}} \quad (3)$$

where:

t_{ae} ... ambient air temperature (TA) - [°C]

Figure 13 shows annual average specific humidity in Prague, which actually increases by 20 %. The similar increase is noticeable for all other locations (*Figures 68 to 71 in Appendix A*) although it is a little bit lower for Marseille (16.5 %) and quite higher for Helsinki (25 %).

When all locations are compared in one *Figure 14*, it needs to be pointed out that due to the climate change, Helsinki and Fichtelberg rise to the current humidity levels in Prague and Hradec Kralove, while those two would match the current conditions in Marseille, which goes even much higher especially in the last period.

2.2.4 Heating and cooling degree hours

Degree hour (similarly to Degree day) is a measurement unit that aims to quantify the expected energy demand of a building based on the location's climate and not the house's design or construction parameters. It is derived solely from ambient air temperature. Total heating degree hours [$K \cdot h$] in a year can be then multiplied by a specific heat loss rate of a building to get the expected heat energy demand:

$$Q_{heat} = (P_{specific} \cdot HDH)/1000 \quad (4)$$

where:

Q_{heat} ... annual heat energy need - [kWh/a]

$P_{specific}$... specific heat loss rate - [W/K]

The heating degree hours (HDH) can be calculated accordingly:

$$HDH = \sum_{i=1}^{8760} (t_{base_H} - t_{ae_i})^+ \quad (5)$$

where:

t_{ae_i} ... hourly average ambient air temperature - [°C]

t_{base_H} ... heating base temperature - [°C]

The base temperature represents an outside temperature above which it is expected that a building would need no heating. It needs to be noted, that the base temperature would actually be different for each building based on its particular function and optimal interior temperature setup. It is basically expected that after the outside temperature reaches above some imaginary base line, the solar and interior gains inside the building would be enough to heat it at least to the optimal interior temperature

range's minimum. But the amount of interior gains would be also different in each house. Therefore the actual annual heat energy consumption might be very different than the calculated heat energy need by using HDH. So while HDH is not the best way to compare the energy demand of different houses, it is nevertheless a decent tool to compare the different locations for the same building, which is exactly the case of this thesis.

- the heating base temperature $t_{base_H} = 15.5\text{ }^\circ\text{C}$
 - as recommended by European Environment Agency [7]

As the HDH is indirectly dependent on ambient air temperature and it was already shown that the annual average temperature would rise due to the global warming, it is only natural that the HDH would decrease. The *Figure 15* shows that while the annual average temperature in Prague increased by $2.9\text{ }^\circ\text{C}$ the HDH actually dropped by significant 32 %. Similar decrease is present in Fichtelberg, Hradec Kralove and Helsinki, while in Marseille the HDH values in distant future are 51 % lower then the recent past values (*Figures 72 to 75 in Appendix A*).

Figure 16 shows that while the HDH would decrease significantly in each location, all cities would remain their own specific heating needs, with Helsinki having the highest, while Marseille having almost none. It can be also highlighted that while the relative decrease was the highest in Marseille, all other locations actually show almost two and half times higher decrease in absolute values which is much more important for the house operating costs.

Similarly to HDH, the cooling degree hours (CDH) aim to quantify the energy needed for cooling. It is calculated similarly:

$$CDH = \sum_{i=1}^{8760} (t_{ae_i} - t_{base_C})^+ \quad (6)$$

where:

t_{ae_i} ... hourly average ambient air temperature - [$^\circ\text{C}$]
 t_{base_C} ... cooling base temperature - [$^\circ\text{C}$]

and

- the cooling base temperature $t_{base_C} = 22.0\text{ }^\circ\text{C}$
 - as recommended by European Environment Agency [7]

It is generally not as commonly used as HDH. Mainly because of the fact that unlike heating demand, the cooling energy need is more dependent on other variables, mainly window solar gains and interior gains from the people and appliances and not on the ambient air temperature. Nevertheless even the CDH can once again reveal the differences among the various locations, the correlation between CDH and the actual cooling energy need would be even much lower than the one between HDH and the

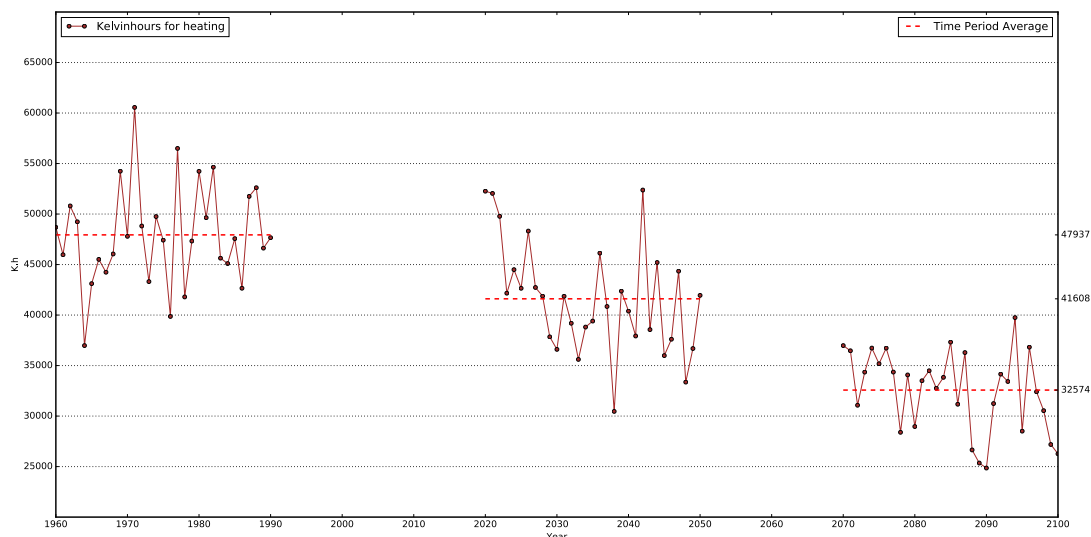


Figure 15 Annual total heating degree hours in Prague

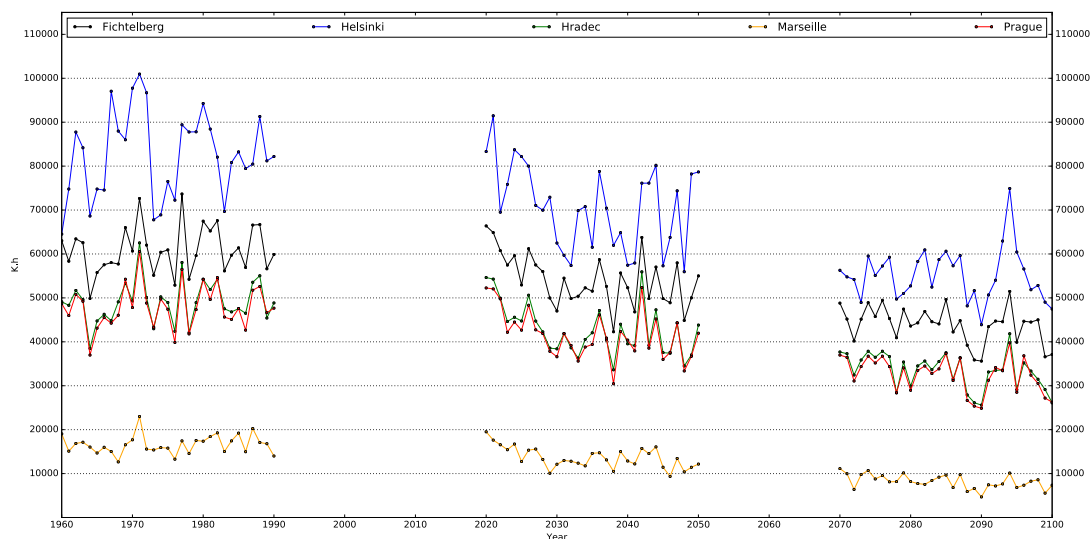


Figure 16 Annual total heating degree hours, all locations

actual heating energy need.

As the CDH is directly dependent on ambient air temperature, the results are almost exactly reversed with the HDH. *Figure 17* depicts that Prague experiences 242 % increase. Similar relative increase can be observed in all locations (*Figures 76 to 79 in Appendix A*) including Marseille where the relative change is again highest (269%).

When all the locations are compared in *Figure 18* it can be observed that this time Marseille experiences not only the highest relative change, but more importantly also the highest absolute increase in CDH between recent past and distant future, which is actually one and half times higher than for all the other four locations combined.

2 Climatic data

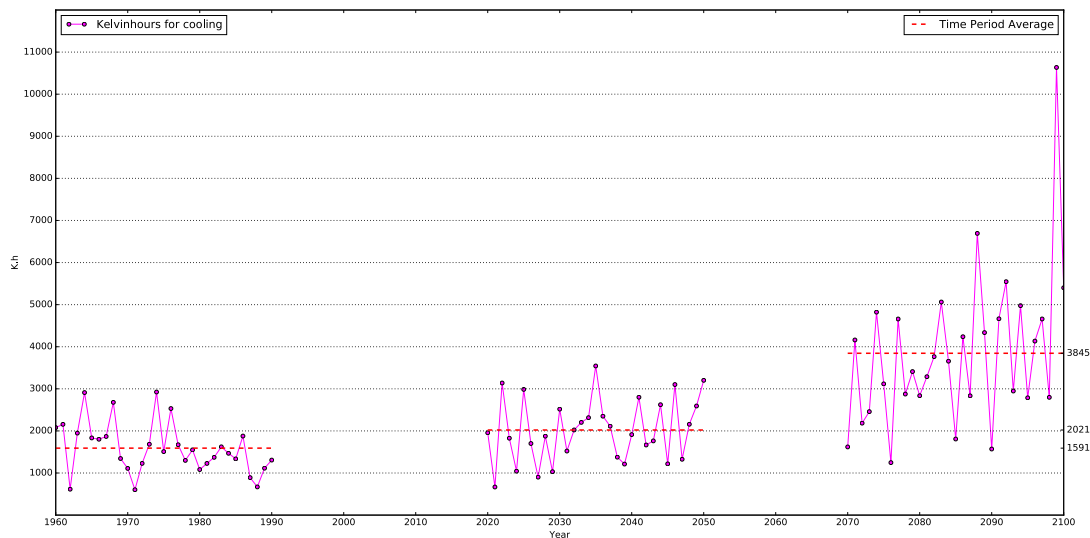


Figure 17 Annual total cooling degree hours in Prague

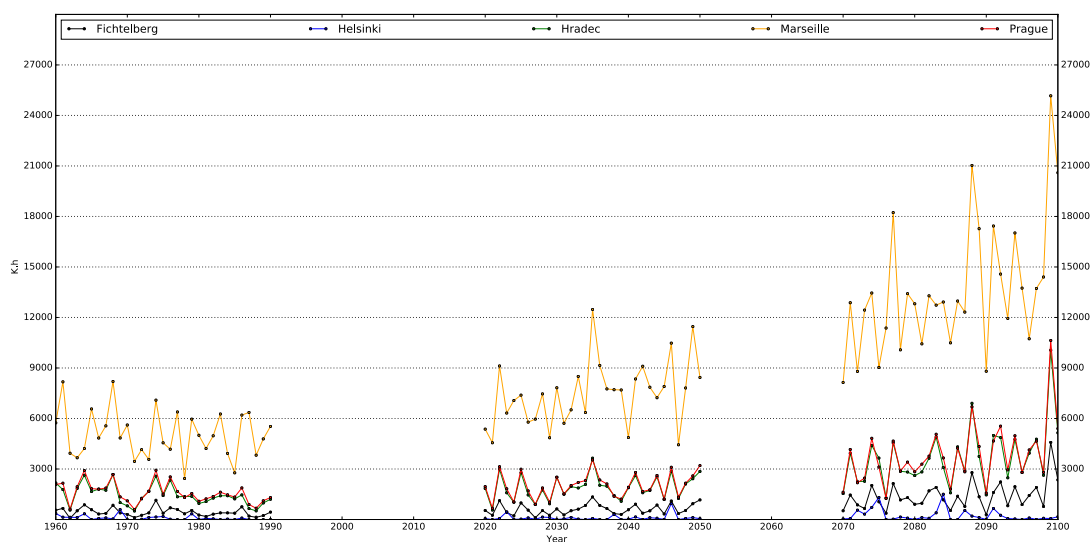


Figure 18 Annual total cooling degree hours, all locations

2.2.5 Wind

Wind speed as a variable is quite difficult to statistically analyze in any useful manner, especially as the effect it can have on energy performance of a house is very hard to express. The analysis here is therefore mainly focused on the wind speed as a variable important for the wind turbine electricity production. Similarly to normal rain (value which is zero most of the year) wind speed keeps at very low values at most of the time during a year, but it is much stronger during few windy hours or days. Calculating the annual average value would therefore be of no use, partly because the wind turbine production's curve is not linear and mainly it has a set minimum wind speed below which it does not produce any electricity.

To be able to quantify the wind turbine potential, Wind speed hour (WSH) unit was designed. The whole calculation is inspired by already existing HDH and CDH and is

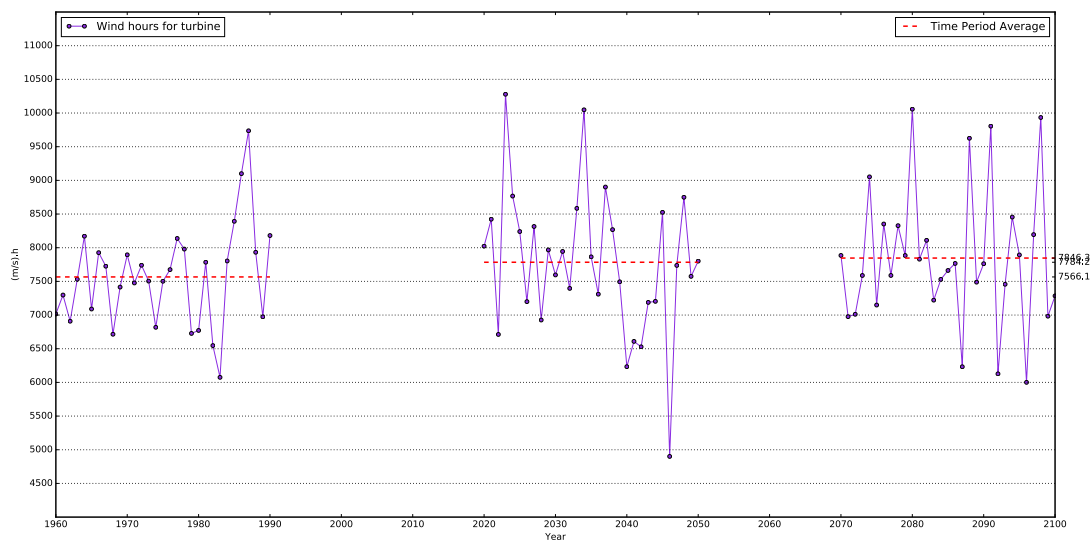


Figure 19 Annual total wind speed hours in Prague

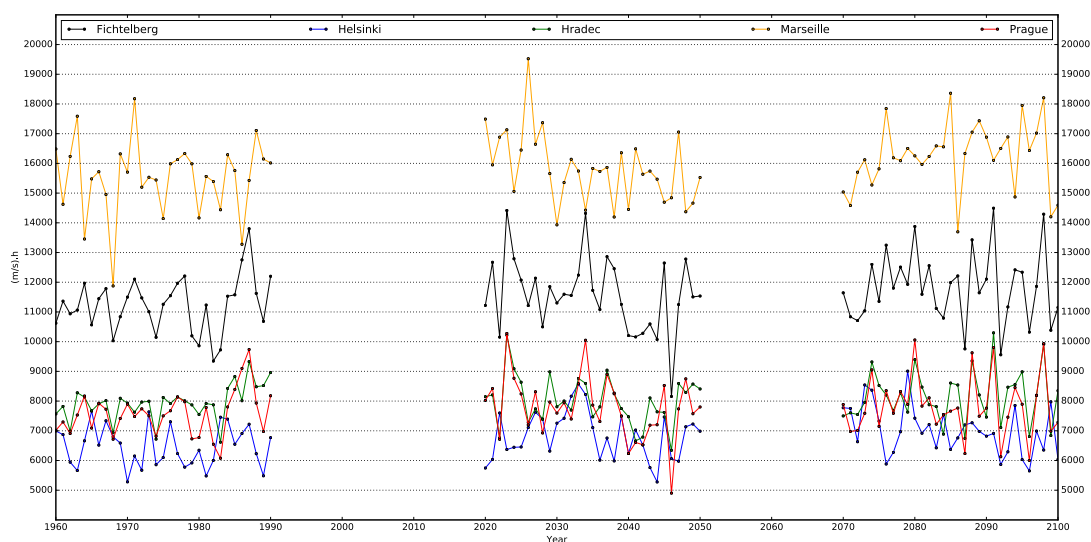


Figure 20 Annual total wind speed hours, all location

very similar, but the units of WSH are $[(m/s) \cdot h]$:

$$WSH = \sum_{i=1}^{8760} (v_{wind_i} - v_{base_W})^+ \quad (7)$$

where:

v_{wind_i} ... hourly average wind speed - $[m/s]$

v_{base_W} ... base wind speed - $[m/s]$

and

- the base wind speed $v_{base_W} = 3.0 m/s$
 - corresponds to the minimum production wind speed for most of the smaller,

vertical axis turbines

The annual electricity production of a wind turbine can be then calculated as follows:

$$P_{WT} = (\alpha \cdot WSH^4 + \beta \cdot WSH^3 + \gamma \cdot WSH^2 + \delta \cdot WSH + \epsilon) / 1000 \quad (8)$$

where:

P_{WT} ... annual wind turbine production - [kWh/a]

$\alpha, \beta, \gamma, \delta, \epsilon$... are parameters describing the specific wind turbine's production curve and can be calculated for any wind turbine either from its manufacturer's specification or from measured production at different wind speeds

While neither Prague (*Figure 19*) nor the other locations (*Figures 80 to 83* in Appendix A) show any significant change due to the climate alteration, the vast differences between the location are depicted in *Figure 20*. Marseille and Fichtelberg show very high potential for the wind turbine electricity production while the rest might probably be below economical viability of such an investment.

2.3 Characteristic year generation

One main objective of this thesis is to be able to use the dataset that stretches over ninety three years and to use the simulation results to compare the house performance in the three different time periods. For that it was necessary to create a script in python that would be able to load the 31 years of data in each time period and return one characteristic year that would consist of real data from the dataset, but would be representing the average of that time period. For each of the twelve months in year the task is to choose one year from the whole time period in which that month's data is the most similar to the data for that month from all years put together. The characteristic average year would then consist of twelve months possibly from twelve different years.

This was done by splitting all values for each variable into histogram bins. The size of a bin is different for each variable based on the absolute minimum and maximum value in the dataset, but the number of bins is the same for all variables. The number of bins in each histogram is 101, mainly because of the variables that range between value 0 and 1. 101 bins allows to use the bin size of 0.1 and still include both 0 and 1. For example, the bin range for ambient air temperature is then from -50 to +50 °C with the bin size 1 °C and from 0 to 1000 W/m² with the bin step 10 W/m² for any irradiance.

A reference histogram for each month was first computed from the data of a particular month over all years in a specific period. Then histograms for the particular month in each year of the period were created. All 31 histograms of the month were then compared with the reference histogram (all histograms were normalized for easy comparison). The similarity measure is represented by the sum of differences between each of the 31 histograms and the reference one. This process of creating and comparing the histograms was done for each variable and the process was repeated for each month

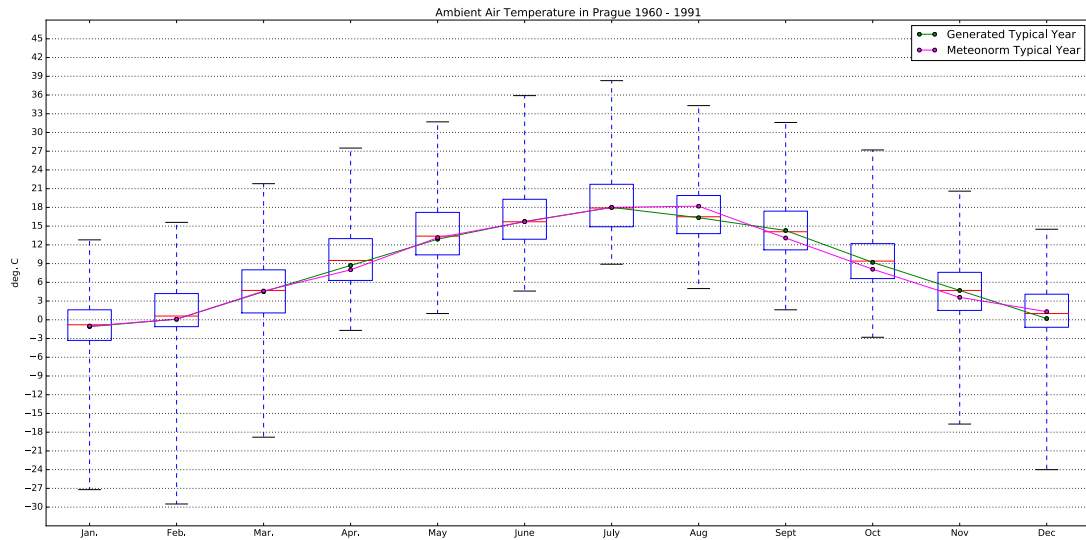


Figure 21 Monthly box plot for Prague 1960 - 1990 which validates the created characteristic year data

in every time period and location.

As it was mentioned several times already, not all the variables have the same importance and not all of them are even going to be used. Therefore, for all the calculated histogram differences, there is also a weight based on the variable and its importance for the climate and the calculation model. The most important is ambient air temperature and then the irradiance. After several iterations, the final weights that were used are as follows: 0.75 for TA, 0.05 for each form of irradiance or radiation (ISGH, ISDH, ILAH, ILTH) and finally 0.05 for Normal Rain, while all the remaining variables' weights are set to 0 (and therefore that variable does not effect the result at all). The weighted difference for each year is the sum of all the variable differences multiplied by the variable's weight. The month of the year with the lowest weighted difference is chosen. After all twelve months were found, the characteristic year is then created by combining their data into one new year data file with 8760 values for each variable. This is then the dataset that is used during the calculation to simulate the house performance in certain location and time period.

In order to validate the created characteristic average years, a monthly box plot was generated for each location and each time period. Monthly median values of the characteristic average year are plotted on top of the boxes. For all the generated typical years, the median values are not only inside the boxes but also very close to the median of the box itself. *Figure 21* also depicts the monthly median values that were generated for the same location and time period (Prague 1960 - 1990) by the Meteonorm software [8]. It can be observed that the monthly median values of the typical year generated for the purposes of this thesis are in every months similar to the median values of the Meteonorm typical year, or are even closer to the median values of the original REMO dataset.

3 Case study

3.1 Case description

The objective of this case study is to take one particular house design and to develop a functional and validated calculation model, then to devise several simulation scenarios and methods how to measure house performance and compare the results not only in different scenarios, but also between various locations and time periods. The last objective is to run parameter optimization to figure out how the house performance is dependent on the chosen parameters.

3.2 Model house

Model house was designed as a very small minimalistic apartment for four people. It has a longitudinal disposition with one bed room at each end and a common living area, kitchen and bathroom in the middle. The entrance as well as majority of the windows is located in the front facade, which was originally designed to face south. As the house was supposed to be fully off-grid, the project includes all the necessary technologies, mainly the photovoltaic panels seamlessly integrated into the construction of the south face of the gable roof. The visualizations and available engineering documentation of the house can be found in *Appendix C*.

Following house description represents the data that is used as an input to the calculation model.

1. House envelope

- Exterior walls
 - $a_{wall} = 106.90 \text{ m}^2$... total area (if there were no windows)
 - $u_{wall} = 0.169 \text{ W/m}^2\text{K}$... thermal transmittance
- Exterior floor above crawl space
 - $a_{floor} = 46.30 \text{ m}^2$... total area
 - $u_{floor} = 0.125 \text{ W/m}^2\text{K}$... thermal transmittance
- Gable roof
 - $a_{roof} = 60.50 \text{ m}^2$... total area
 - $u_{roof} = 0.164 \text{ W/m}^2\text{K}$... thermal transmittance
- Front facade windows
 - $a_{win_{max}} = 30.36 \text{ m}^2$... the maximum square area of the front wall that could be glassed

- $f_{glassed} = 0.35$ [-] ... portion of the front wall that is glassed
(default value that represents original design and is due to be changed during the optimization as explained in *Section 3.4.2*)
- $a_{win} = a_{win_{max}} * f_{glassed} = 10.63 \text{ m}^2$... actual square area of the windows
- $f_{frame} = 0.15$ [-] ... portion of the window frame
- $a_{glass} = a_{win} * (1 - f_{frame}) = 9.03 \text{ m}^2$... actual square area of the glass within the windows
- $u_{win} = 0.640 \text{ W/m}^2.K$... thermal transmittance
- $g = 0.6$ [-] ... solar energy transmittance
- $f_g = 0.95$ [-] ... factor reducing solar energy transmittance for non perpendicular solar rays
- $f_{sh} = 0.72$ [-] ... average passive shading factor
- f_{frame} and u_{win} values were calculated for $f_{glassed} = 0.35$ [-] but for simplification of the calculation model the same values are used during the optimization for any $f_{glassed}$ values even though the actual f_{frame} and u_{win} value would slightly differ based on actual window size)

2. Environment parameters

- $v_{air} = 100 \text{ m}^3$... interior air volume
- $n_{50} = 0.6 \text{ ACPH}$... infiltration when pressurized to 50 Pascals
- $c_{int} = 15.0 \text{ MJ/K}$... thermal capacity active in the interior
- $\rho_{air} = 1.171 \text{ kg/m}^3$... density of the air
- $c_{air} = 1010 \text{ J/kg.K}$... specific heat capacity of the air
- $c_{water} = 4180 \text{ J/kg.K}$... specific heat capacity of the water
- $t_{int_{min}} = 20.0 \text{ }^\circ\text{C}$... minimum interior temperature (for heating system purposes)
- $t_{int_{max}} = 27.0 \text{ }^\circ\text{C}$... maximum interior temperature (for cooling system purposes)
- $t_{opt_{min}} = 23.0 \text{ }^\circ\text{C}$... optimal interior temperature range's minimum (for active shading and ventilative cooling purposes)
- $t_{opt_{max}} = 25.0 \text{ }^\circ\text{C}$... optimal temperature range's maximum (for active shading and ventilative cooling purposes)

3. Building geometry

- $\alpha = 0 \text{ }^\circ(\text{south})$... front facade azimuth
- $\gamma_{roof} = 40.0 \text{ }^\circ$... gable roof slope
- $\gamma_{wall} = 90.0 \text{ }^\circ$... front facade slope

3.3 Calculation model

The calculation model is programmed in Python 2.7.2. The code is divided into multiple classes. Each class represents either energy gain, energy loss or energy accumulation. There is a minimum set of classes which is necessarily for the simulation to be able to run. It would then represent a simulation of an empty house, with no inhabitants, and no technical systems. More "energy" classes can be then used to make the model more complex, ideally to have one class for each house construction or system. One class can be also initiated more than once. For example window class has to be initiated separately for each window that differs in its technical properties or in parameters like its azimuth, glazing or passive shading.

There are also some classes that are used solely to process some input data and return them in a desired way. The simulation itself is one of them. Other important "processing" class is Occupancy, which simulates real-like behavior of house's inhabitants and determines whether they are outside or inside, cooking or sleeping. Lastly it is Solar Calculator, which uses Irradiance on horizontal plane to calculate Irradiance on a tilted plane.

Within each class is a set of member variables, which are set to the right value at the beginning of the simulation, when a class instance is initiated. In each class, there are also defined many member functions which contain all the necessary equations and logic describing physical actions that the class represents. The member functions from various classes are then called upon during the simulation in a specific order. This happens repetitively in each calculation step - in this case one hour. As all the operations within the energy classes are calculated in Watts and the length of the step is one hour, the whole simulation model operates in Watt hours. Even for classes where the interest is in values in other units - for example temperature, the energy status is first calculated in Watt hours and then the temperature is deduced based on the specific heat capacity.

The simulation itself is started from a configuration process file, where it is possible to set up for what location and time period the weather data is loaded, what classes would be used and what return data is wanted to be printed, saved or plotted into a graph. All the necessarily pieces of information about the house itself are at the beginning of the simulation file. To create a calculation for another house, it is needed to make a new instance of the simulation and to change all the necessarily data and the beginning, but its not needed to change the actual simulation process and its decision making, because it is controlled from the process file by turning whole classes (or their parts) on and off.

1. The minimum set of classes to run the simulation:

Consumption

- calculates electricity consumption based on occupancy and system loads

Gains

- calculates interior heat gains based on occupancy and consumption

Transmission

- calculates heat loss or gain by transmission based on interior and exterior temperature

Ventilation

- calculates heat loss or gain by ventilation based on interior and exterior temperature
- without inhabitants or active ventilation system, the class is still needed to calculate the infiltration
- active ventilation changes its power based on occupancy
- can include heat recuperation unit
- can be enabled for ventilative cooling at maximum fan power when empty or by opening windows (and increasing infiltration) when occupied to prevent overheating

Window

- calculates interior solar gains based on irradiance on corresponding window's plane
- passive window shading is set up as an average value during class initiation
- active window shading can be enabled

Environment

- operates as an accumulation class for all the heat gains and losses inside the house
- calculates the interior temperature based on the specific heat capacity of the environment and its current energy state
- calculates the total heating and cooling energy needs as well as heating and cooling peak loads if ideal heating and cooling source option is enabled

Grid

- represents electric power grid
- counts total electricity consumption from the grid
- can serve only as a backup source if other renewable sources or battery are enabled
- can be disabled when generator is present

Occupancy

- for each step (hour) returns occupancy value based on the initial setting:
 - 0 for unoccupied house (longterm)
 - 1 for occupied house but with no people currently inside

3 Case study

- 2 for people inside
- 3 for people inside and cooking
- 4 for people inside and sleeping
- can be set up as either idealized (same every week) or simulated occupancy (randomized based on total percentage desired)

Solar Calculator

- uses global and diffuse irradiance on horizontal plane, ground reflectance(albedo), latitude, longitude, time and meridian from the weather data to calculate global and diffuse irradiance on tilted plane based on its azimuth and slope

2. Extra classes that might be used:

a) Water related systems in the house:

Accumulation

- represents large insulated water tank to store the spare energy from heat or renewable electricity sources
- can also function as a hot water tank, if there is no separate hot water tank

Hot water

- represents smaller insulated water tank used to prepare hot water for shower and tap

Shower

- calculates energy consumed from hot water tank and hot water usage in shower based on occupancy
- counts total water consumption in shower
- can include heat recuperation from waste water

Tap

- calculates energy consumed from hot water tank and hot water usage from tap based on occupancy
- counts total water consumption from tap
- can include heat recuperation from waste water

Toilet

- counts total water consumption in toilet based on occupancy
- if turned off, represents composting toilet

Rain water

- represents large water tank that collects all the rain water from the roof surface
- calculates the water volume in the tank based on hourly precipitation and water consumption in shower

Grey water

- represents large water tank that collects all the waste water from the shower and tap
- calculates the water volume in the tank based on water consumption in toilet, shower and tap

Well water

- represents energy consumption necessary to draw the fresh water from a well
- can include large fresh water tank placed in higher altitude than the house to which the water is drawn when suitable (for example to consume extra renewable production during peak hours) and which later supplies the house with water by gravitational force
- calculates the fresh water volume in the tank based on water consumption

b) **Renewable and off-grid systems:**

Battery

- represents home battery to store electricity produced by renewable or backup sources which is then provided for the consumption when needed
- counts the number of cycles that the battery has made during the simulation

Photovoltaic

- represents array of photovoltaic panels
- calculates electricity production based on irradiance on corresponding tilted plane

Photothermic

- represents array of photothermic panels
- calculates heat energy production based on irradiance on corresponding tilted plane

Wind

- represents a small wind turbine
- calculates electricity production based on wind speed

Generator

- represents backup electricity source
- calculates electricity production, number of times and total time when turned on and total amount of fuel consumed

c) **Heating or cooling systems:**

Stove

- represents biomass burning stove
- calculates heat energy production, number of times and total time when in use and total amount of fuel burned
- can include water heat exchanger which splits energy production between environment and accumulation watter tank based on its efficiency

Heat Pump

- represents a heat pump unit that can be used both to provide heat energy to accumulation tank or cool energy to air cooling exchanger
- counts the electricity consumed based on provided energy and the unit's coefficient of performance (CoP)

Air Heating

- represents air heating exchanger by hot water from accumulation tank
- provides heat energy from accumulation tank to environment based on heat need and ventilation air flow

Air Cooling

- represents air cooling exchanger by cold water from reversed heat pump unit
- provides cooling energy based on demand and ventilation air flow

Heating

- represents hot water heat radiator
- provides heat energy from accumulation tank to environment based on heat need and its maximum power output

Simulation process which repeats in each step:

1. Get the occupancy status.
2. Calculate renewable energy sources' production (if Photovoltaic, Photothermic or Wind present).

3. Calculate the transmission heat loss or gain.
4. Calculate the ventilation heat loss or gain.
5. Calculate the interior solar heat gains.
6. Calculate the electricity consumption.
7. Calculate the interior heat gains.
8. Accumulation tank accepts energy from stove water heat exchanger when the stove is on (if Accumulation and Stove present).
9. Use the RES electricity production to cover the electricity consumption (if any RES present).
10. Use the possible RES electricity overproduction to charge the battery (if RES and Battery present).
11. Use the possible electricity overproduction to heat water in the hot water tank to desired optimum temperature (if RES and Hot water present).
12. Use the possible electricity overproduction to draw water from the well to fresh water tank up to a maximum level (if RES and Well water present).
13. Use the possible electricity overproduction to power the heat pump to provide energy to the accumulation tank up to a maximum temperature (if RES, Accumulation and Heat pump present).
14. Use the possible electricity overproduction to heat water in the accumulation water tank up to a maximum temperature (if RES and Accumulation present).
15. Count the possible electricity overproduction that the system was not able to use (if RES present).
16. Cover the possible remaining electricity consumption from battery (if Battery present).
17. Use the heat from accumulation tank to heat the water in hot water tank up to a desired optimum temperature (if Accumulation and Hot Water present).

3 Case study

18. Use the electricity from the battery to heat the water in hot water tank up to a desired minimum temperature (if Battery and Hot Water present).
19. Start the electricity backup generator if battery voltage drops to a set maximum depth of discharge (if Battery and Generator present).
20. Cover the electricity consumption from the generator or the grid (if Generator or Grid present).
21. Use the electricity from the generator or the grid to charge the battery to an optimum state of charge (if Battery and Generator or Grid present).
22. Use the electricity from the generator or the grid to heat the water in hot water tank to a desired minimum temperature (if Hot Water and Generator or Grid present).
23. Calculate the water usage in shower, tap and toilet and update the state of all the water tanks present (if any water related system present).
24. Calculate additional interior heat gains from various system inefficiencies and losses.
25. Calculate total interior gains.
26. Balance the environment energy state with the energy gains and losses from transmission and ventilation and solar and interior gains.
27. Calculate the heating or cooling energy need and the system load necessary to cover it (if ideal heating and cooling enabled).
28. Environment accepts energy from the stove if the stove is on (if Stove present).
29. Environment accepts heat energy from accumulation tank via air heating system (if Accumulation and Air Heating present).
30. Environment accepts heat energy from accumulation tank via heating system (if Accumulation and Heating present).
31. If there is not enough energy for heating in accumulation tank start the stove for the next step (if Accumulation and Stove present).
32. Heat the accumulation tank from the grid to a optimum temperature if electric heating enabled (if Accumulation and Grid present).

3.4 Simulation settings

As mentioned in previous section, the whole simulation can be set up in a process file before being started. Not only it is possible to enable or disable whole classes, but also some vital parts of the classes, for example active exterior window shading. This allows different simulation scenarios to be created and to analyze the differences in the results.

3.4.1 Simulation scenarios

Simulation settings used for the purposes of this thesis:

1. Scenario 1

- No inhabitants
 - Occupancy value 0 at all times
 - Permanent system consumption at 100 W
- Minimum active ventilation
 - Fixed at 0.3 ASPH ($30 \text{ m}^3/h$)
 - Ventilator consumption 50 W per ASPH (15 W for 0.3 ASPH)
 - Exhaust air heat recuperation unit with 90 % efficiency
 - Recuperator by-pass active for temperatures above optimal range maximum ($25.0 \text{ }^\circ\text{C}$) when exterior temperature is lower
- Active shading disabled
- No ventilative cooling

2. Scenario 2

- 4 inhabitants with idealized occupancy (same every day)
 - Occupancy value 1 (outside) from 10 am to 6 pm
 - Occupancy value 4 (sleeping) from 12 am to 7 am
 - Occupancy value 3 (cooking) at 8 am and again at 8 pm
 - Occupancy value 2 (inside) the rest of the time
- electricity consumption based on occupancy value:
 - 1 (outside): 50 W
 - 2 (inside): 150 W
 - 3 (cooking): 1000 W
 - 4 (sleeping): 50 W

3 Case study

- consumption goes up by 50 W for lighting when occupancy is 2 or 3 and diffuse irradiance is below 10 W/m^2
- interior gains based on occupancy value
 - 1 (outside): 0 W per person
 - 2 (inside): 120 W per person
 - 3 (cooking): 120 W per person
 - 4 (sleeping): 50 W per person
- active ventilation power and ventilator consumption based on occupancy value
 - 1 (outside): 0.5 ASPH (50 m^3/h and 25 W)
 - 2 (inside): 1.0 ASPH (100 m^3/h and 50 W)
 - 3 (cooking): 1.0 ASPH (100 m^3/h and 50 W) + infiltration also goes up by 1.0 ASPH
 - 4 (sleeping): 0.7 ASPH (70 m^3/h and 35 W)

3. Scenario 3

- active exterior window shading is enabled
 - shading is activated when interior temperature raises above optimal range maximum (25.0 $^{\circ}C$)
 - it applies additional shading factor of 0.2
 - it is deactivated when interior temperature drops below optimal range minimum (23.0 $^{\circ}C$)

4. Scenario 4

- active ventilative cooling to prevent overheating
 - ventilative cooling is activated when interior temperature raises above optimal range maximum (25.0 $^{\circ}C$) and is also higher than exterior temperature by at least 2 degrees
 - the system runs at 3.0 ASPH (300 m^3/h and 150 W) when occupancy is 1
 - when the occupancy is 2, 3 or 4, the ventilation runs regularly based on occupancy and the infiltration goes up by 3.0 ASPH instead
 - it is deactivated when interior temperature drops below optimal range minimum (23.0 $^{\circ}C$)

A. No heating or cooling system

- No heating system present
- No cooling system present

B. Added ideal heating and cooling system

- For all the Scenarios above, the ideal heating and cooling system is enabled. It represents imaginary heat and cool energy source with unlimited power and instant (within an hour) heat or cool distribution.
- Ideal heating system delivers heat energy to environment based on calculated heat need
 - It keeps the interior temperature at set minimum value (20.0 °C)
- Ideal cooling system delivers cool energy to environment based on calculated cool need
 - It keeps the interior temperature at set maximum value (27.0 °C)

3.4.2 Parameter optimization

The simulation scenarios 1B to 4B with ideal heating and cooling enabled can also be used to perform parameter optimization or rather to determine the effect of a certain parameter on the performance of the house.

Due to the house design described in *Section 3.2*, the main thing that can be most easily customized during the production is total window area size. And as majority of windows is placed in one front facade of the house, its orientation (azimuth) should be also very crucial for the house performance. Therefore it was decided to set up an optimization scenario by changing percentage of the front wall that would be glassed between 0 and 100 % by 5 % and the azimuth from -180 ° to +180 ° (with -90 ° being east, +90 ° being west and 0 ° being south) by 15 °.

The simulation was run for each combination of 21 values for glazing and 25 values for azimuth. Two values were obtain as the result - annual heating and cooling energy need (in kWh/a). The resulting performance of the house was then measured by a cost function mentioned below:

$$f_{cost} = w_{heat} \cdot Q_h + w_{cool} \cdot Q_c \quad (9)$$

where:

f_{cost} ... cost function result
 Q_h ... annual heating energy need - [kWh/a]
 Q_c ... annual cooling energy need - [kWh/a]
 w_{heat} ... weight for heating - [-]
 w_{cool} ... weight for cooling - [-]

and

$$w_{heat} + w_{cool} = 1 \quad (10)$$

Using the different sets of the weights allows to devise various optimization scenarios and to use the cost function value to evaluate the result. The lower the value, the better the performance of the house. In some situations it might be more valuable to have higher heating need and lower or none cooling energy demand, therefore the weight for

3 Case study

heating would be set high and the weight for cooling would be set low. In the other situation, when the low heating need is appreciated and a higher cooling energy demand is not a problem, the weights would be setup in opposite manner.

1. Optimization weights set 1

- represents a scenario where there is no cooling system installed and therefore the lowest heating consumption is preferred
 - $w_{heat} = 1.0$
 - $w_{cool} = 0.0$

1. Optimization weights set 2

- could represents a scenario where there are both heating and cooling systems present and both are electric, but while cool energy need correlates with own electricity production (for example from photovoltaic panels), heat energy need does not
 - $w_{heat} = 0.7$
 - $w_{cool} = 0.3$

2. Optimization weight set 3

- could represent a scenario where there are both heating and cooling systems present and both are using a source with the same mixture of renewable and non-renewable energy and the goal is to minimize the house's energy footprint on the Earth
 - $w_{heat} = 0.5$
 - $w_{cool} = 0.5$

3. Optimization weight set 4

- could represent a scenario where there are both heating and cooling systems present but while heating energy comes from a renewable source, cooling system uses mostly the energy which comes from the non-renewable source
 - $w_{heat} = 0.3$
 - $w_{cool} = 0.7$

4. Optimization weight set 5

- last scenario could represent a house where there is either no heating system present or where there is cooling system which uses only the energy which comes from the non-renewable
 - $w_{heat} = 0.0$
 - $w_{cool} = 1.0$

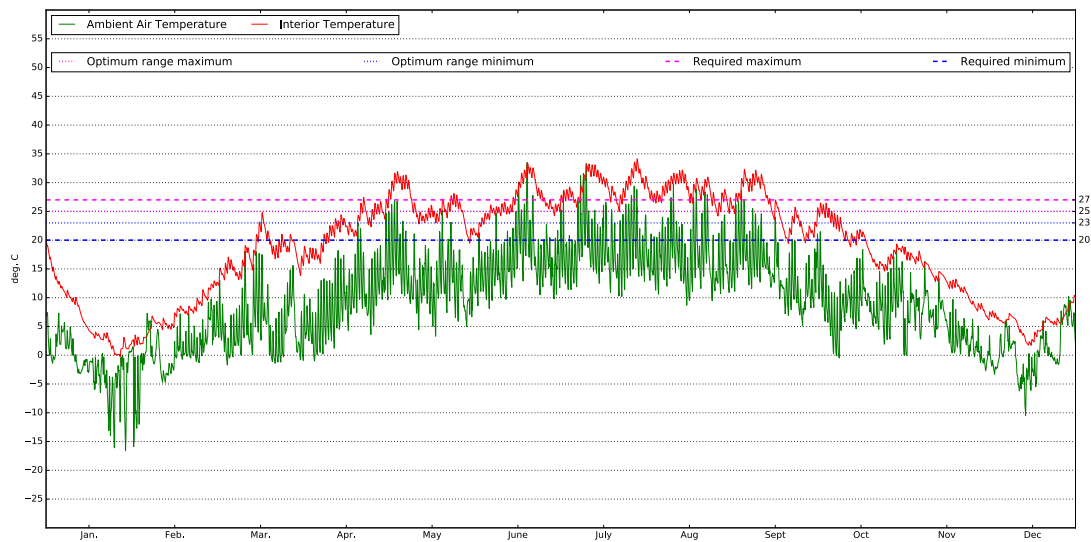


Figure 22 Exterior and interior temperature for Scenario 1A in Prague 1960 - 1990

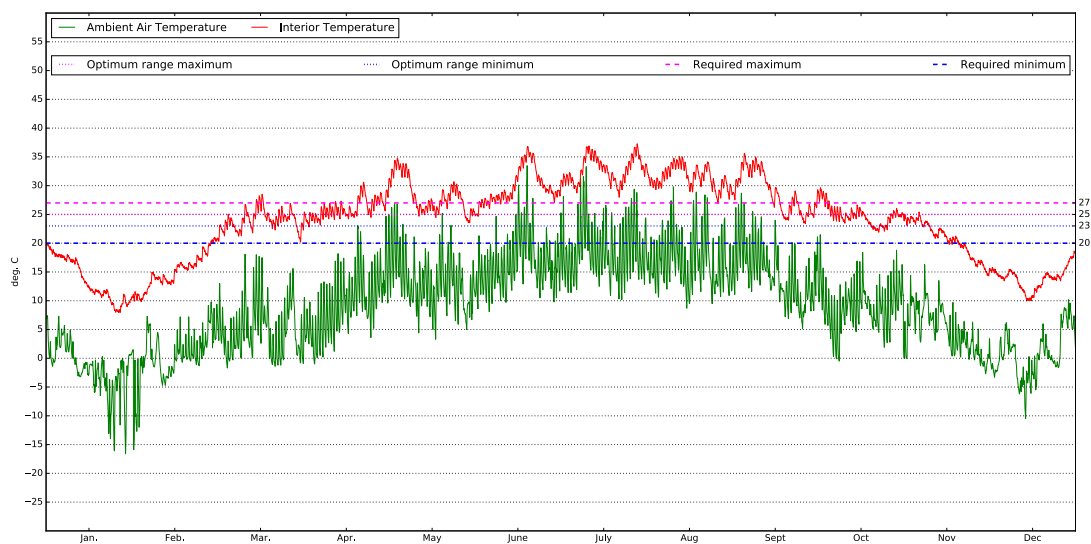


Figure 23 Exterior and interior temperature for Scenario 2A in Prague 1960 - 1990

3.5 Results

In the first part of the calculation, the simulation was run for each location and time period with fixed parameters of glazing at 35 % of the front wall, which was in turn fixed to face south by setting the azimuth to 0 °. The output of the simulation contains hourly values from each class, as well as annual summary values at the end of the simulation. In order to be able to visually compare the results for various locations, but mainly to depict how the available systems in the house deal with the effects of climate change, interior temperature was used as the results for scenarios 1A to 4A (which were described in *Section 3.4.1*). Interior temperature was plotted together with ambient air temperature, and with horizontal lines that represent optimum temperature range (dotted lines) and the minimum and maximum temperatures that are used for heating and cooling system (dashed lines).

3 Case study

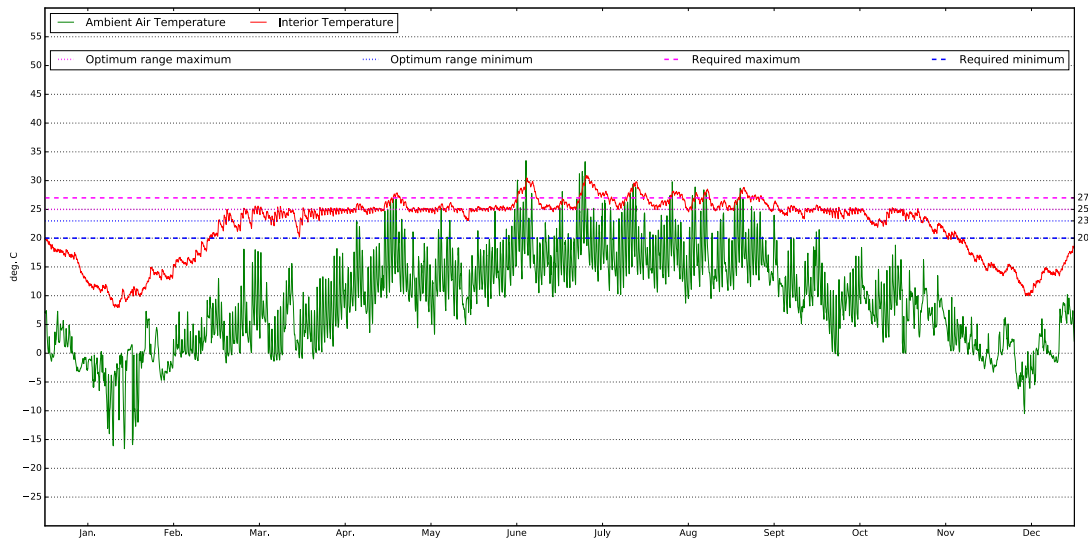


Figure 24 Exterior and interior temperature for Scenario 3A in Prague 1960 - 1990

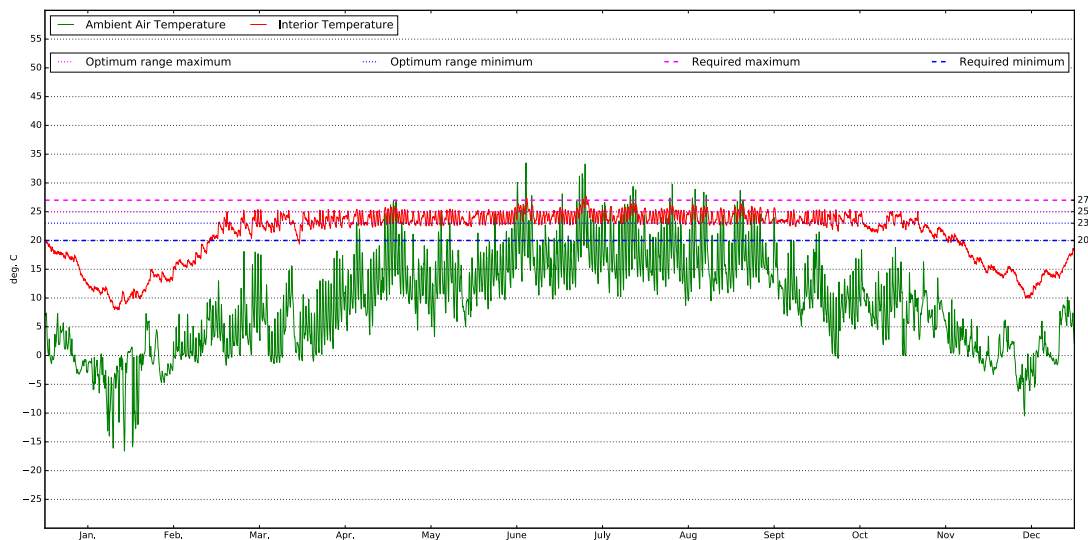


Figure 25 Exterior and interior temperature for Scenario 4A in Prague 1960 - 1990

As can be observed in *Figure 22*, which shows interior temperature behavior for Scenario 1A (empty house with minimum ventilation) in recent past in Prague, the interior temperature follows the ambient temperature with almost constant margin but reacts to the changes in TA with slight time shift. The time shift would have been much higher if the thermal mass of the house was higher, but because the house is very light, the interior temperature responds very quickly to changes in exterior temperature. The effect of the air heat recuperating unit is very low, because the volume of the exchanged air is very little in this scenario.

In the 2A scenario, the house is already inhabited and as the *Figure 23* shows, the presence of people adds to the environment large interior gains that cause the margin between interior and exterior temperature to further increase. With no systems present to regulate the temperature, the house suffers from overheating for the recent past data period in Prague.

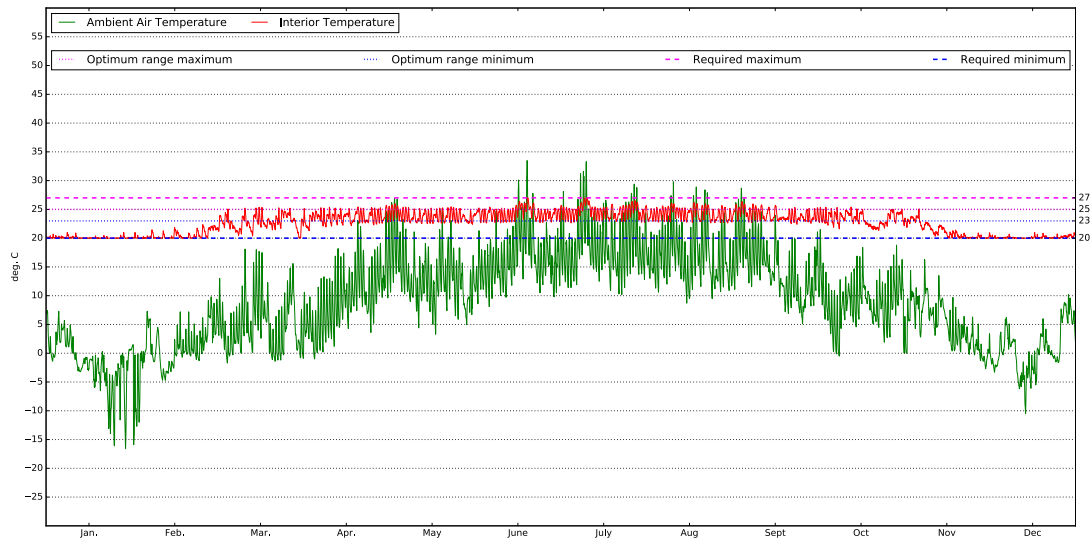


Figure 26 Exterior and interior temperature for Scenario 4B in Prague 1960 - 1990

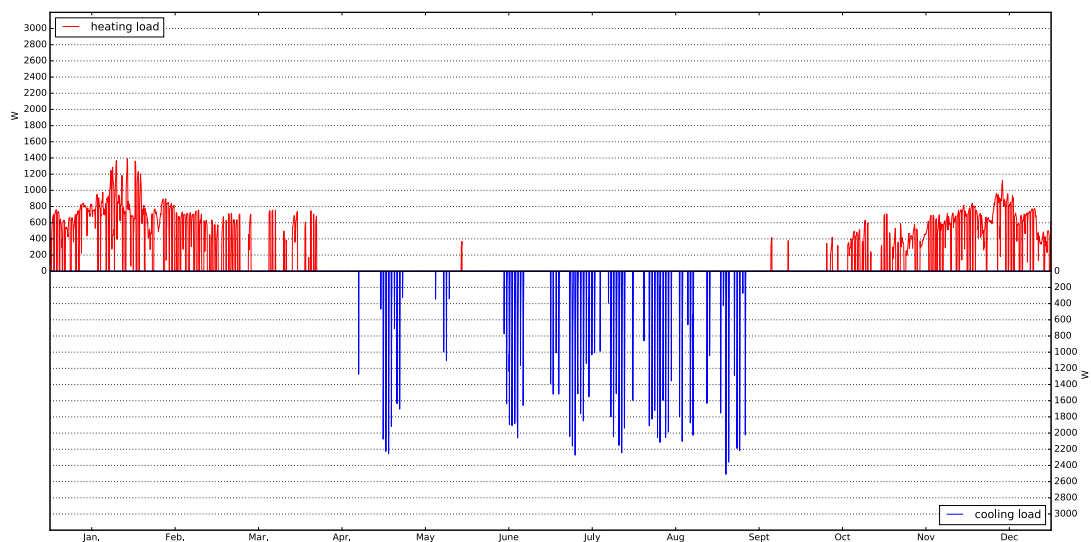


Figure 27 Heating and cooling loads for Scenario 1B in Prague 1960 - 1990

With the active window exterior shading enabled in scenario 3A, it can be easily spotted in *Figure 24* how the shading activates when the interior temperature reaches $25\text{ }^{\circ}\text{C}$ (magenta dotted line) and the temperature then decreases. Once it crosses the lower boundary of optimal range at $23\text{ }^{\circ}\text{C}$ (blue dotted line), the shading is deactivated and the temperature rises again. The effect of the shading is only able to prevent further interior gains and cannot get rid of the energy gains already obtained, which come not only through the windows, but mainly from the inhabitants and their electricity consumption. Because of that, it can be observed, that in Prague 1960 - 1990 from April to September, the active shading is not sufficient to lower the interior temperature below $23\text{ }^{\circ}\text{C}$ and therefore it would remain activated whole that time.

In scenario 4A, the use of ventilating system for ventilative cooling is also enabled and as can be seen in *Figure 25*, the combined effect of active shading and ventilative

3 Case study

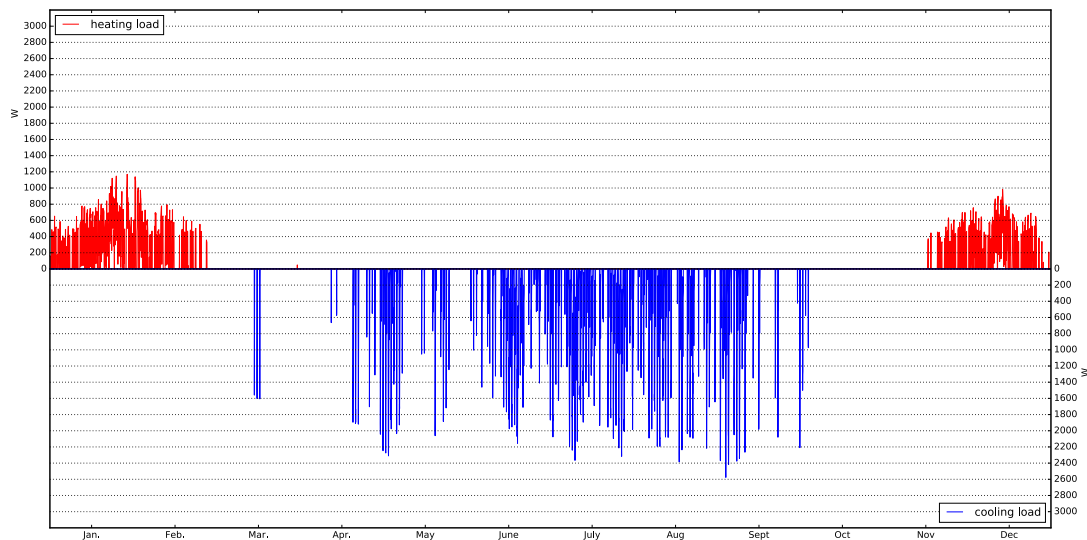


Figure 28 Heating and cooling loads for Scenario 2B in Prague 1960 - 1990

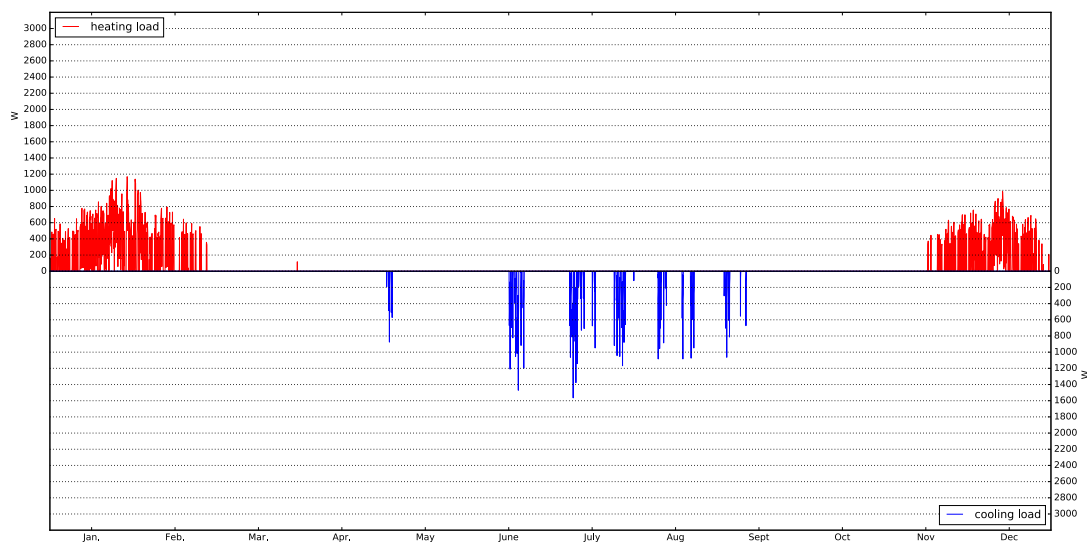


Figure 29 Heating and cooling loads for Scenario 3B in Prague 1960 - 1990

cooling is enough to keep the interior temperature within its optimum range most of the time. There are only several warm days in the typical year for Prague 1960 - 1990, when the interior temperature peaks over the $25\text{ }^{\circ}\text{C}$ line. When the other locations are examined (*Figures 84 to 87 in Appendix B*) it can be seen, that the same description applies for Hradec Kralove and Fichtelberg. In Helsinki, the active shading and ventilative cooling are enough to keep the temperature within the optimum range the whole year. In Marseille, on the other hand, the both systems have to be active almost the whole year, but from June to September, they are not enough to prevent the interior overheating, but the maximum temperature does not reaches higher then $29.1\text{ }^{\circ}\text{C}$.

The last plot in the first part of the simulation, which is the *Figure 26*, shows how the interior temperature is kept between the set minimum and maximum when the ideal heating and cooling systems are activated.



Figure 30 Heating and cooling loads for Scenario 4B in Prague 1960 - 1990

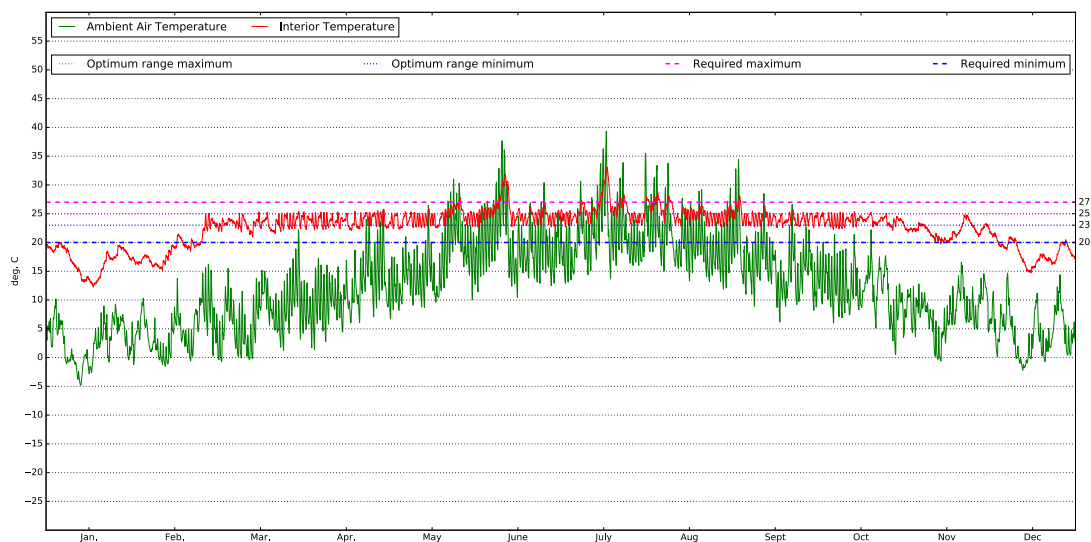


Figure 31 Exterior and interior temperature for Scenario 4A in Prague 2070 - 2100

In the second part of the calculation, the scenarios 1B to 4B were used. The presence of the ideal heating and cooling system allows to calculate the annual heat and cool energy need. The heating and cooling loads were also obtained from the simulation as an hourly output. The interior temperature is regulated by the system between set minimum of 20 °C and maximum of 27 °C. To be able to visually compare the results, the hourly heat and cool loads were plotted.

Scenario 1B for Prague 1960 - 1990 in *Figure 27* shows that the total cooling energy demand is twice lower than the heating energy need, but the cooling is required in larger, less frequent peak loads, while the necessary heating load are much more constant.

The presence and activity of the inhabitants in the house changes the heat and cool energy needs entirely as can be seen in *Figure 28* for Scenario 2B. While the maximum peak loads remain almost the same as in the previous scenario, the annual heat need is

3 Case study

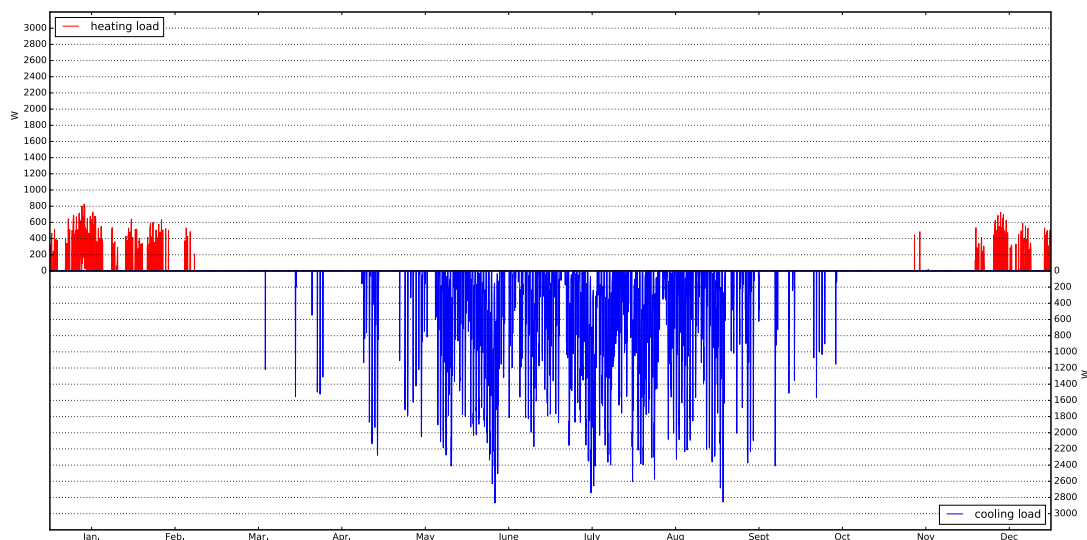


Figure 32 Heating and cooling loads for Scenario 2B in Prague 2070 - 2100

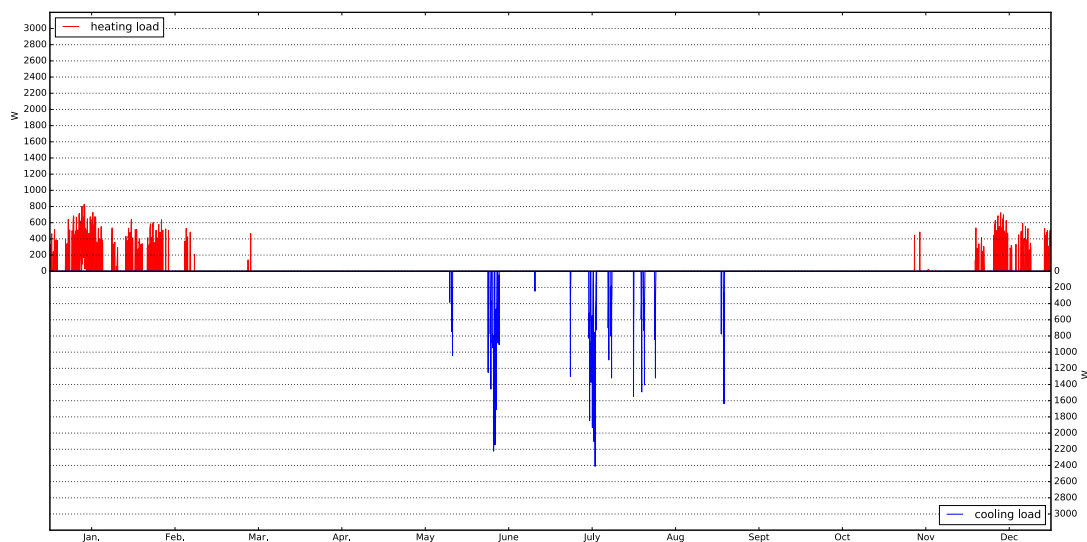


Figure 33 Heating and cooling loads for Scenario 4B in Prague 2070 - 2100

more than 60 % lower and the annual cool need goes up by more than 250 %.

Figure 29 with scenario 3B with recent past in Prague depicts how the effect of good exterior window shading manages to significantly reduce the cooling need. While the peak cooling loads are halved, the annual cool energy need is reduced by 87 %. When the *Figure 29* is compared with the *Figure 24*, it can be noted, that the cooling loads in scenario 3B directly correspond with the warm days in scenario 3A, when the interior temperature reaches over the required maximum temperature of 27 °C.

The scenario 4B for current climate conditions in Prague represented by the period 1960 - 1990 in the *Figure 30* confirms the original design of the house, which aimed for the passive house requirements and no need for cooling system. The specific heating energy demand is therefore 14.37 kWh/m² · a while there is almost no cooling energy demand. That is mainly because of the fact how efficient the ventilative cooling is in a

very small house with little to none thermal mass.

The results for the scenario 4B in other locations (*Figures 89,91,93 and 95 in Appendix B*) allow to actually compare how would the same original design work in other locations. The specific annual heating demand is very similar in Hradec Kralove ($13.1 \text{ kWh/m}^2 \cdot a$), while in Fichtelberg ($18.35 \text{ kWh/m}^2 \cdot a$) it is already above the passive standard ($15.0 \text{ kWh/m}^2 \cdot a$), but in Helsinki ($38.21 \text{ kWh/m}^2 \cdot a$) the need is almost tripled. In Marseille, there is actually no heat energy need at all. And for all the locations, it can be stated that there is either no cooling energy demand (Helsinki and Fichtelberg) or that it is so low (Hradec Kralove and Marseille) that it would not justify the installation of the cooling system in the house.

So far all the plots represented the recent past, but the same figures were generated also for the near and distant future. While no two simulation results are the same, there is no point of comparing all the graphs for all the scenarios in all the locations. The differences from scenario 1A all the way to scenario 4B follow the same pattern in near or in distant future as in recent past, which was described previously. Also as it was already analyzed in *Section 2.2*, the difference in the data between the recent past and the near future is much smaller than when compared to the distant future. It is therefore probably most interesting to compare the changes between the recent past and the distant future on the plots for Scenarios 4A and 4B. Within each time period, the effect of the active shading and ventilative cooling in each location can be best seen when the plots for scenarios 2B and 4B are compared.

Figure 31 depicts scenario 4A in Prague's distant future, and it is apparent that the interior temperature manages to remain much higher in the winter and it almost no longer drops below $15 \text{ }^\circ\text{C}$. The house systems for the overheating prevention (active shading and ventilative cooling) are still quite effective but they have to be in operation already from early March and till late October. Also the days when the ambient air temperature reaches way above the interior temperature and causes it to pass the required maximum of $27 \text{ }^\circ\text{C}$ are much more numerous.

Similarly *Figure 33* shows the system loads of the house in Prague 2070 - 2100 with the ideal heating and cooling systems enabled (scenario 4B). It is quite clear how the heating system reacts to the higher interior temperature with much lower and less frequent heating loads. The cooling loads are still not continuous but rather present in large separated peaks. This is mainly because the cooling source in this scenario is idealized and the maximum peak load is not limited. The *Figure 33* can be also compared with the *Figure 32* to realize the effect of system in scenarios 3 and 4, and how much energy is actually saved on cooling by effective shading and clever use of the ventilation system.

This comparison of scenarios 2B and 4B is very demonstrative in other locations as well. *Figures 96 and 97 in Appendix B* for Helsinki show, that even in the coldest location of the dataset, the specific annual cooling demand would be noticeable - $10.83 \text{ kWh/m}^2 \cdot a$ in the scenario 2B, but in scenario 4B there is actually none. The same two scenarios in distant future of Marseille (*Figures 102 and 103 in Appendix B*) show the decrease in the annual cooling energy need by 72%.

The annual values of the simulation results were organized into *Tables 1 to 4*. Each

3 Case study

table represents one simulation scenario (*Table 1* for scenario 1 and so on). For the simulation scenario part A the table displays the minimum and maximum interior temperature that is reached inside the house in each location and time period, when no heating or cooling system are present. The second part of each table corresponds with the part B of the simulation scenarios and shows the specific annual heat need necessary to raise the annual minimum interior temperature to 20 °C and also the specific annual cooling energy demand necessary to keep the annual maximum interior temperature at 27 °C. The titles of the table columns stand for:

$t_{int_{min}}$... annual minimum interior temperature - [°]
 $t_{int_{max}}$... annual maximum interior temperature - [°]
 Q_{hs} ... specific annual heat need - [kWh/m² · a]
 Q_{cs} ... specific annual cooling energy demand - [kWh/m² · a]
TP1 ... time period 1960 - 1990
TP2 ... time period 2020 - 2070
TP3 ... time period 2070 - 2100

The third part of the calculation uses some of the scenarios from previous calculations and performs the parameter optimization for the glazing value and the azimuth. It was already mentioned in the *Section 3.4.2* how the result of each simulation was processed into a cost function value. For each location in each time period, the simulation had to be run 525 times. To be able to visually compare the results, a heat map with 21 x 25 values was generated using the calculated 525 values of the cost function. The values for glazing changing from 0 to 100 % are on the y axis and the azimuth values changing from -180 ° to +180 ° are on the x axis. For the values of glazing or azimuth between those that were used in the simulation (for example glazing 32.1 % or azimuth 123°), the values of the cost function were interpolated using 'spline16' method, already available in the Python's matplotlib package, that was used to generate the heat map. The color bar below each heat map shows how the colors are scaled between the lowest and the highest cost function values.

The heat map plots were first generated for all the location and time periods in scenario 4B with the heating and cooling weights set to previously devised optimization scenarios. *Figure 34* shows the result for Prague 1960 - 1990 with the weight set to 100 % for heating and 0 % for cooling. It can be clearly seen that if the cooling energy demand is not an issue, the house designed with approximately 70 % glazing in the south wall achieved the lowest heating energy need. The worst performance, which is in this case represented by the highest heat need, would have the house with a fully glazed north facade.

The opposite weight set (100 % for cooling and 0 % for heating) for the same scenario 4B in recent past in Prague is depicted in *Figure 35*. As can be seen, when the concerns are reversed, the minimum cooling energy demand was achieved for either the house with no windows, or the house with the windows facing north while the highest demand would be met, when fully glazed facade faces south.

In the simulations for scenario 4B (results for glazing 35 % and azimuth 0 ° can be checked in *Table 4*), the shading and active ventilation systems are very effective and significantly reduce the cooling energy demand, which causes all the optimization results, where the weight for heating is not zero, to be almost identical to the result in

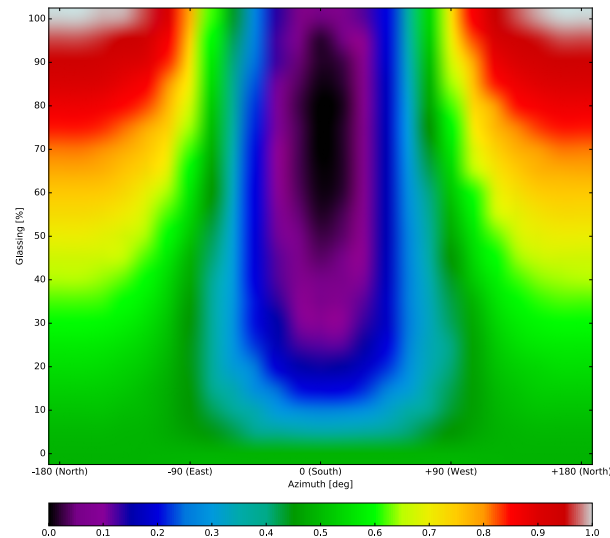


Figure 34 Parameter optimization results for Scenario 4B in Prague 1960 - 1990 with 1.0 weight for heating and 0.0 weight for cooling

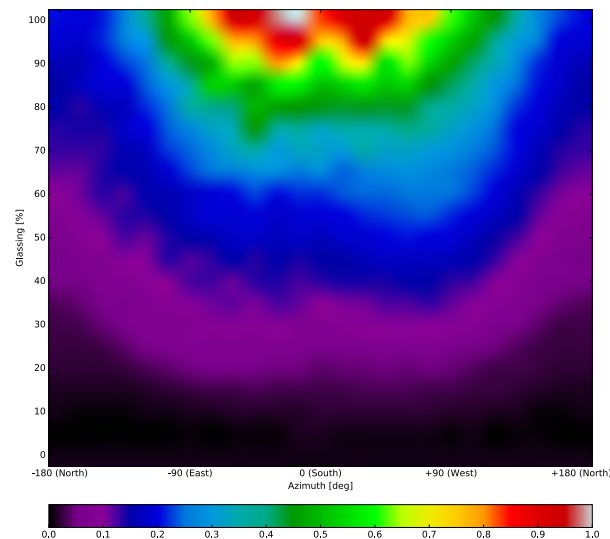


Figure 35 Parameter optimization results for Scenario 4B in Prague 1960 - 1990 with 0.0 weight for heating and 1.0 weight for cooling

Figure 34. Similarly in Marseille the heating energy need is so close to zero in all the time periods in scenario 4B (but also 2B and 3B), and therefore all the optimization results for Marseille where the weight for cooling is not set to zero are almost identical to the result in *Figure 35*.

The only exception where the results are not totally one sided was found for the scenario 4B in Prague in 2070 - 2100 (*Figures 105 to 109 in Appendix B*), where the heating and cooling needs are quite evenly balanced and therefore it can be observed how the cost function results gradually change with the predefined weights. It can be observed, that in this scenario the optimum glazing changes between 20 and 60 % based on the weight set used.

3 Case study

	Scenario 1A						Scenario 1B					
	$t_{int_{min}} [^{\circ}C]$			$t_{int_{max}} [^{\circ}C]$			$Q_{hs} [kWh/m^2 \cdot a]$			$Q_{cs} [kWh/m^2 \cdot a]$		
	TP1	TP2	TP3	TP1	TP2	TP3	TP1	TP2	TP3	TP1	TP2	TP3
Helsinki	-7.4	-4.3	-1.6	32.2	32.1	33.4	70.58	62.35	54.39	1.89	3.04	2.93
Fichtelberg	-2.8	0.8	2.8	30.9	32.1	34.8	45.98	41.18	35.85	2.36	3.37	5.70
Hradec	1.3	1.2	2.8	34.3	37.0	38.2	36.31	32.31	27.26	7.69	11.79	14.19
Prague	-0.3	2.6	4.6	34.1	34.3	39.3	36.88	31.15	26.67	8.34	10.28	14.90
Marseille	12.8	13.2	16.8	37.5	40.0	43.6	7.04	6.65	2.35	20.36	26.13	38.40

Table 1 The annual simulation results in scenarios 1A and 1B

	Scenario 2A						Scenario 2B					
	$t_{int_{min}} [^{\circ}C]$			$t_{int_{max}} [^{\circ}C]$			$Q_{hs} [kWh/m^2 \cdot a]$			$Q_{cs} [kWh/m^2 \cdot a]$		
	TP1	TP2	TP3	TP1	TP2	TP3	TP1	TP2	TP3	TP1	TP2	TP3
Helsinki	0.5	3.4	6.3	34.5	35.1	36.4	38.15	30.16	24.11	6.53	9.79	10.83
Fichtelberg	5.1	8.2	9.9	34.2	34.6	37.6	18.08	15.19	10.91	9.32	12.73	16.00
Hradec	8.7	8.9	10.6	37.7	39.8	41.1	13.03	10.63	6.91	20.24	26.71	32.85
Prague	7.6	10.5	12.1	37.2	37.1	42.7	14.28	8.43	6.02	21.35	25.57	32.55
Marseille	19.8	19.8	20.0	40.2	42.7	46.6	0.01	0.02	0.00	42.86	52.20	70.54

Table 2 The annual simulation results in scenarios 2A and 2B

	Scenario 3A						Scenario 3B					
	$t_{int_{min}} [^{\circ}C]$			$t_{int_{max}} [^{\circ}C]$			$Q_{hs} [kWh/m^2 \cdot a]$			$Q_{cs} [kWh/m^2 \cdot a]$		
	TP1	TP2	TP3	TP1	TP2	TP3	TP1	TP2	TP3	TP1	TP2	TP3
Helsinki	0.5	3.4	6.3	26.2	27.4	28.1	38.16	30.17	24.13	0.00	0.08	0.16
Fichtelberg	5.1	8.2	9.9	29.3	29.4	30.5	18.11	15.19	10.92	0.67	0.40	2.31
Hradec	8.7	8.9	10.6	31.3	32.3	34.0	13.04	10.64	6.92	2.47	5.10	8.65
Prague	7.6	10.5	12.1	31.0	31.4	36.5	14.28	8.44	6.02	2.79	3.60	10.04
Marseille	19.8	19.8	20.0	34.0	36.1	40.7	0.01	0.02	0.00	13.68	19.50	33.18

Table 3 The annual simulation results in scenarios 3A and 3B

	Scenario 4A						Scenario 4B					
	$t_{int_{min}} [^{\circ}C]$			$t_{int_{max}} [^{\circ}C]$			$Q_{hs} [kWh/m^2 \cdot a]$			$Q_{cs} [kWh/m^2 \cdot a]$		
	TP1	TP2	TP3	TP1	TP2	TP3	TP1	TP2	TP3	TP1	TP2	TP3
Helsinki	0.5	3.4	6.3	25.5	25.9	25.8	38.21	30.21	24.19	0.00	0.00	0.00
Fichtelberg	5.1	8.2	9.9	26.6	26.8	27.6	18.35	15.25	11.01	0.00	0.00	0.06
Hradec	8.7	8.9	10.6	28.4	28.0	30.3	13.10	10.70	6.92	0.17	0.24	1.78
Prague	7.6	10.5	12.1	27.9	28.5	33.4	14.37	8.46	6.05	0.15	0.26	3.02
Marseille	19.8	19.5	20.0	29.3	31.3	36.0	0.01	0.02	0.00	1.56	6.15	19.50

Table 4 The annual simulation results in scenarios 4A and 4B

3.6 Discussion

Based on the weather data and climate change analysis, it was expected that the heating demand would become much lower or even non-existent in some locations. This was confirmed by the simulation results, where the annual heat energy need actually dropped by 40 - 65 % in each location (except for Marseille where the heating demand was already zero in the recent past). That is even higher decrease than what was originally suggested by the heat degree hours analysis.

It was also expected that the cooling energy demand would become much more prevailing or that the house would experience problems with overheating without any cooling system. This was actually disproved by the results and the cooling energy need did not increase significantly and while in Marseille 2070 to 2100 the specific cooling energy need reaches $19.5 \text{ kWh/m}^2 \cdot \text{a}$ it would be still considered quite energy efficient, especially when the original design includes photovoltaic panels seamlessly integrated into the south-facing part of the gable roof. Because the electricity production from photovoltaic panels correlates highly with the cooling load, it might be possible to be able to cover the whole cooling energy consumption from house's own renewable production, especially in Marseille, where the potential for the solar energy use is the highest.

In Helsinki and Fichtelberg, the cooling energy demand would still remain zero, even in distant future, and in Prague and Hradec the actual specific cooling need would remain between 1.5 and $3.0 \text{ kWh/m}^2 \cdot \text{a}$, which basically means 2 - 3 weeks in the summer, when the interior temperature actually reaches above $30 \text{ }^\circ\text{C}$ without cooling system. While for some people that might justify the necessity for cooling system, others may just get used to the warmer climate and the building code might change accordingly. It would most definitely not cause every house to be equipped with a cooling unit.

4 Conclusion

The calculation model was set up in a way that tries to describe all processes in the house as realistically as possible, including the human behavior. The precision of the simulation results were tested against other software and the functionality of the calculation model was thus validated. Nevertheless, there are still many calculations that are only simplified and can be further improved.

At this point of the development, all the thermal calculations are done within one node represented by the environment class and all the thermal mass of the house is also represented only by one value. More complex model could be devised by splitting the environment class into multiple subclasses. There would be one subclass for each different construction of the exterior envelope with defined layers and their physical parameters. The model would be simulating a temperature behavior inside each subclass and calculating the interior temperature based on the surface temperatures of the subclasses. Also the calculation of the exterior surface temperature could include the effects of the short and long wave radiation and the wind exposure, rather than using only the ambient air temperature.

The results showed very good functionality of the model house. But it was especially apparent, that in every single location the interior environment would suffer from overheating if the active shading and ventilative cooling systems were not so effective. The high efficiency of those systems should be put to further examination. Both active and passive window shading is represented only by estimated values of average shading factors.

Factor $f_{sh} = 0.72$ [-] for average passive shading should represent combined passive shading effects of window's own reveal and overhead, surrounding environment, glass smear, and so on. It is only estimated value, that would be different in every situation and would also change with the movement of the sun in the sky. The used f_{sh} value might have been too low and improved calculations can be done in the future to make it more precise.

Active shading, which is in the house design represented by semi translucent white textile, that would automatically roll out on the exterior side of the window, is expected to add another shading factor of 0.2 (reducing the interior solar gains by additional 80 %). While this value is provided by the manufacturer, it was obvious in the simulation result plots for scenarios 3A and 4A, that the shading textile would have to remain rolled out more than half of the year to have desired effect. Because the textile is only semi transparent and semi translucent, it would definitely cause the house user discomfort and might be expected that the inhabitants would try to deactivate the shading system most of the time, despite the risks of interior overheating.

Active use of ventilation system for ventilative cooling proved to be even more effective in reducing the interior temperature than the active shading by the results of the sim-

ulation scenario 4A. The ventilative system was set up to simulate a situation where people would open the small window in the bathroom in the back facade and the larger windows in the front facade to increase the infiltration by cross window ventilation and it was estimated that three air volume changes per hour would be thus achieved. This value might have been estimated too high and also it might not be able to achieve it consistently, because outside wind direction and speed might influence it significantly.

When the occupants are not present to open the windows, system would use maximum fan power in ventilation unit, which would also cause the electric consumption to raise equivalently. The ventilated air contains approximately 33 Wh/K per ACPH. The ventilative cooling system uses the ventilation system to raise the ACPH by 2.0 and the fan consumption by 100 W . If the system were to achieve at least the CoP of 1.0 (therefore invest 100 Wh of electricity to get rid of 200 Wh of excess heat) the ambient air temperature would have to be at least $3 \text{ }^\circ\text{C}$ lower than the interior air temperature. And while this prerequisite was set in the simulation, there are still two issues to be faced. If the electricity to run the fan is not produced in the house by any possible RES and therefore has to be paid for, CoP of 1.0 is really very inefficient and the users might either choose to disable the ventilative cooling system or/and install other cooling system, that might have much higher CoP.

Other issue with the efficiency of the ventilative cooling is that the actual air temperature on the inlet to the house might be actually much higher than the ambient air temperature in the dataset. It depends on the location of the inlet, possible irradiance or shading of the place, the wind, presence of vegetation in near surrounding and so on. This is unfortunately hard to predict and calculate. Some possible solution, that would actually even increase the CoP of the system might include having an earth-air heat exchanger that would precool the air in the summer. Other option is to use the water drawn from the well that would be used to water the garden and use it first in water-air heat exchanger to cool the air. The plants would even benefit from the higher water temperature. But those options are very situational and cannot be generally available every time.

The parameter optimization showed that the model house was originally designed quite correctly with the glazing of 35% and facing south. That would apply also in other locations with similar or colder climate than in Prague and even in distant future. But when moved to a warmer location, like Marseille, where the heating energy demand is basically non-existent, it might be indeed effective way of reducing the cooling energy demand to turn the house around, and let the windows face north and place the photovoltaic panels on the other side of the gable roof, to still face south.

Bibliography

- [1] et al Cook J. “Consensus on consensus: a synthesis of consensus estimates on human-caused global warming”. In: *Environmental Research Letters* (2016).
- [2] 2018. URL: <https://www.remo-rcm.de>.
- [3] D. Jacob. “A note to the simulation of the annual and inter-annual variability of the water budget over the Baltic Sea drainage basin”. In: *Meteorology and Atmospheric Physics* 77 (1-4 2001), pp. 61–73.
- [4] 2018. URL: <https://www.remo-rcm.de/060230/index.php.en>.
- [5] 2018. URL: https://www.climateforculture.eu/index.php?inhalt=team.partners#partner_21.
- [6] 2018. URL: <https://www.climateforculture.eu/index.php?inhalt=project.climatechange>.
- [7] 2018. URL: <https://www.eea.europa.eu/data-and-maps/indicators/heating-degree-days>.
- [8] 2018. URL: <http://www.meteonorm.com/>.

Appendix A

Weather Data Analysis - Additional Figures

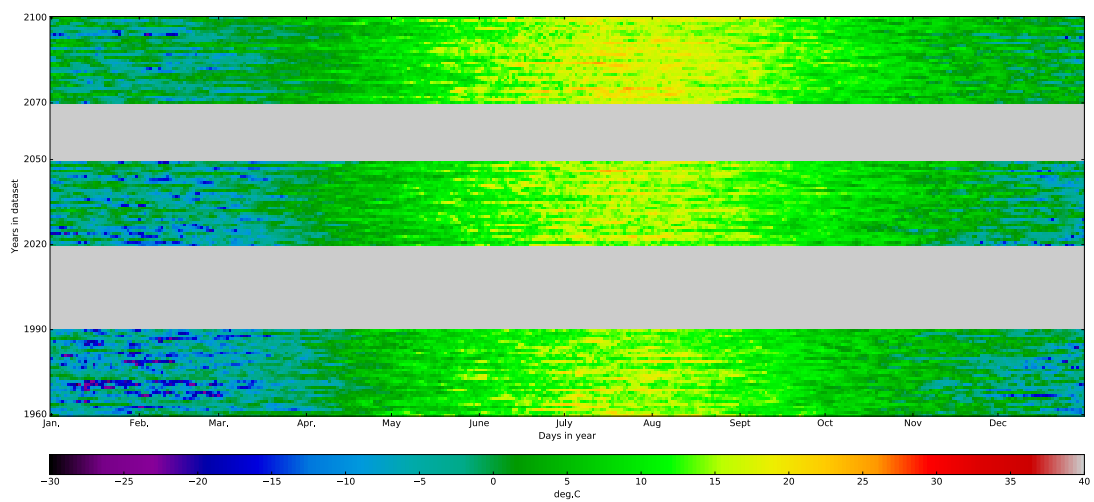


Figure 36 Daily average temperatures in Helsinki

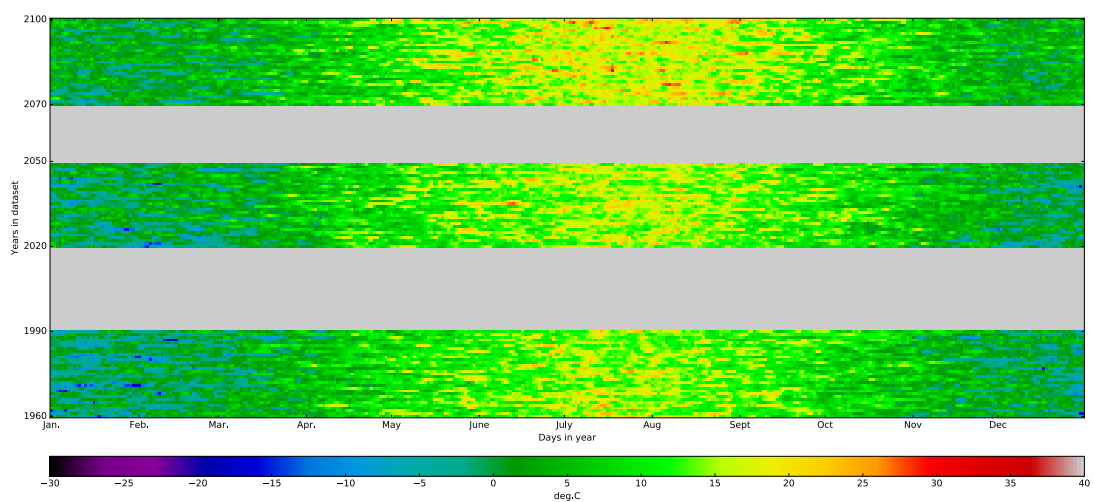


Figure 37 Daily average temperatures in Fichtelberg

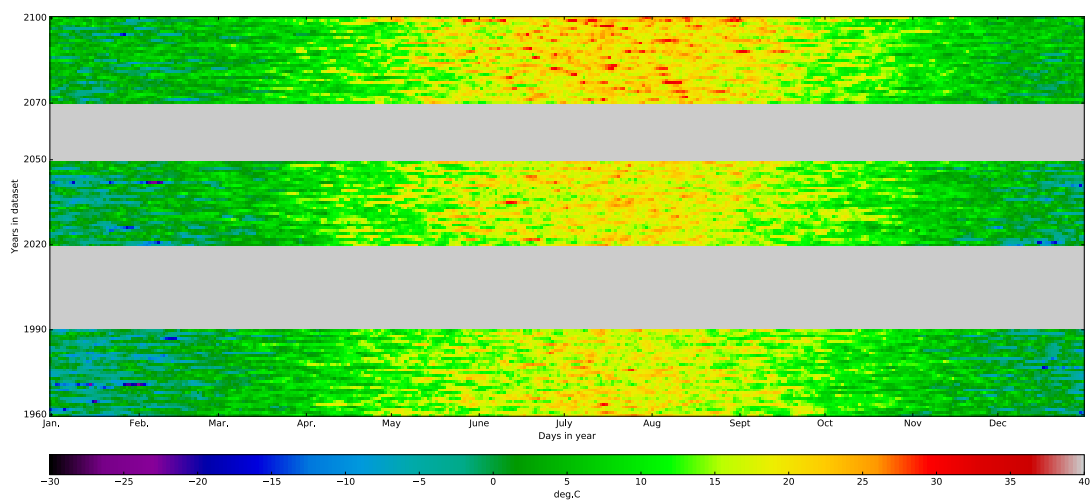


Figure 38 Daily average temperatures in Hradec

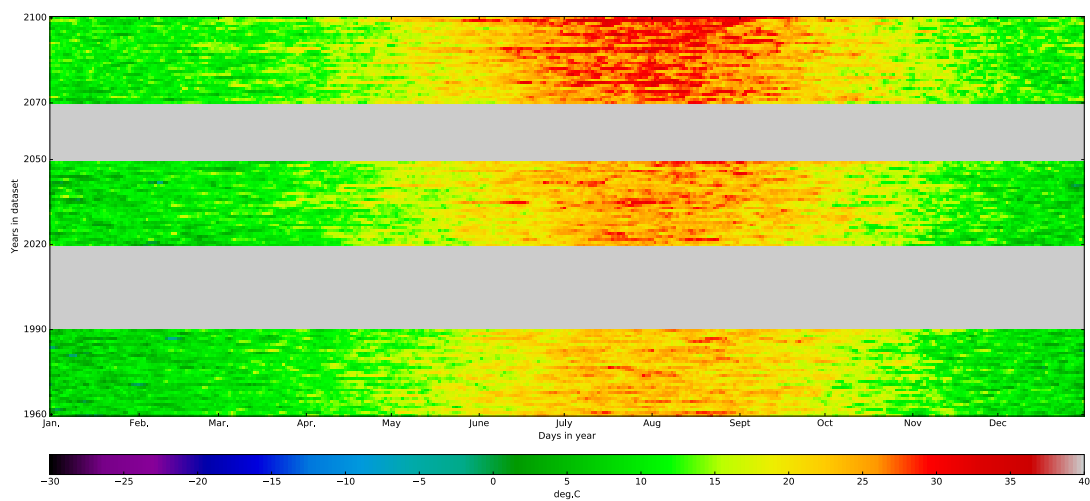


Figure 39 Daily average temperatures in Marseille

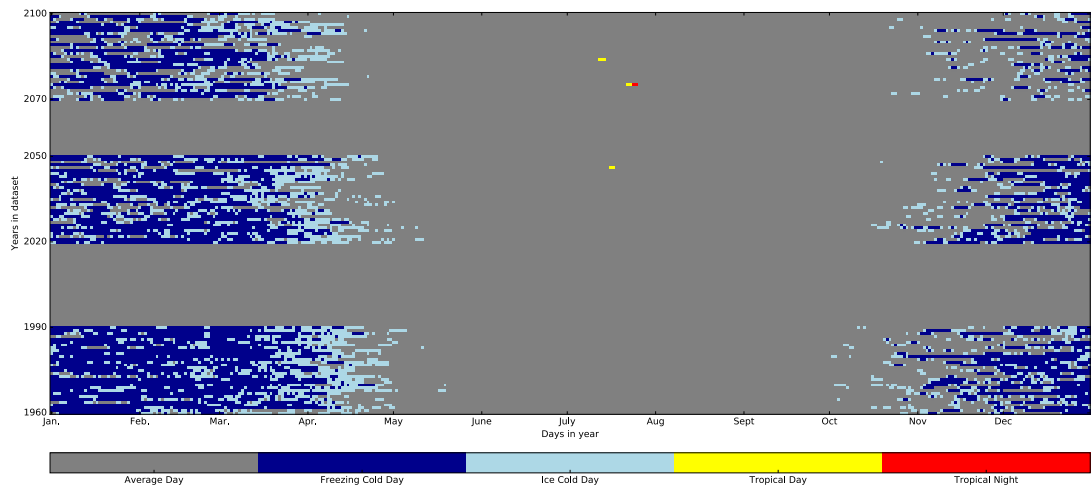


Figure 40 Atypically hot and cold days in Helsinki

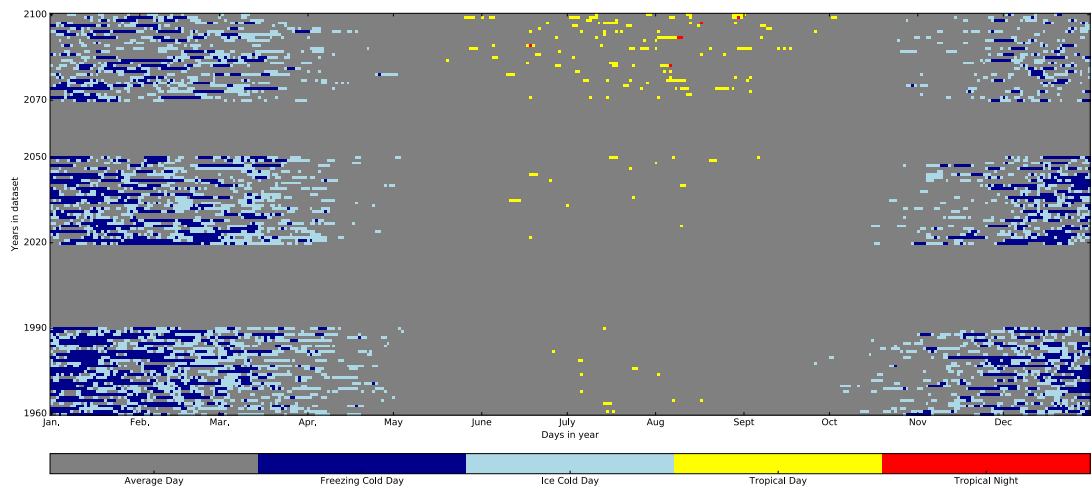


Figure 41 Atypically hot and cold days in Fichtelberg

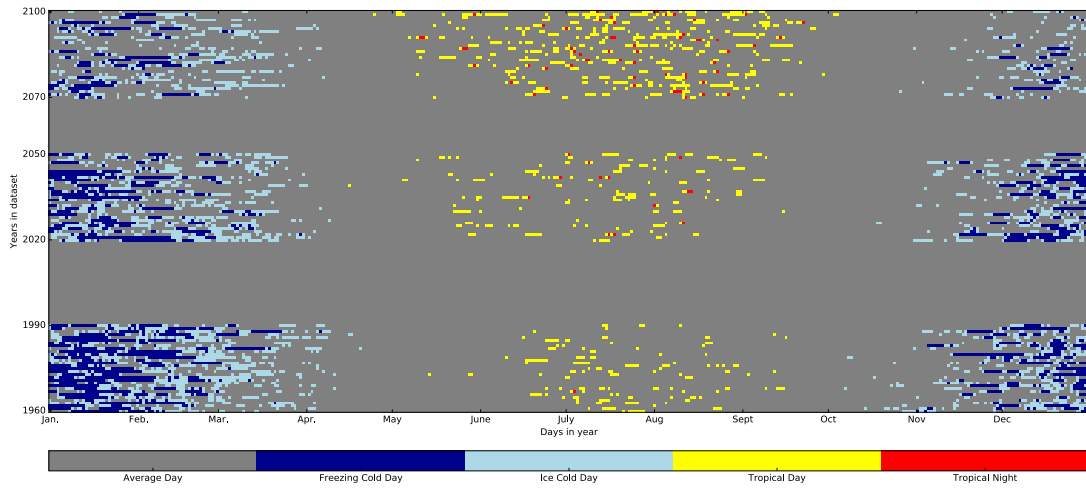


Figure 42 Atypically hot and cold days in Hradec

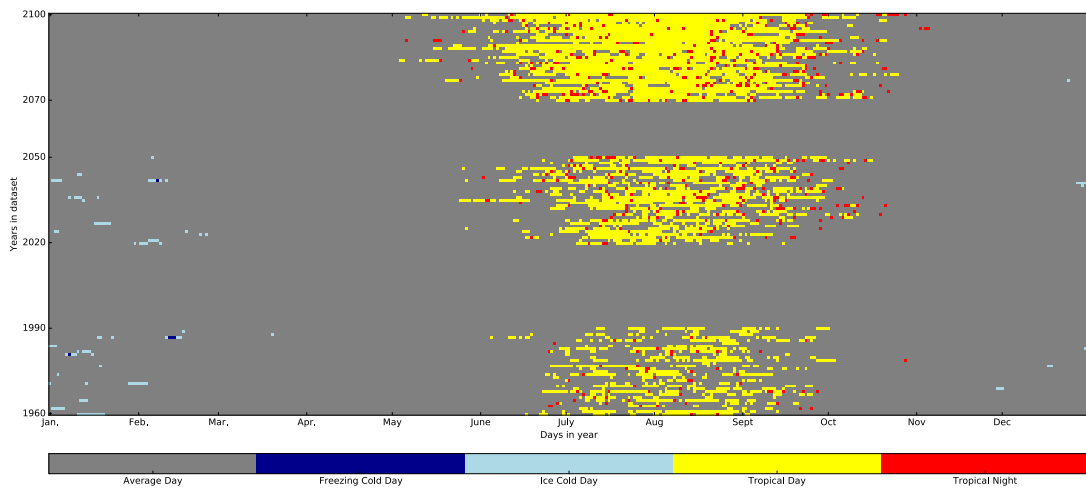


Figure 43 Atypically hot and cold days in Marseille

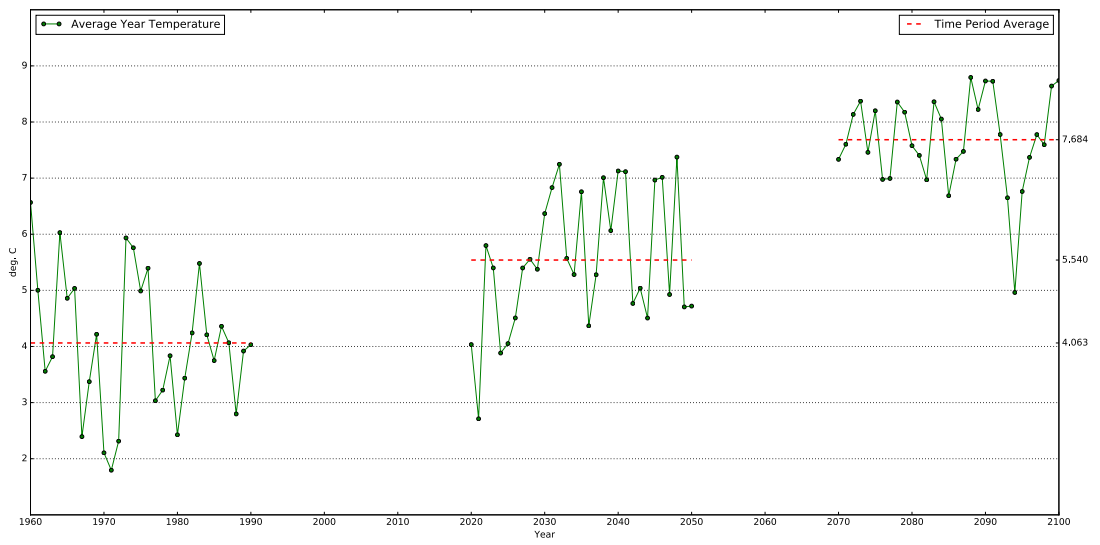


Figure 44 Annual average temperatures in Helsinki

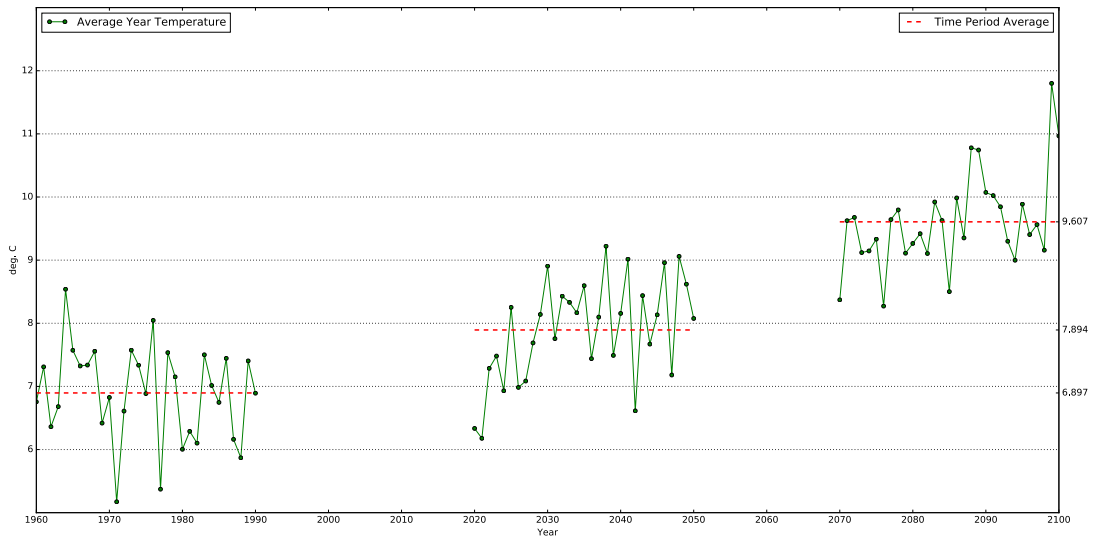


Figure 45 Annual average temperatures in Fichtelberg

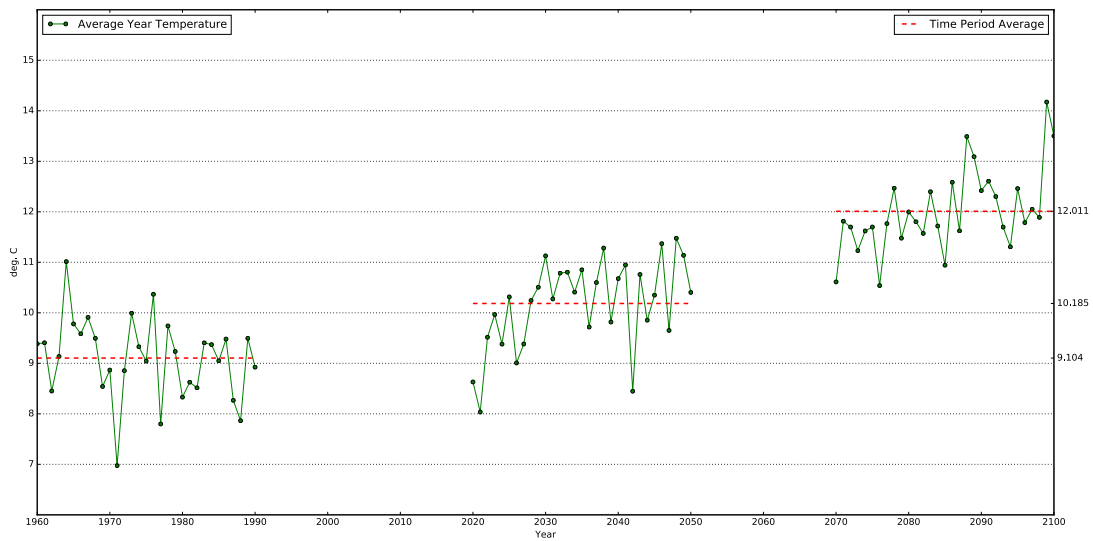


Figure 46 Annual average temperatures in Hradec

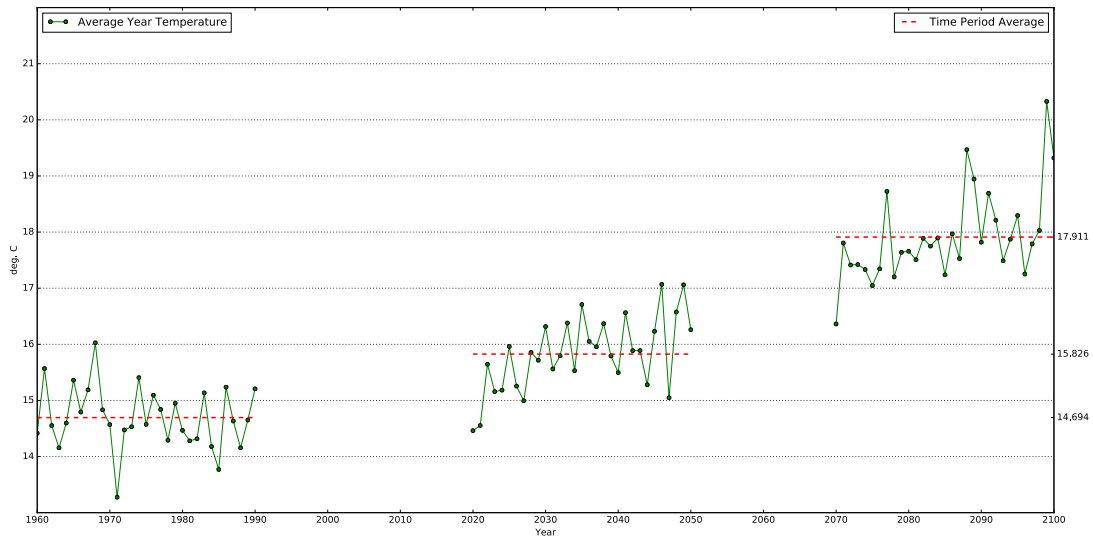


Figure 47 Annual average temperatures in Marseille

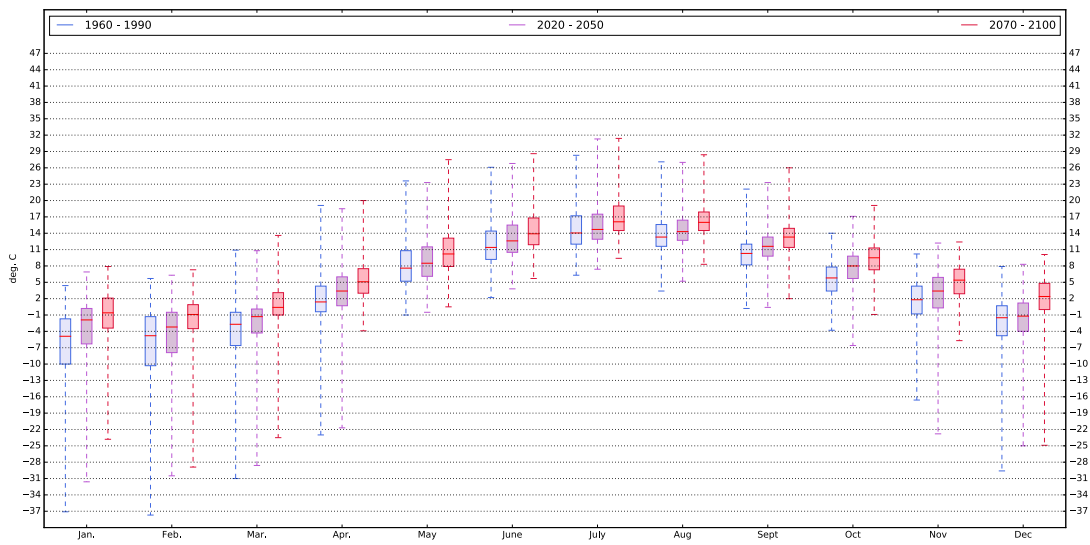


Figure 48 Monthly box-plot for temperatures in all time periods in Helsinki

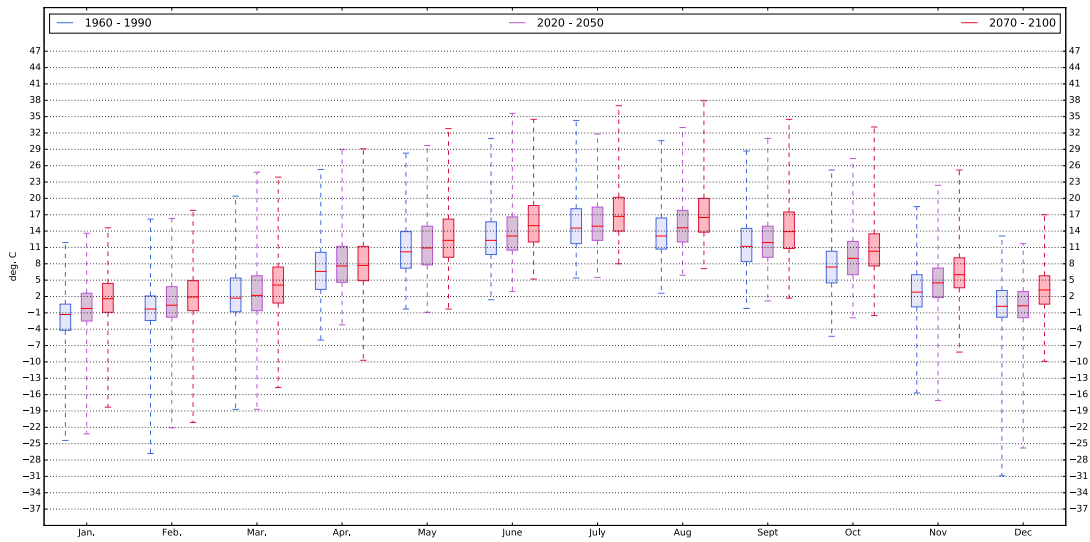


Figure 49 Monthly box-plot for temperatures in all time periods in Fichtelberg

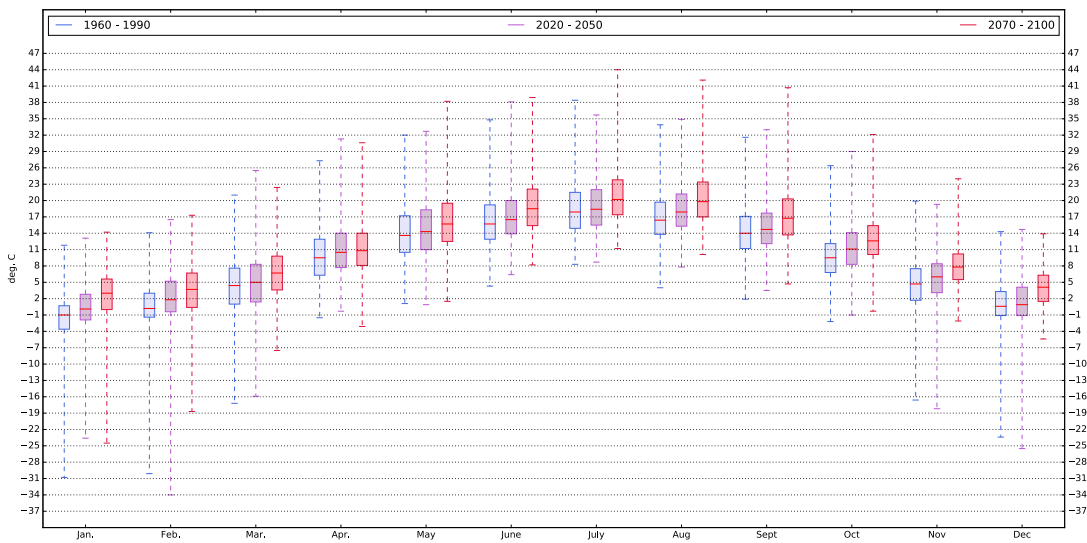


Figure 50 Monthly box-plot for temperatures in all time periods in Hradec

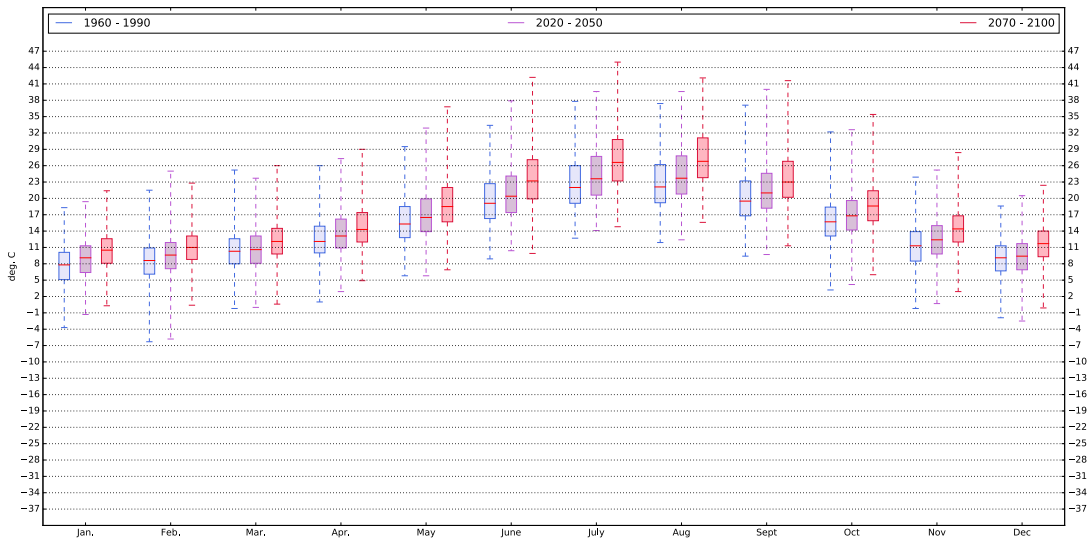


Figure 51 Monthly box-plot for temperatures in all time periods in Marseille

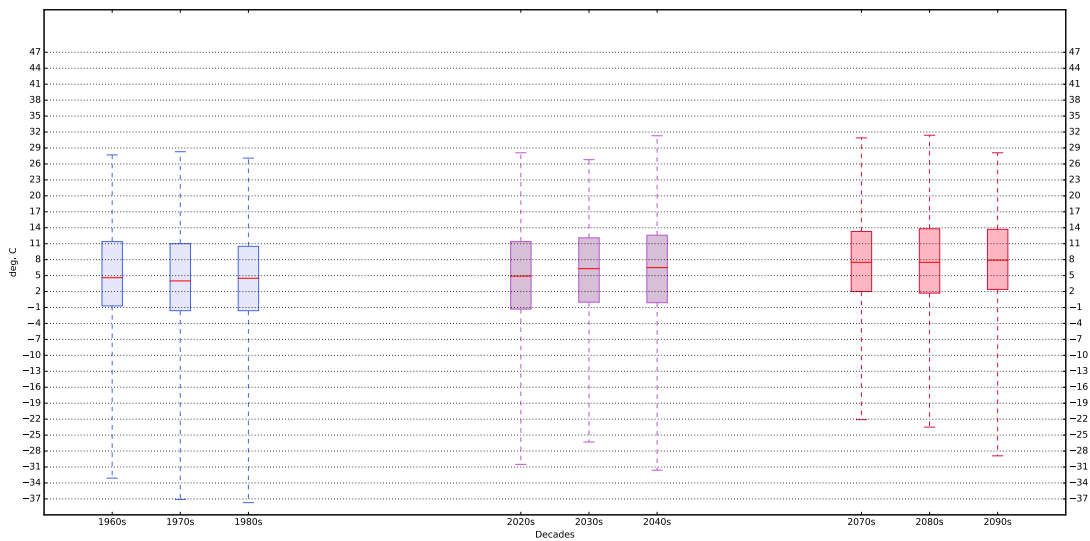


Figure 52 Box-plot for temperatures in decades in Helsinki

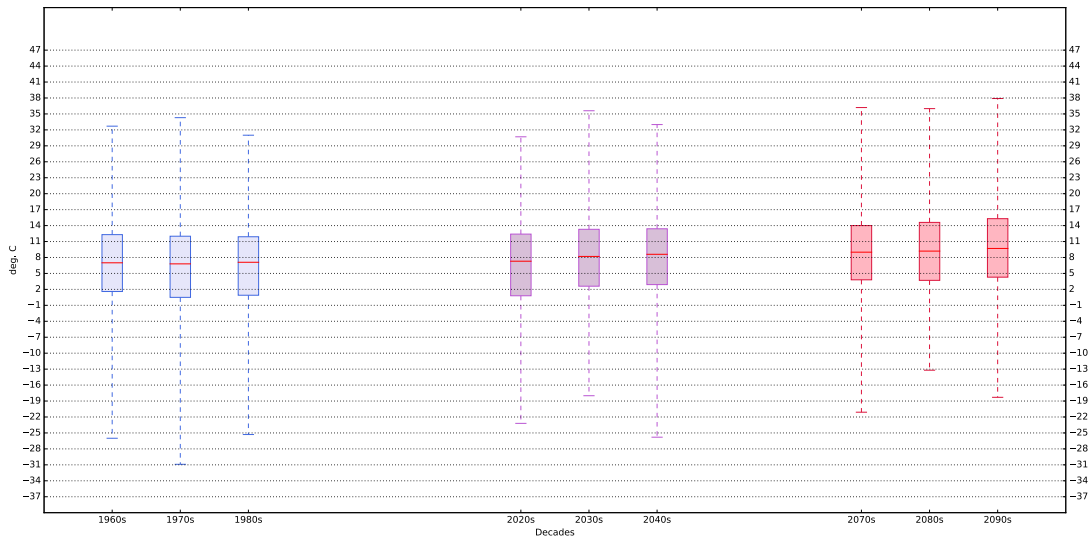


Figure 53 Box-plot for temperatures in decades in Fichtelberg

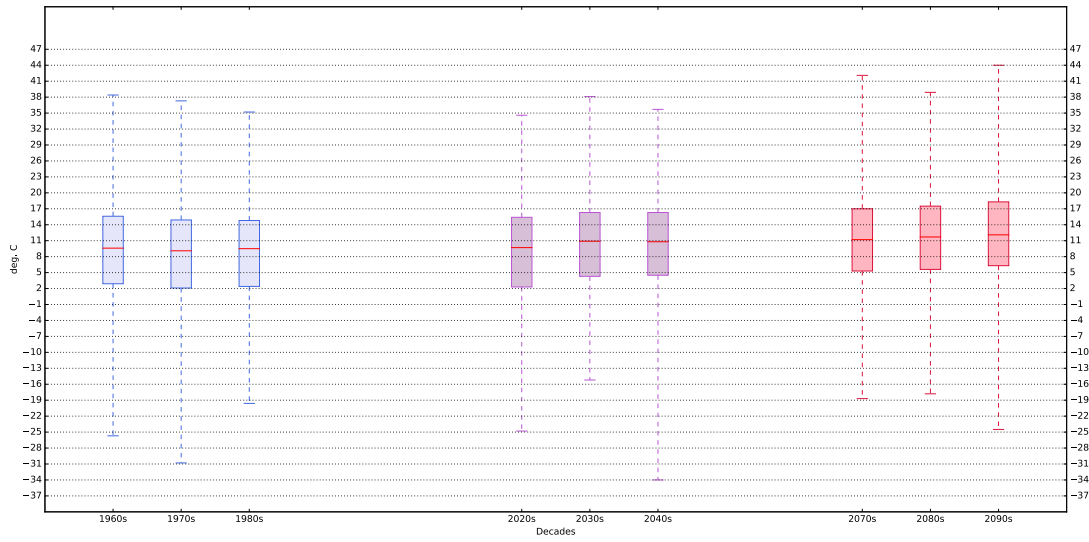


Figure 54 Box-plot for temperatures in decades in Hradec

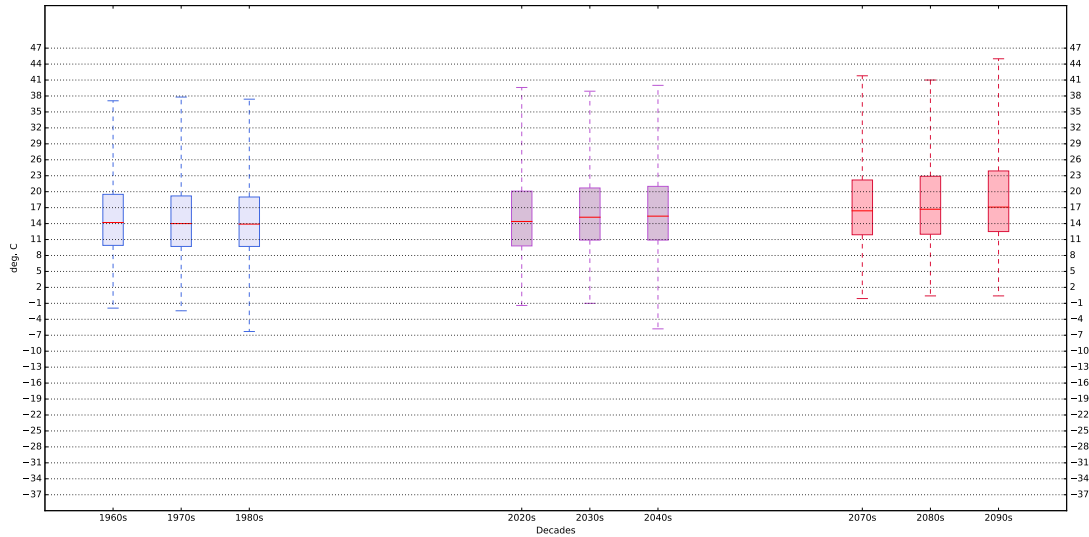


Figure 55 Box-plot for temperatures in decades in Marseille

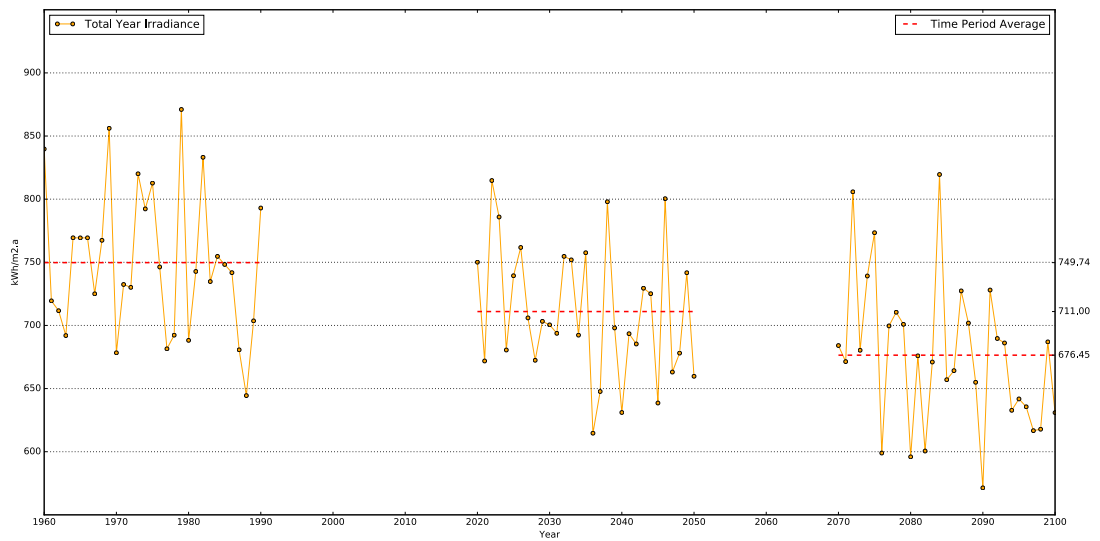


Figure 56 Annual summary of global irradiance in Helsinki

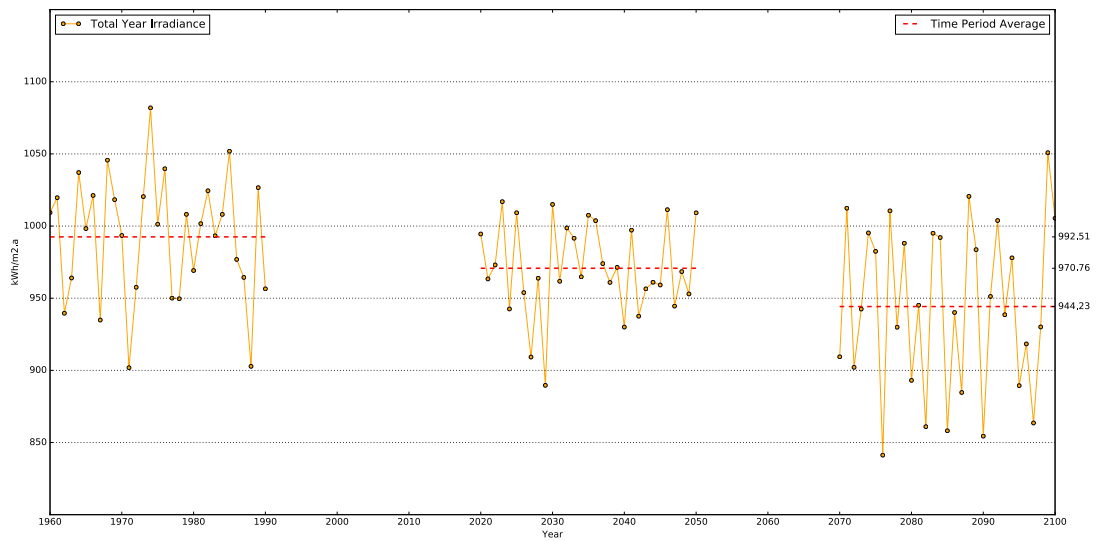


Figure 57 Annual summary of global irradiance in Fichtelberg

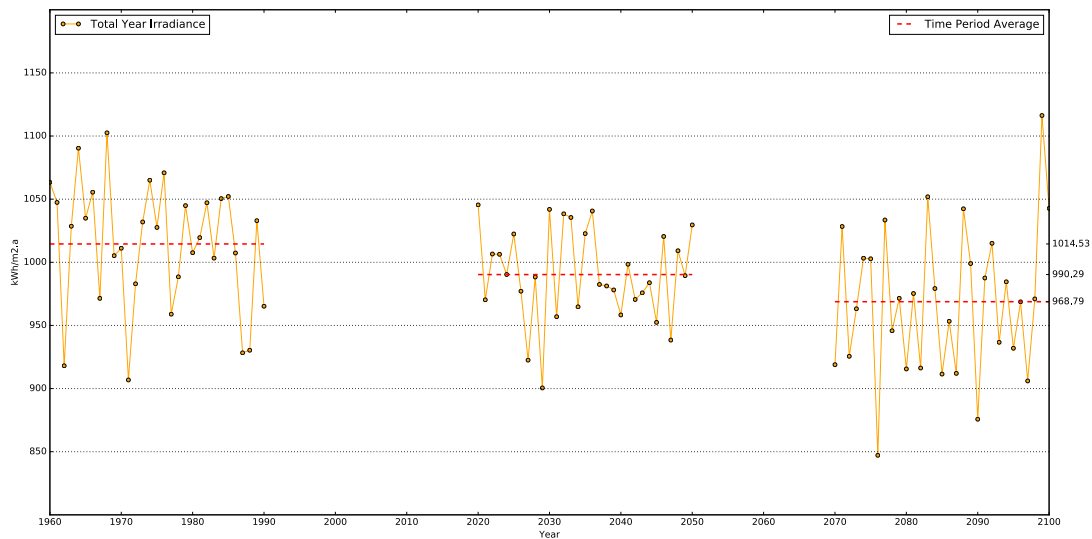


Figure 58 Annual summary of global irradiance in Hradec

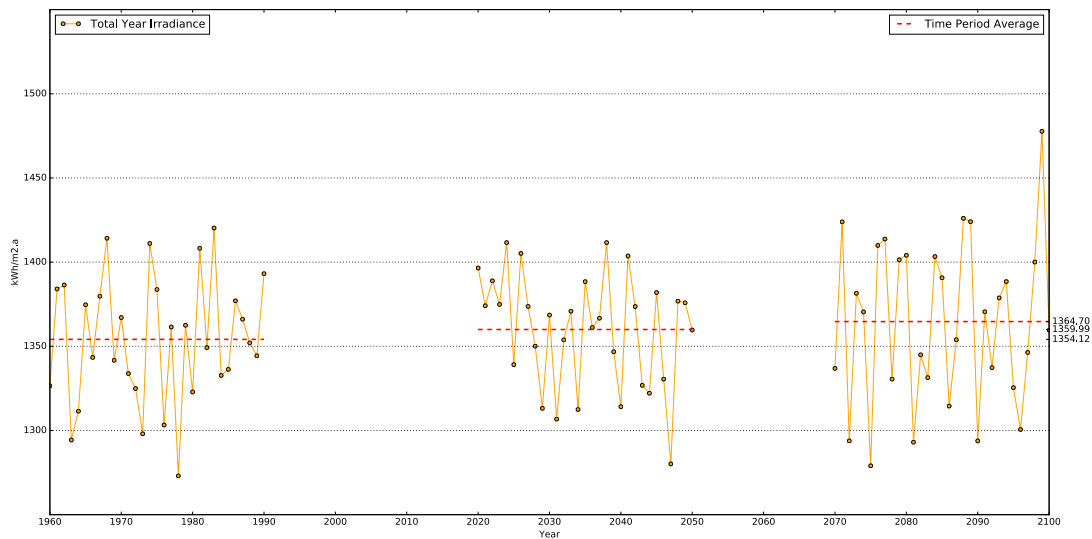


Figure 59 Annual summary of global irradiance in Marseille

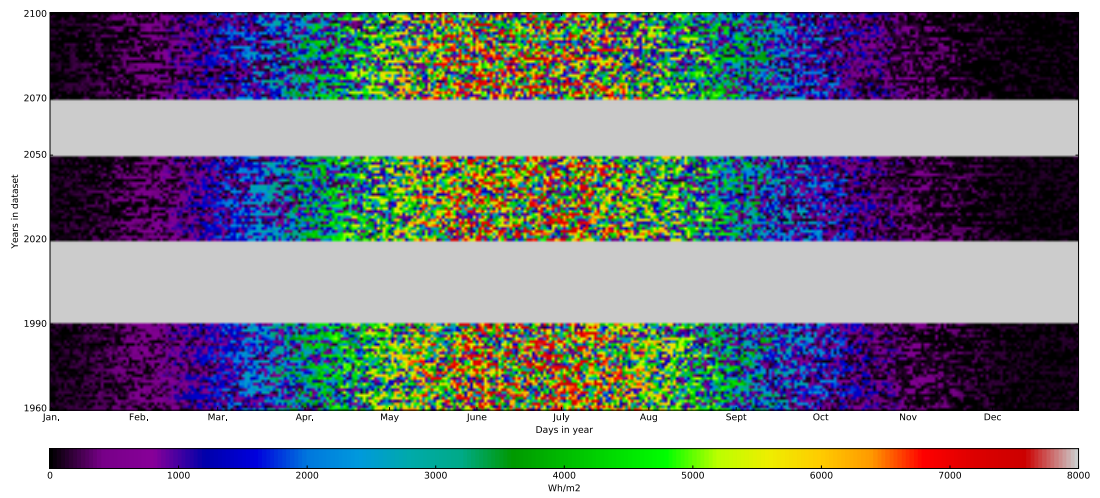


Figure 60 Daily summary of global irradiance in Helsinki

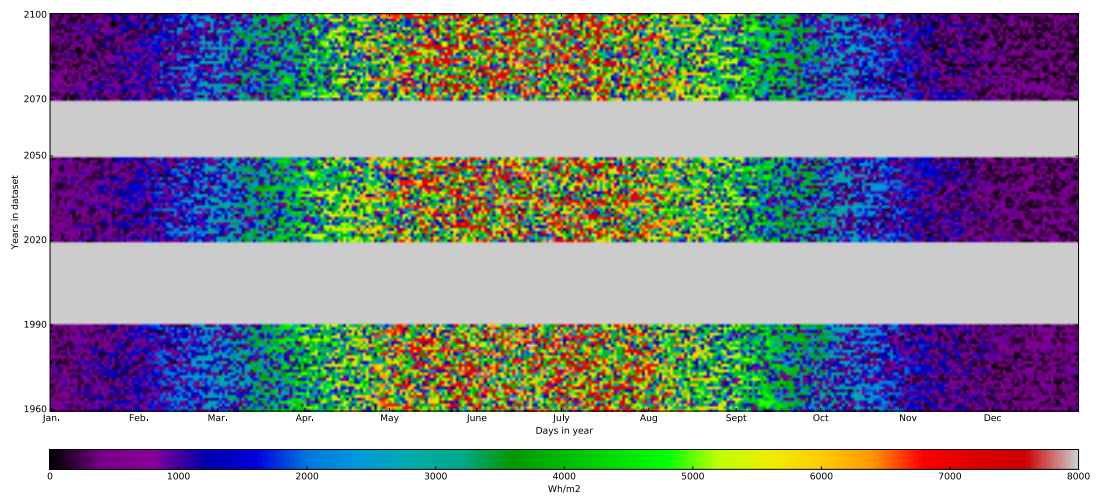


Figure 61 Daily summary of global irradiance in Fichtelberg

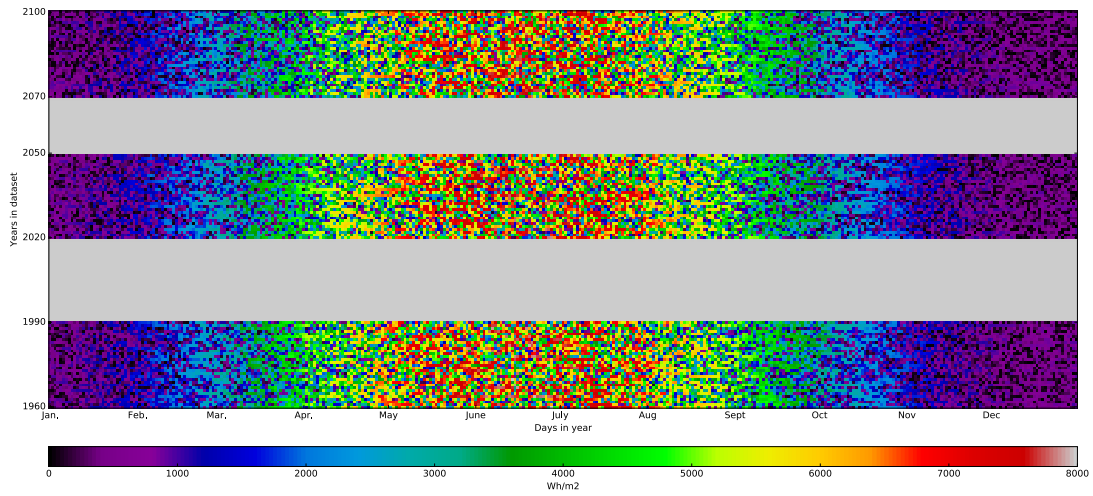


Figure 62 Daily summary of global irradiance in Hradec

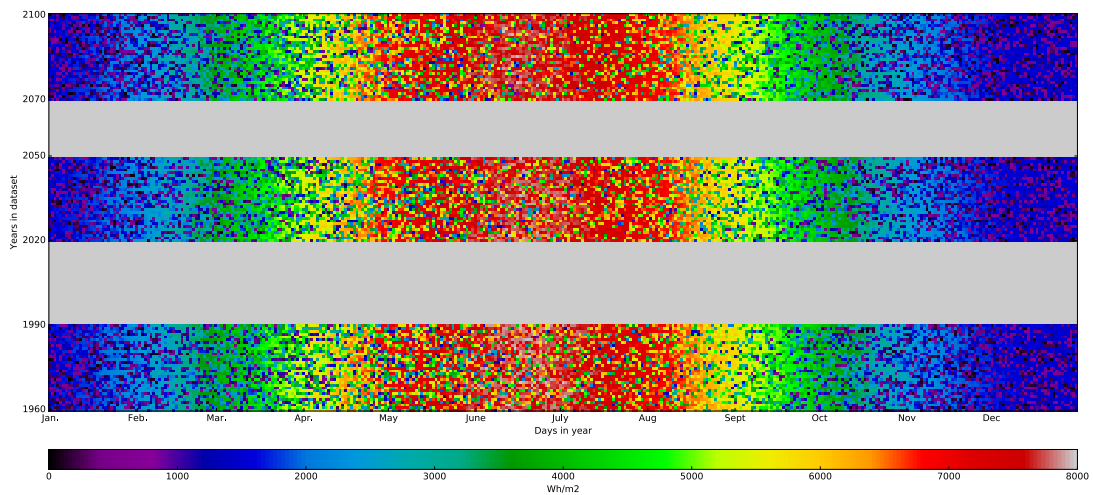


Figure 63 Daily summary of global irradiance in Marseille

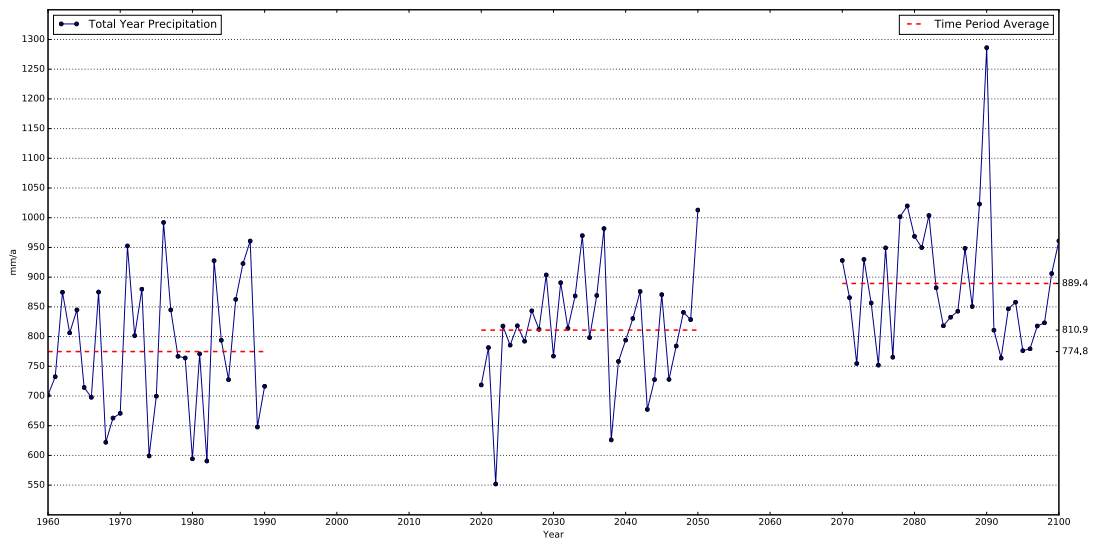


Figure 64 Annual precipitation in Helsinki

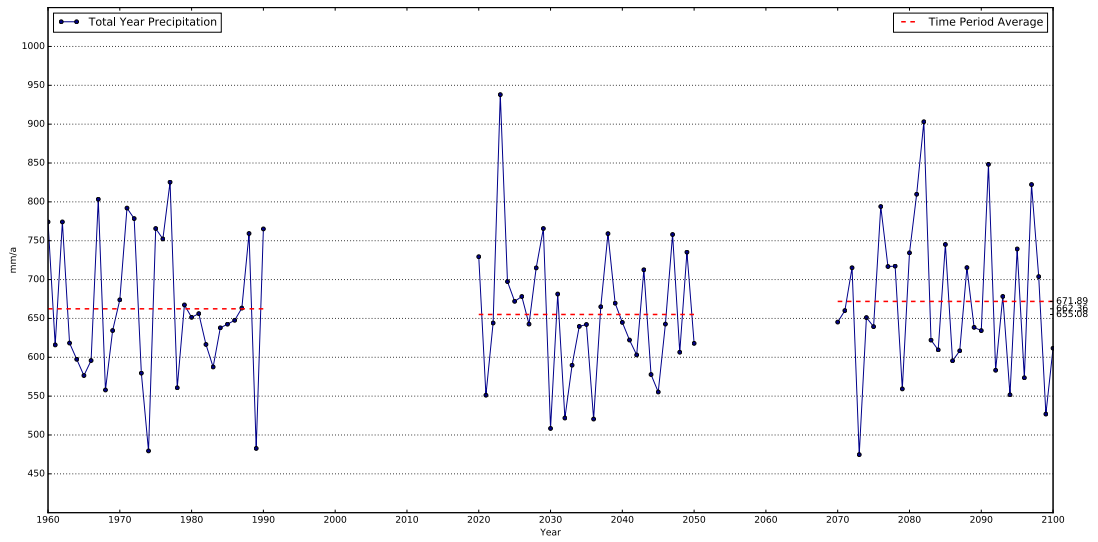


Figure 65 Annual precipitation in Fichtelberg

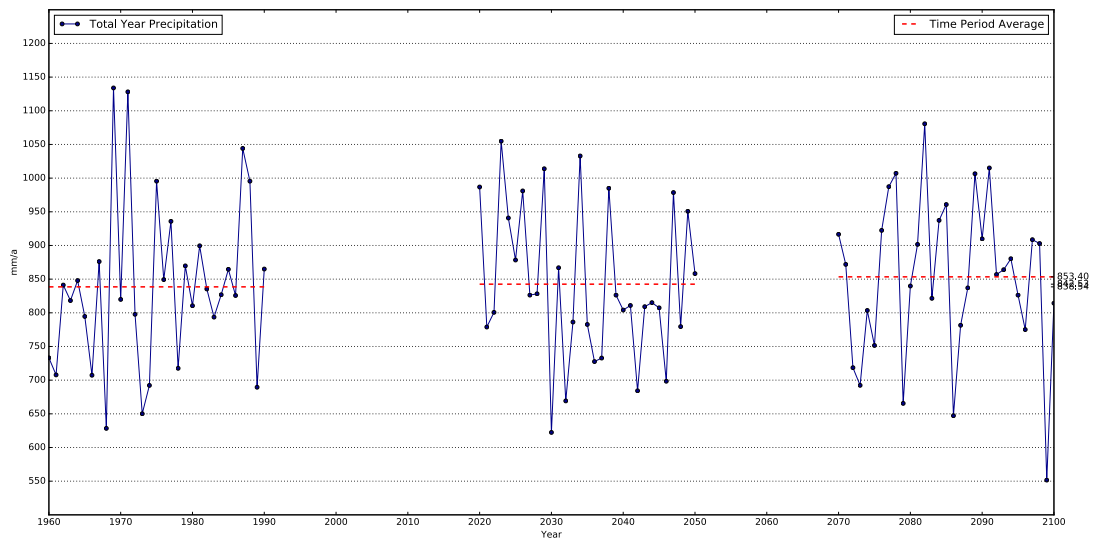


Figure 66 Annual precipitation in Hradec

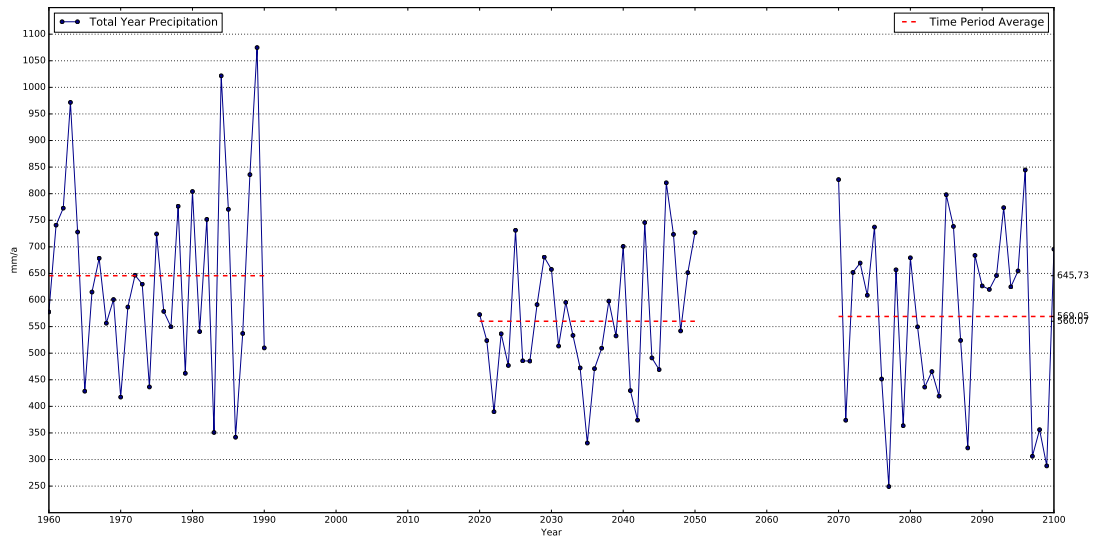


Figure 67 Annual precipitation in Marseille

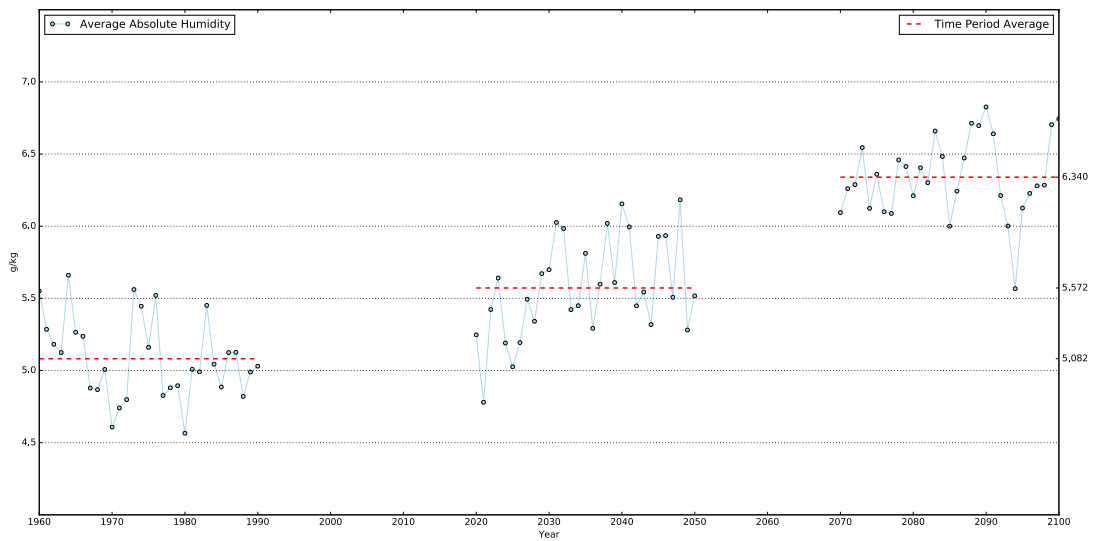


Figure 68 Annual average specific humidity in Helsinki

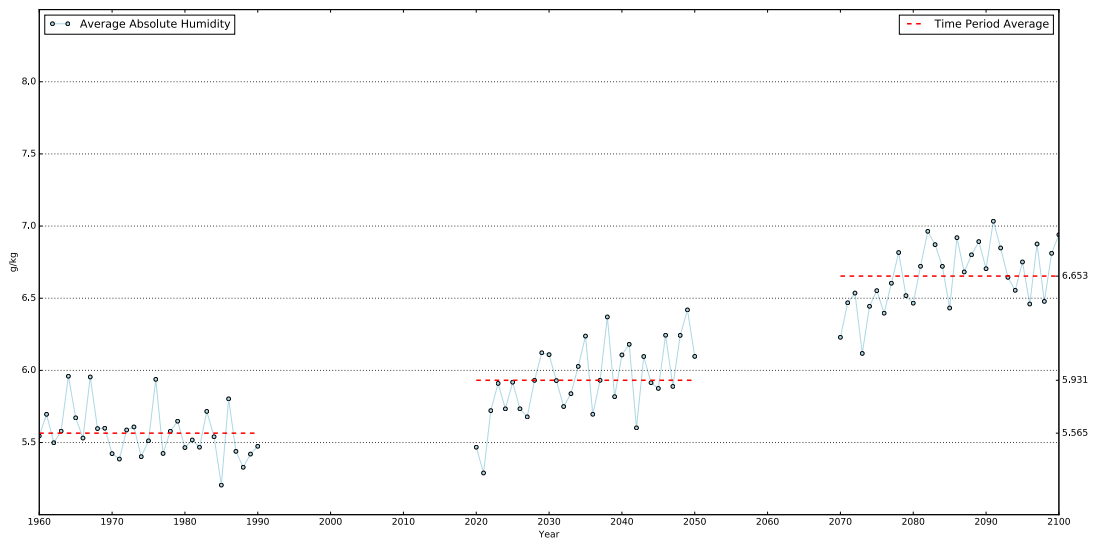


Figure 69 Annual average specific humidity in Fichtelberg

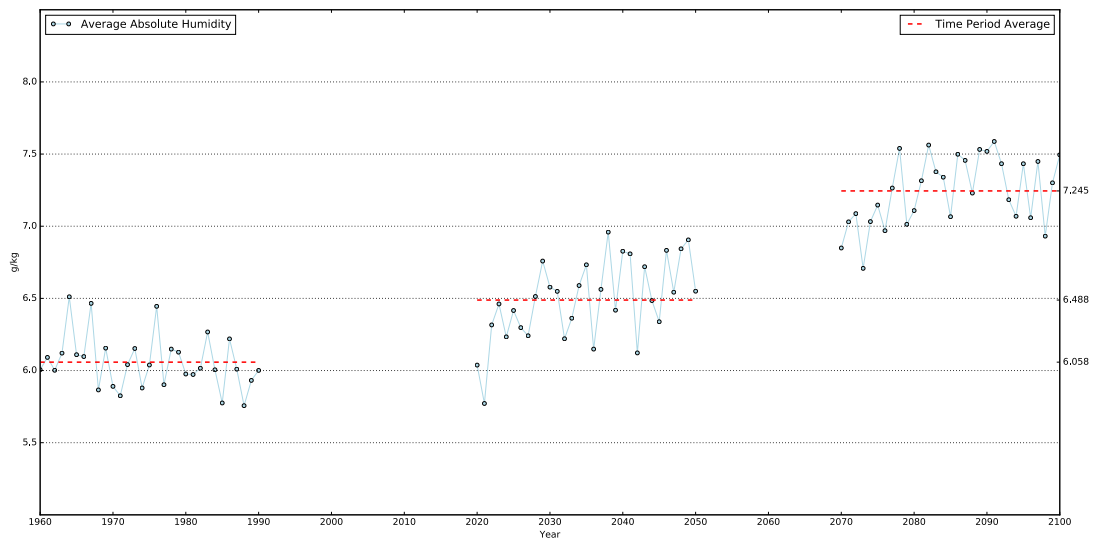


Figure 70 Annual average specific humidity in Hradec

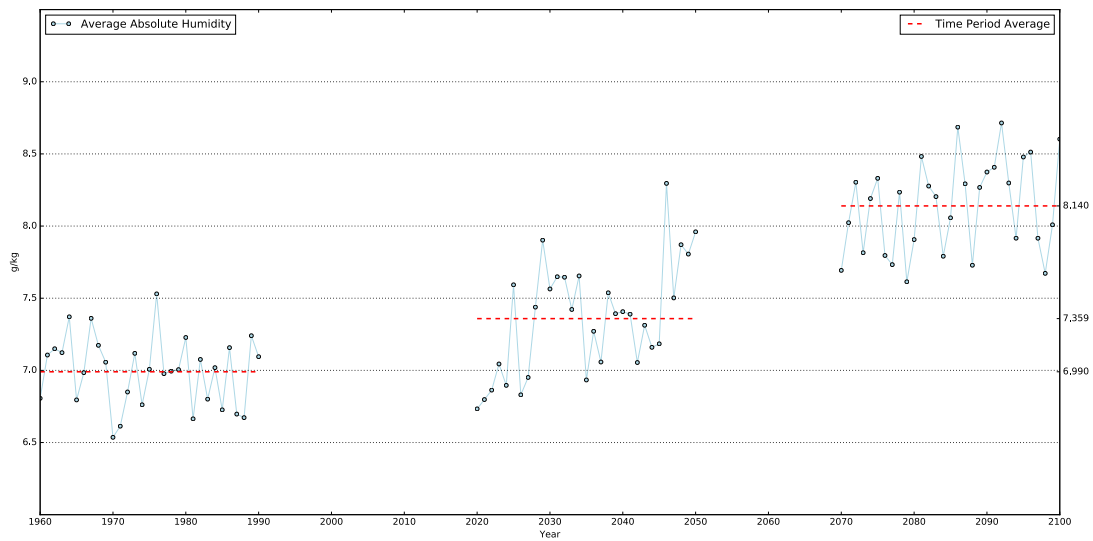


Figure 71 Annual average specific humidity in Marseille

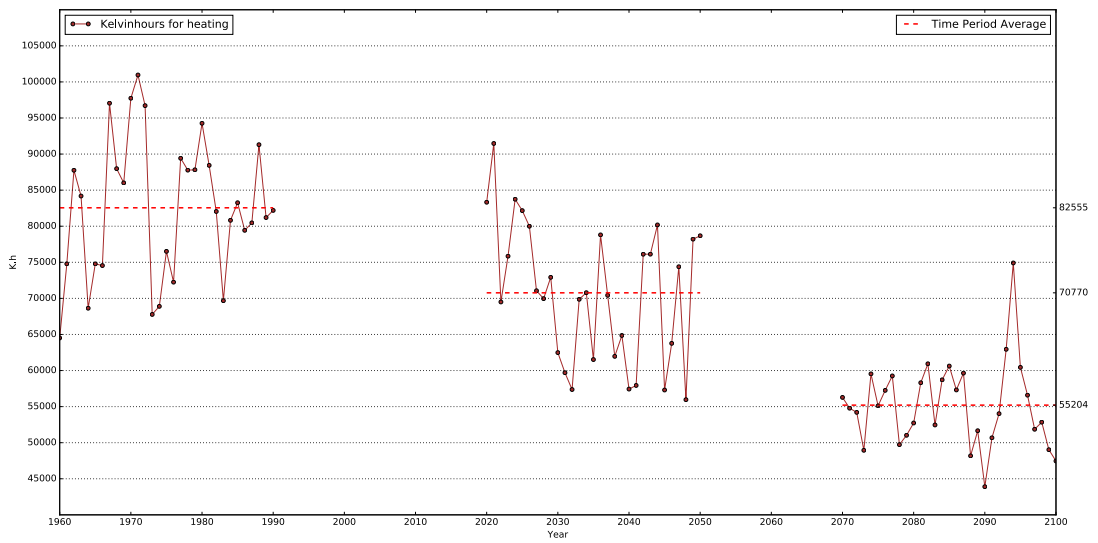


Figure 72 Annual total heating degree hours in Helsinki

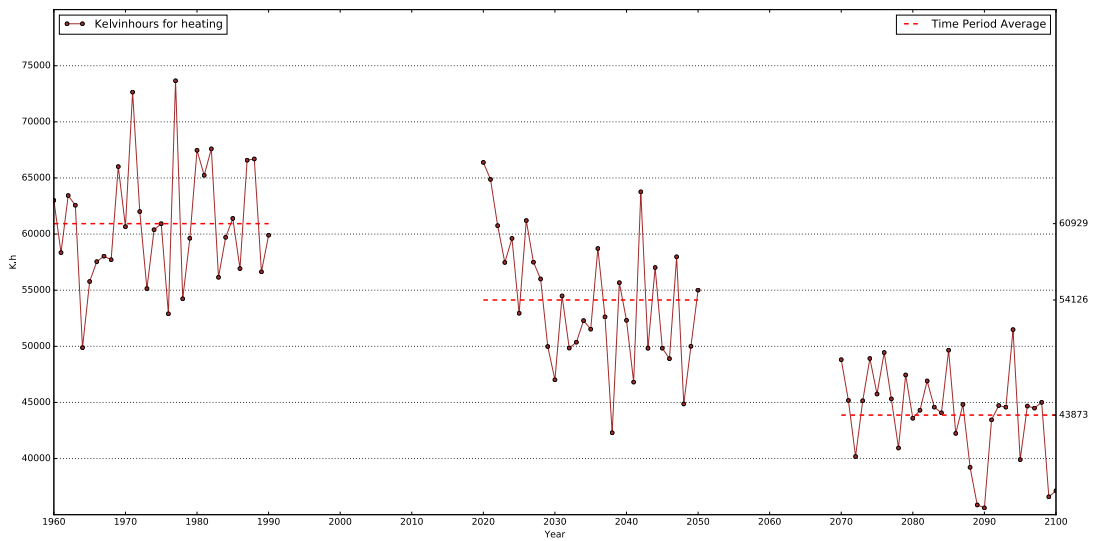


Figure 73 Annual total heating degree hours in Fichtelberg

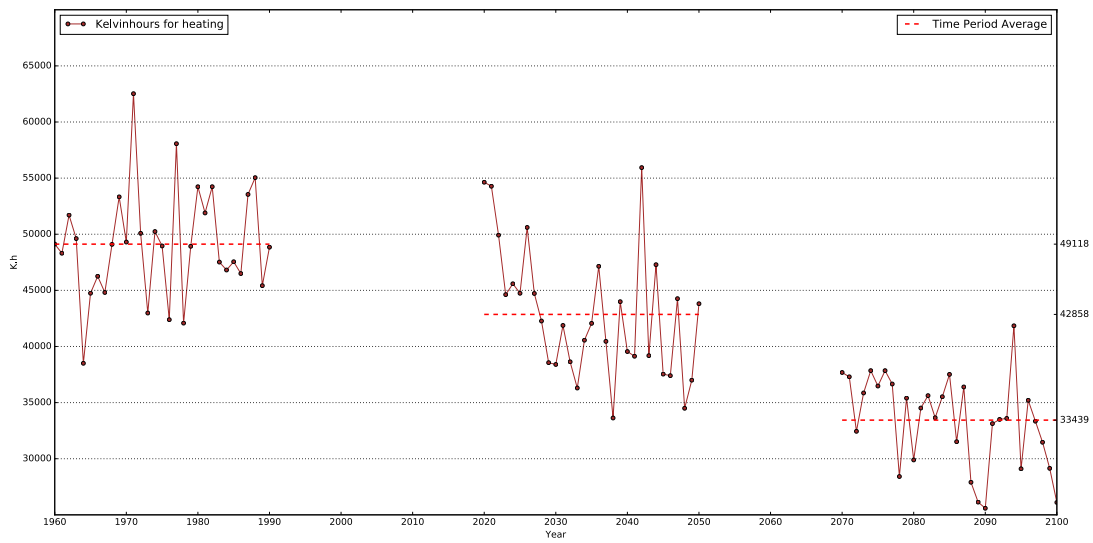


Figure 74 Annual total heating degree hours in Hradec

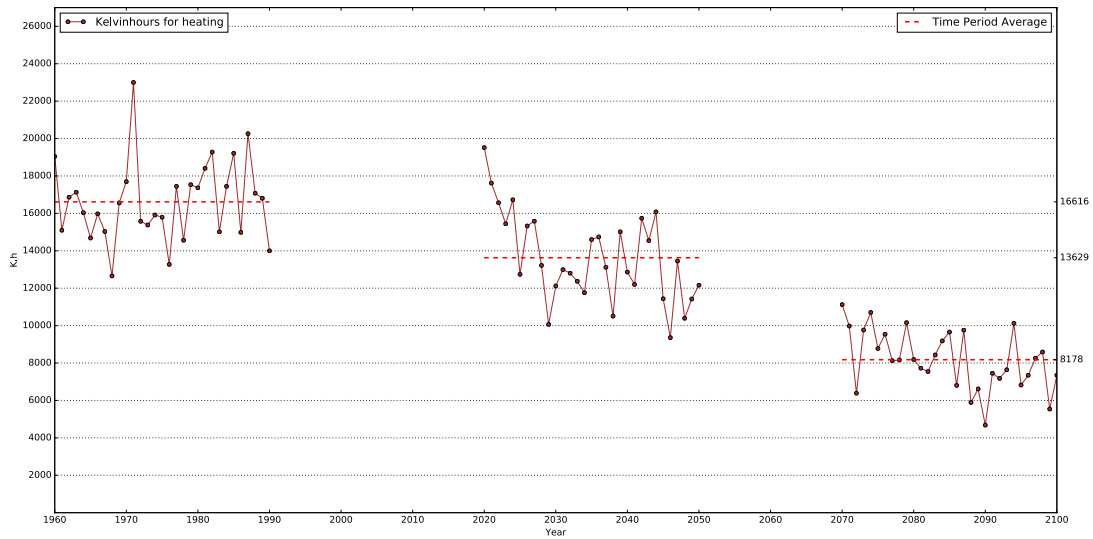


Figure 75 Annual total heating degree hours in Marseille

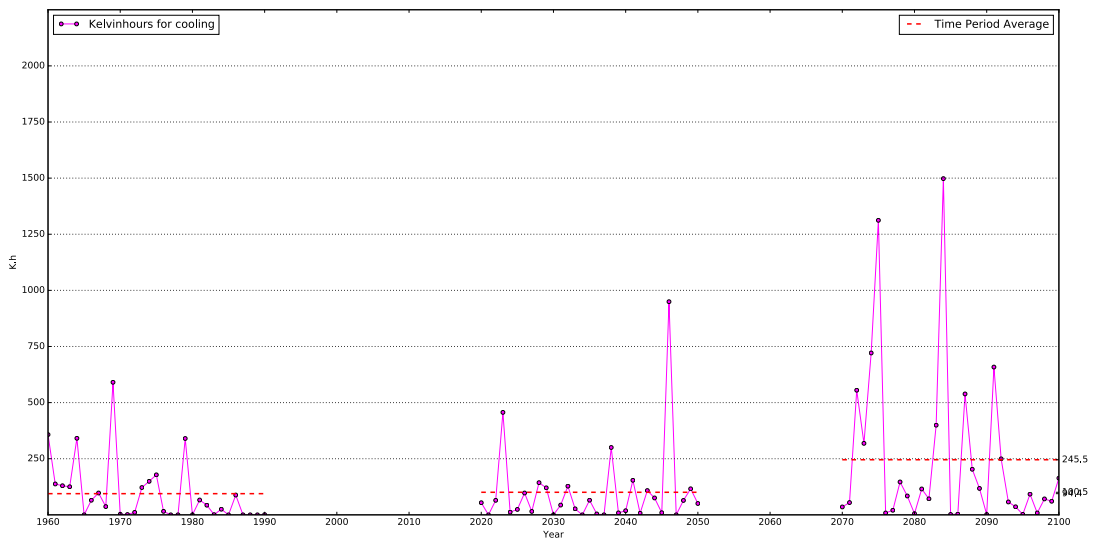


Figure 76 Annual total cooling degree hours in Helsinki

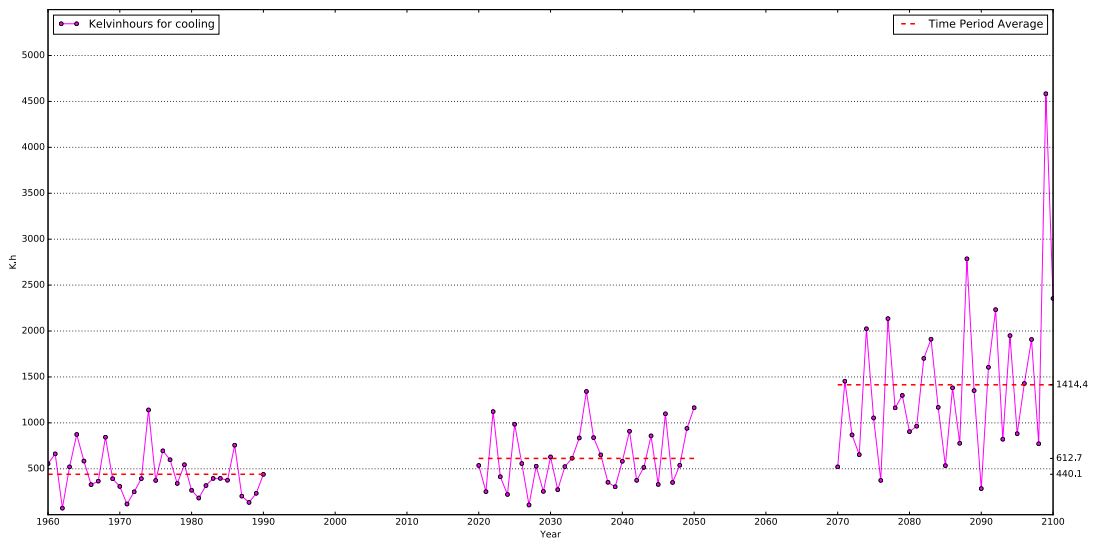


Figure 77 Annual total cooling degree hours in Fichtelberg

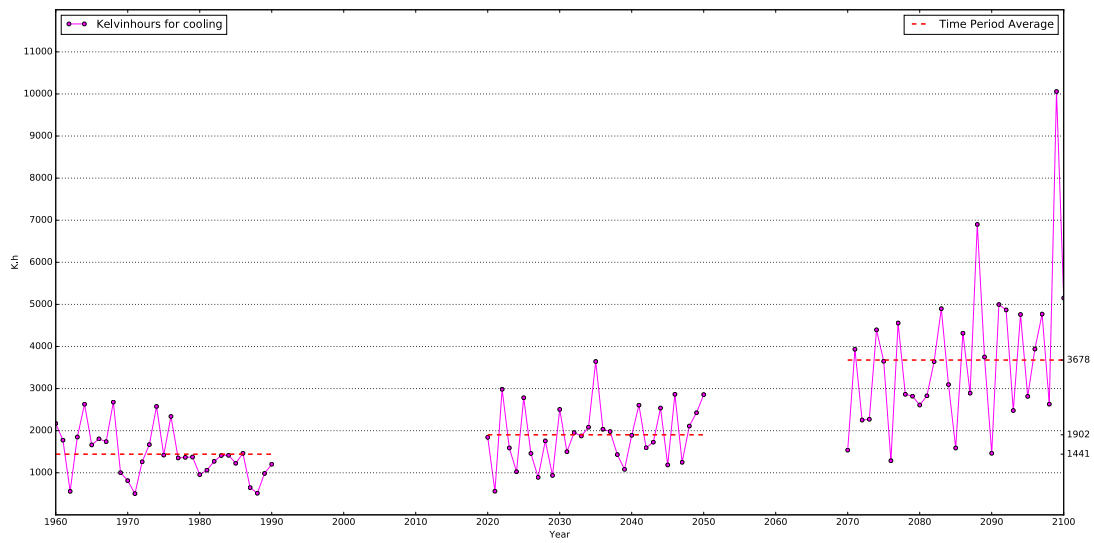


Figure 78 Annual total cooling degree hours in Hradec

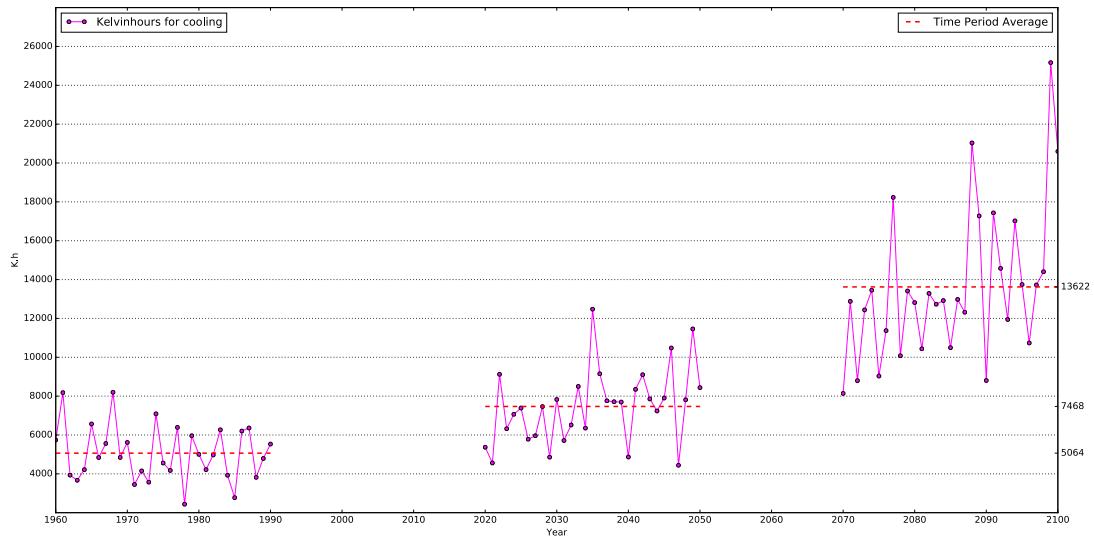


Figure 79 Annual total cooling degree hours in Marseille

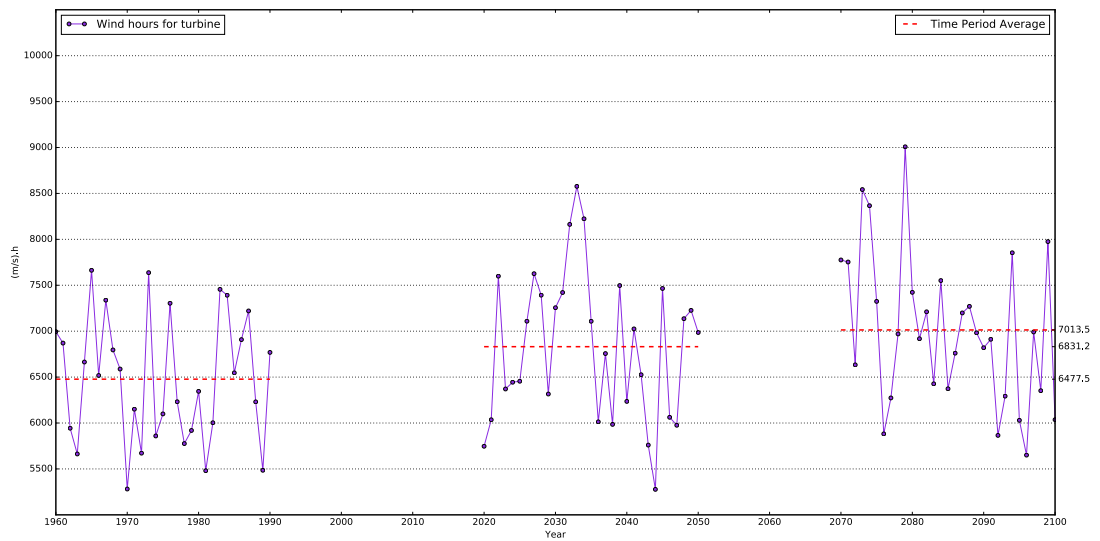


Figure 80 Annual total wind speed hours in Helsinki

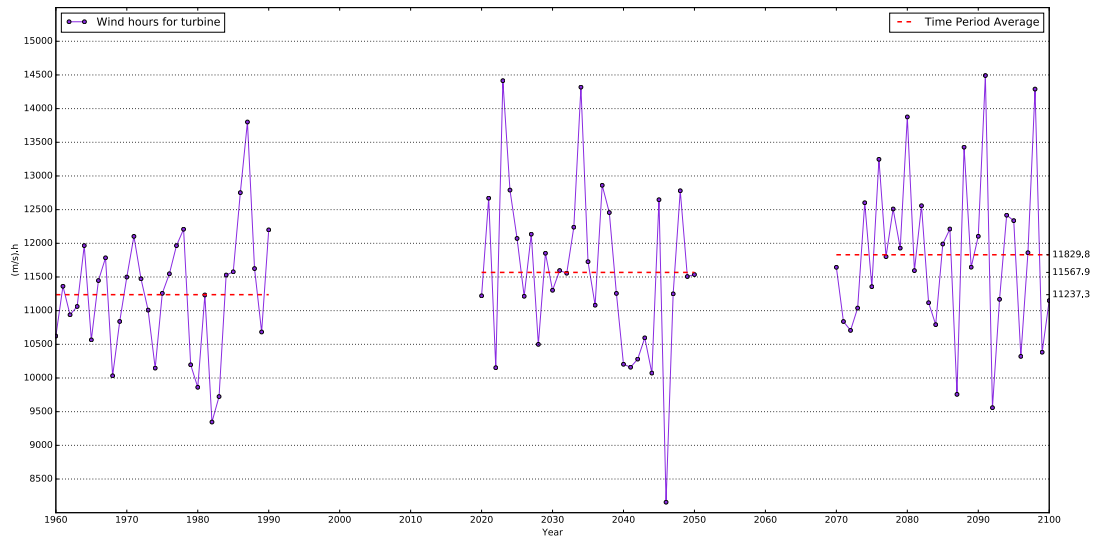


Figure 81 Annual total wind speed hours in Fichtelberg

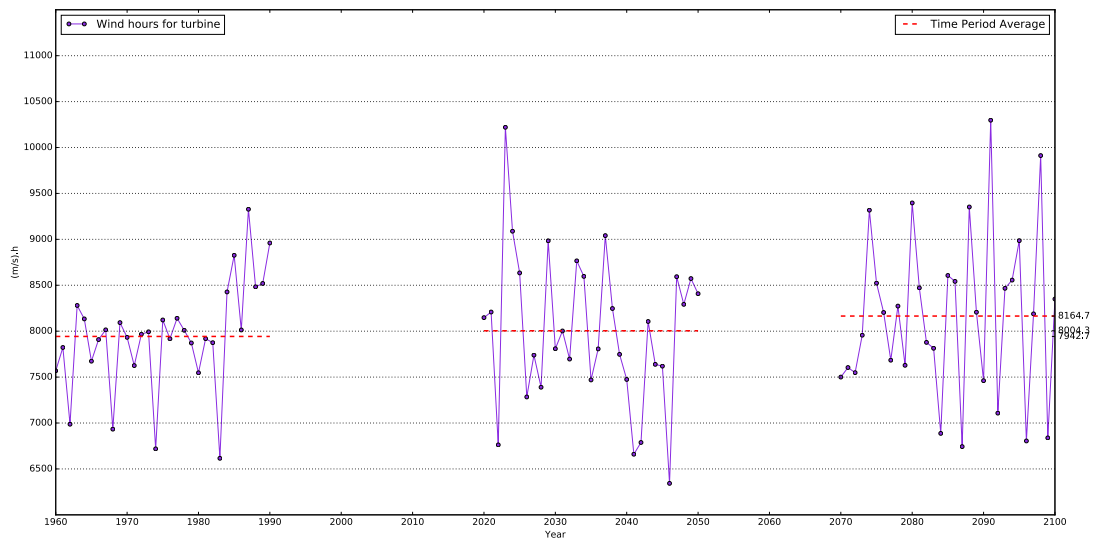


Figure 82 Annual total wind speed hours in Hradec

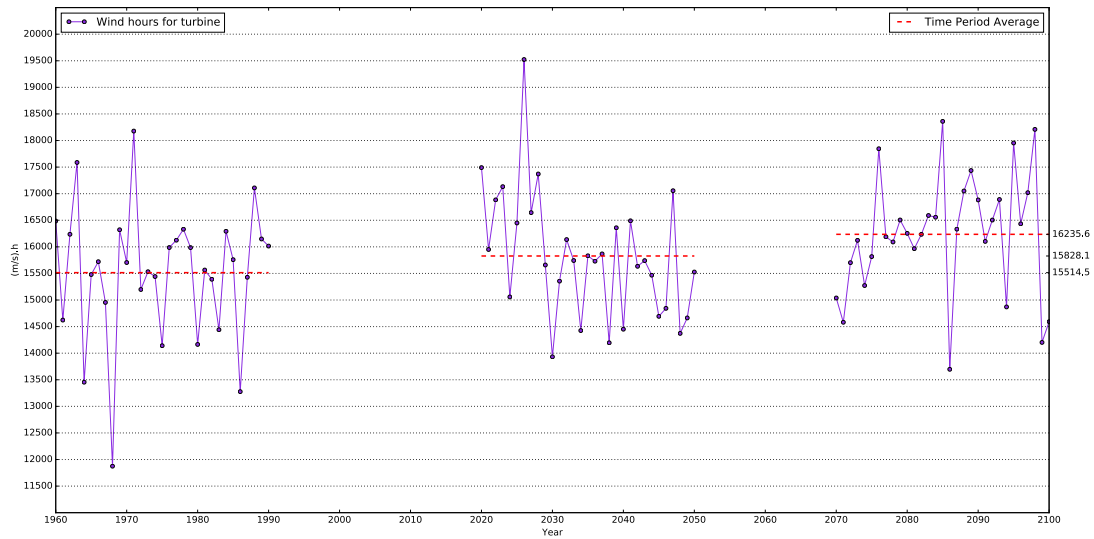


Figure 83 Annual total wind speed hours in Marseille

Appendix B

Case Study Results - Additional Figures

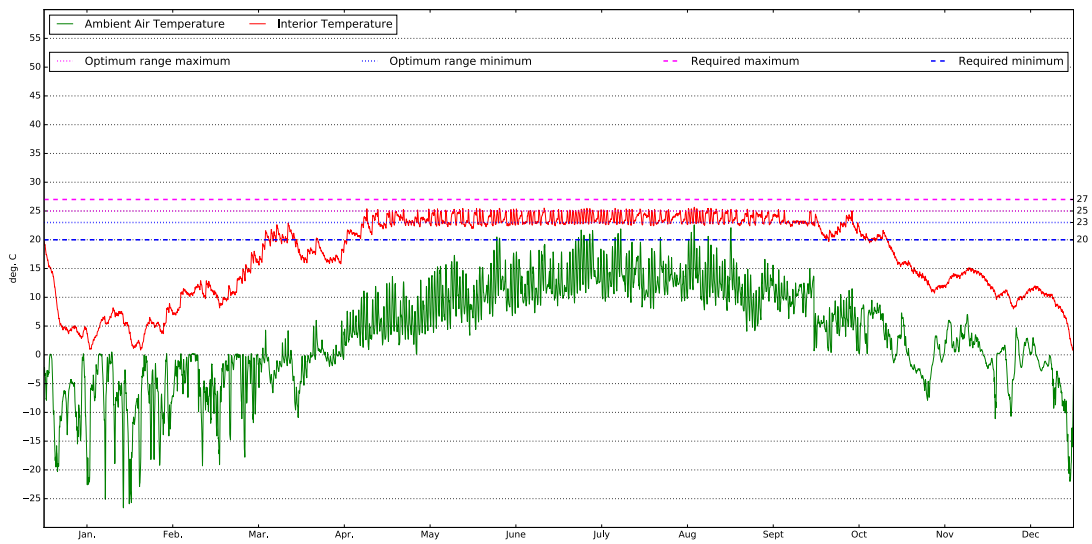


Figure 84 Exterior and interior temperature for Scenario 4A in Helsinki 1960 - 1990

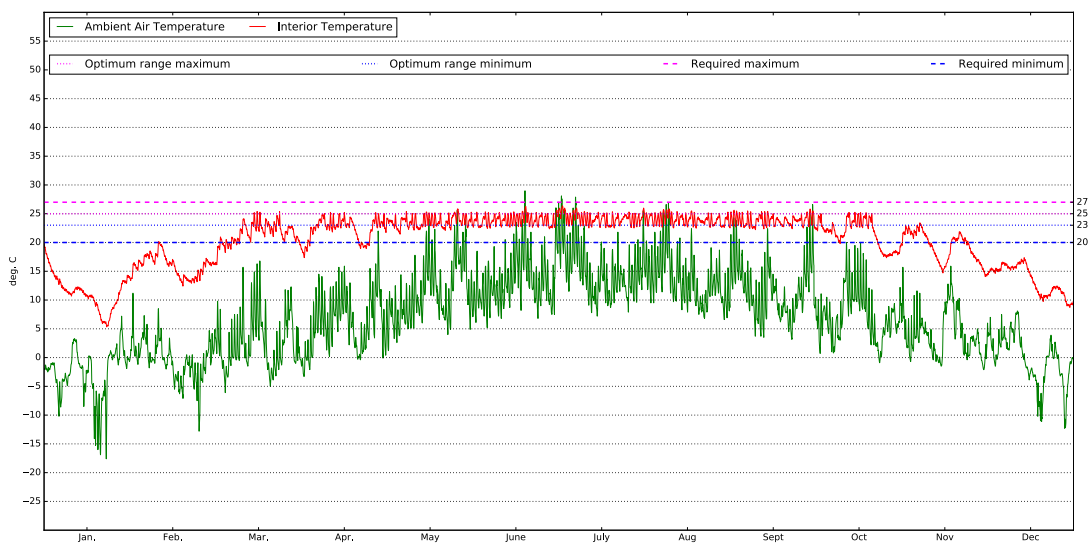


Figure 85 Exterior and interior temperature for Scenario 4A in Fichtelberg 1960 - 1990

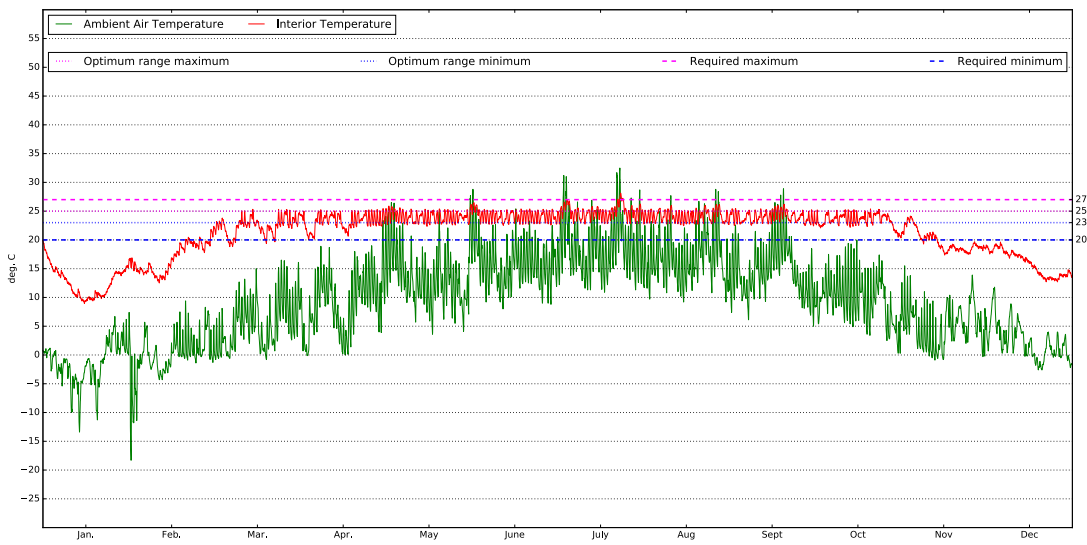


Figure 86 Exterior and interior temperature for Scenario 4A in Hradec 1960 - 1990

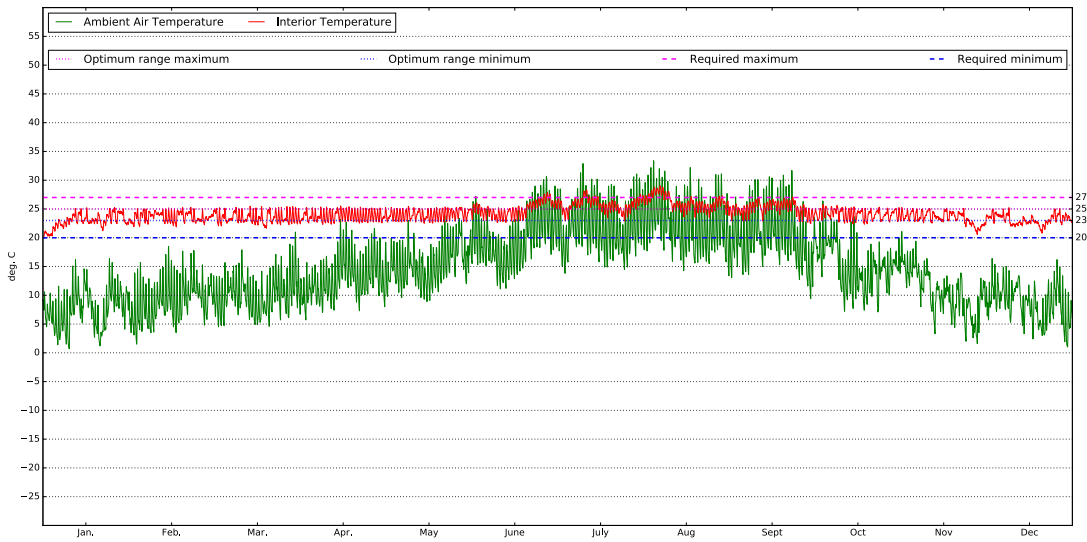


Figure 87 Exterior and interior temperature for Scenario 4A in Marseille 1960 - 1990

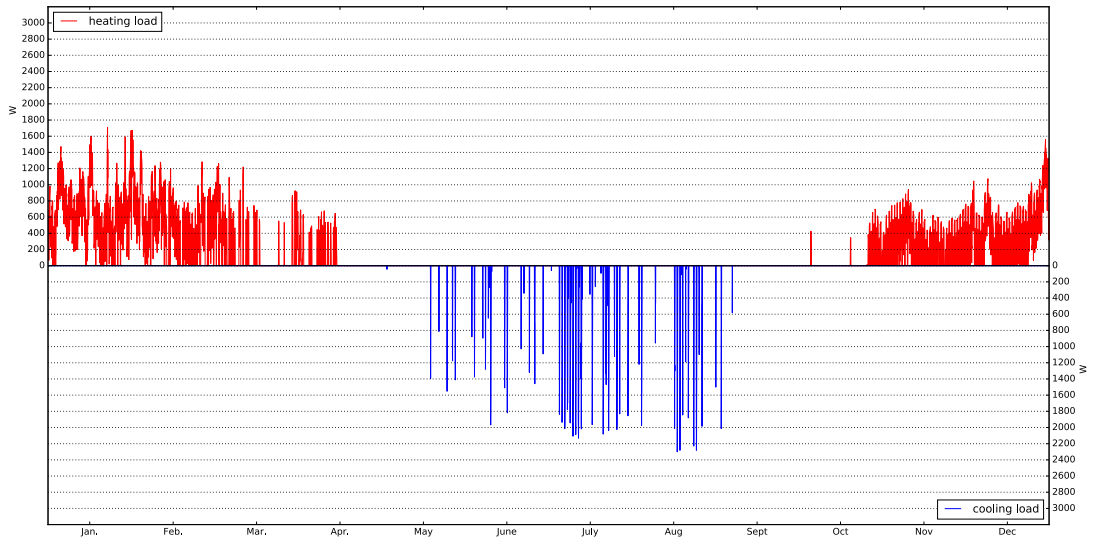


Figure 88 Heating and cooling loads for Scenario 2B in Helsinki 1960 - 1990

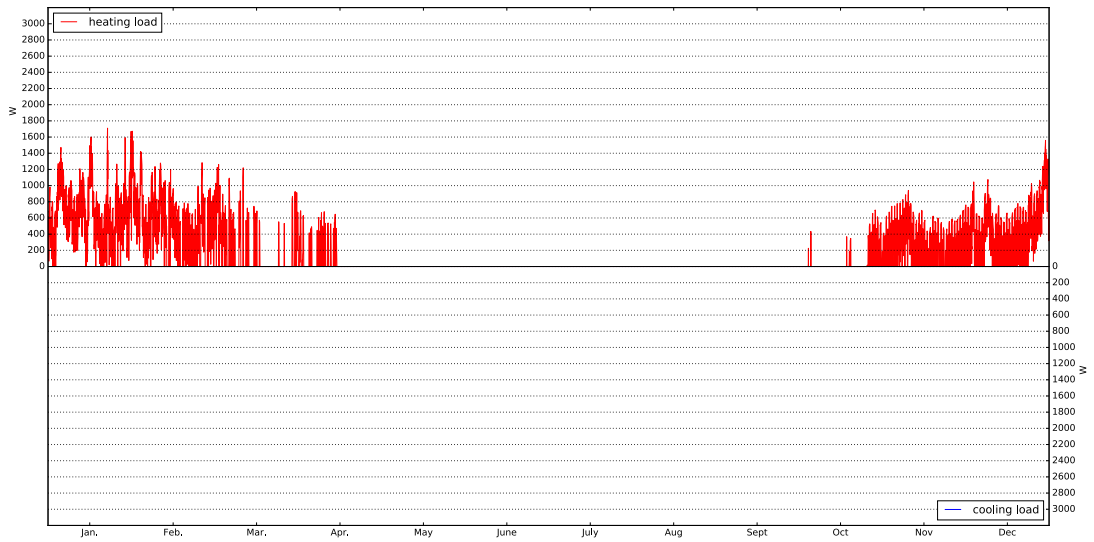


Figure 89 Heating and cooling loads for Scenario 4B in Helsinki 1960 - 1990

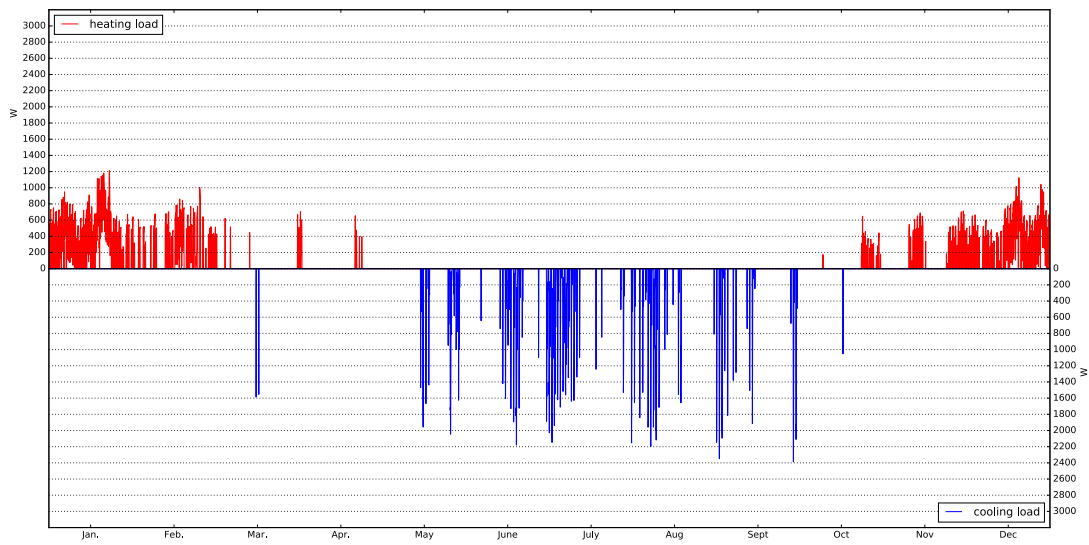


Figure 90 Heating and cooling loads for Scenario 2B in Fichtelberg 1960 - 1990



Figure 91 Heating and cooling loads for Scenario 4B in Fichtelberg 1960 - 1990

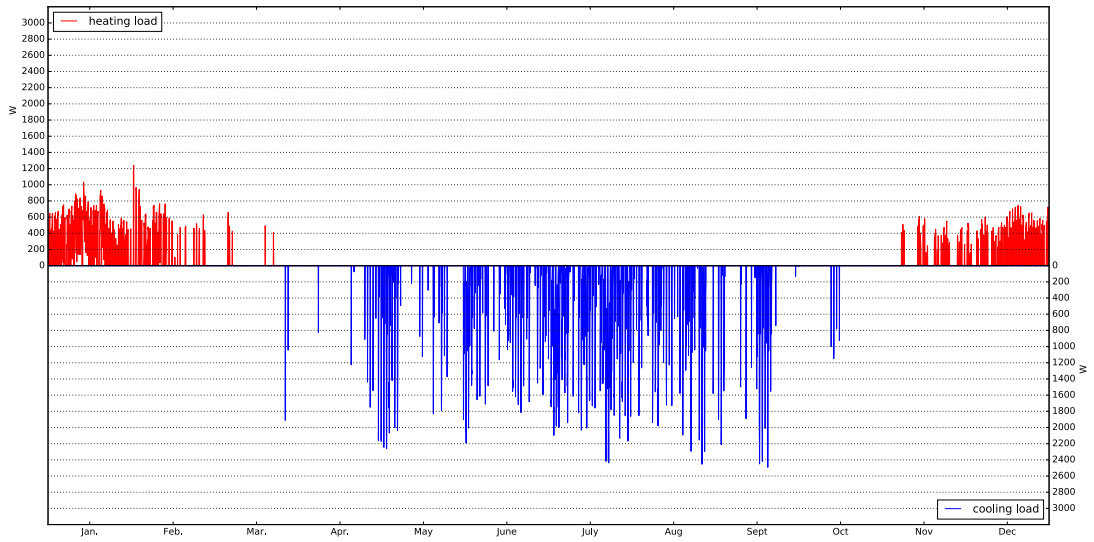


Figure 92 Heating and cooling loads for Scenario 2B in Hradec 1960 - 1990

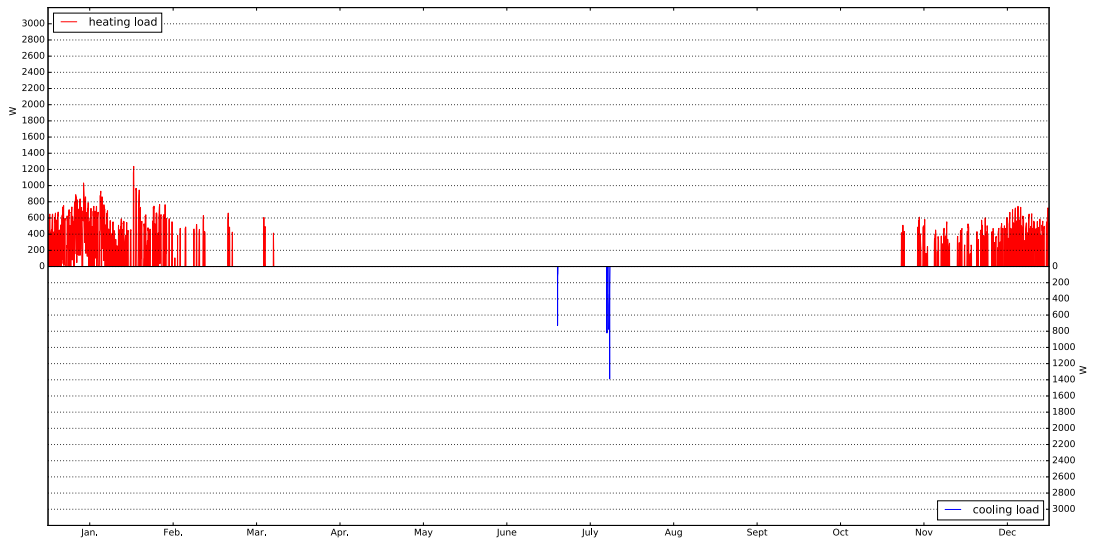


Figure 93 Heating and cooling loads for Scenario 4B in Hradec 1960 - 1990

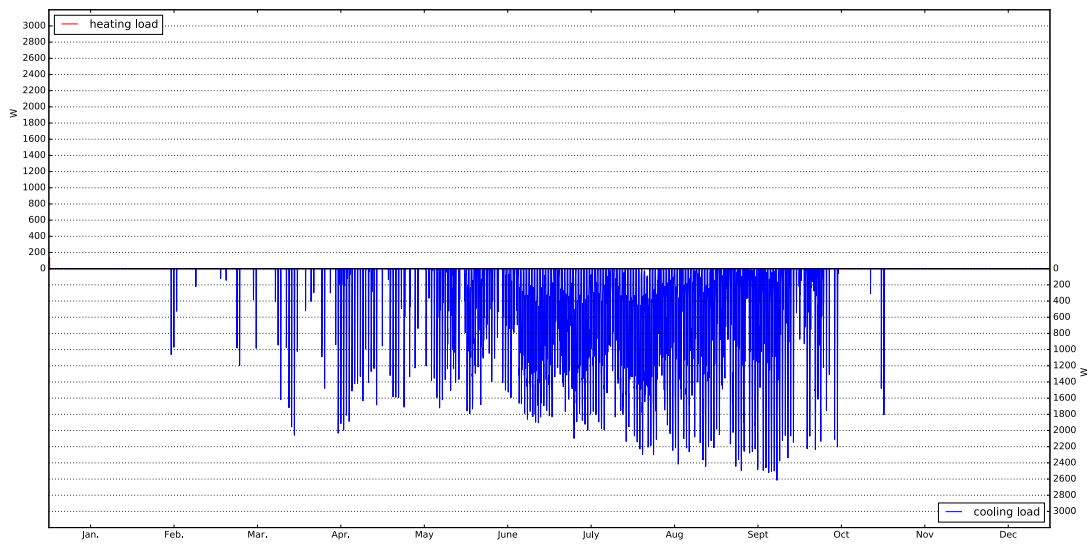


Figure 94 Heating and cooling loads for Scenario 2B in Marseille 1960 - 1990

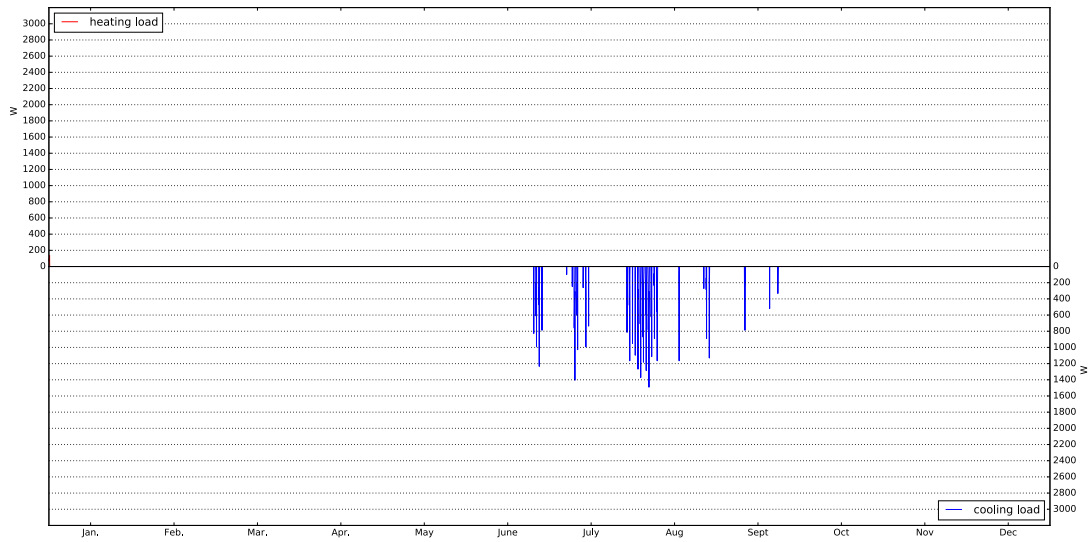


Figure 95 Heating and cooling loads for Scenario 4B in Marseille 1960 - 1990

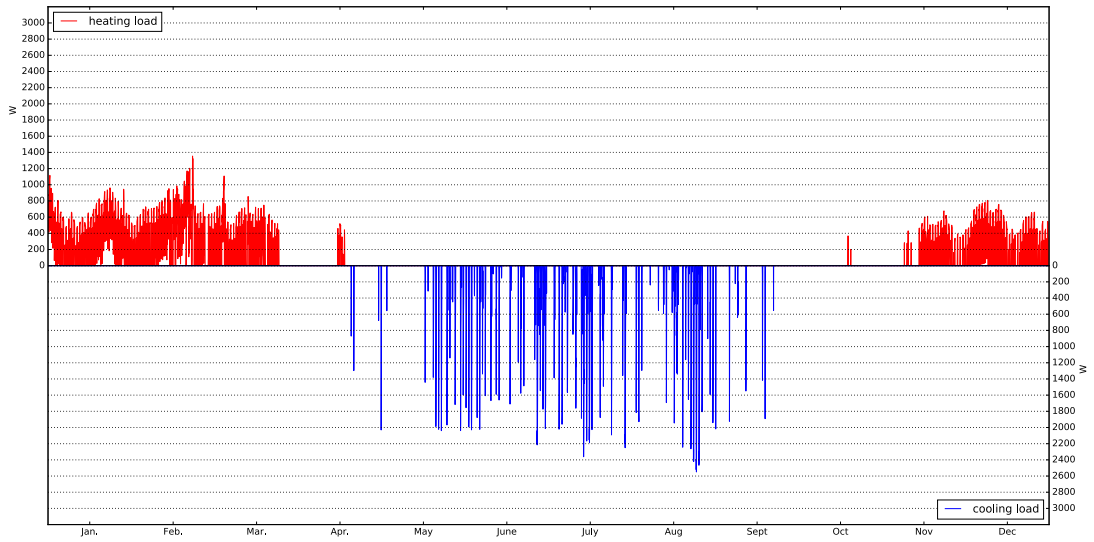


Figure 96 Heating and cooling loads for Scenario 2B in Helsinki 2070 - 2100



Figure 97 Heating and cooling loads for Scenario 4B in Helsinki 2070 - 2100

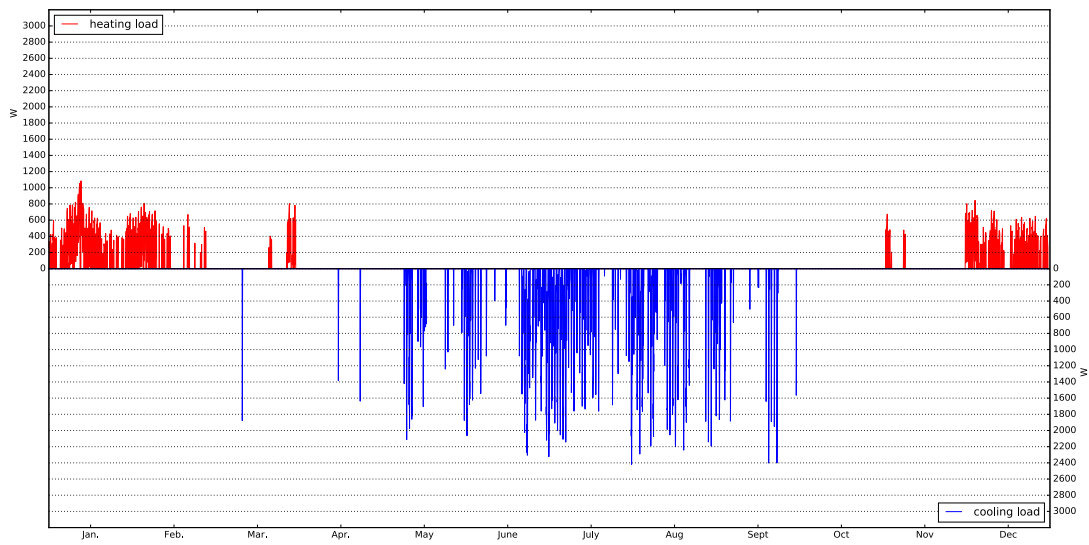


Figure 98 Heating and cooling loads for Scenario 2B in Fichtelberg 2070 - 2100



Figure 99 Heating and cooling loads for Scenario 4B in Fichtelberg 2070 - 2100

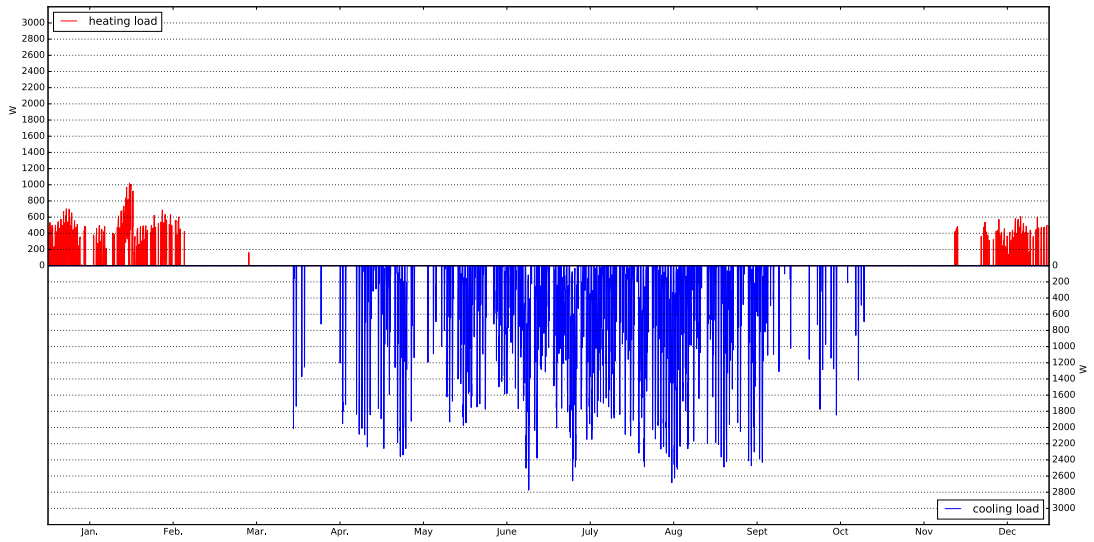


Figure 100 Heating and cooling loads for Scenario 2B in Hradec 2070 - 2100

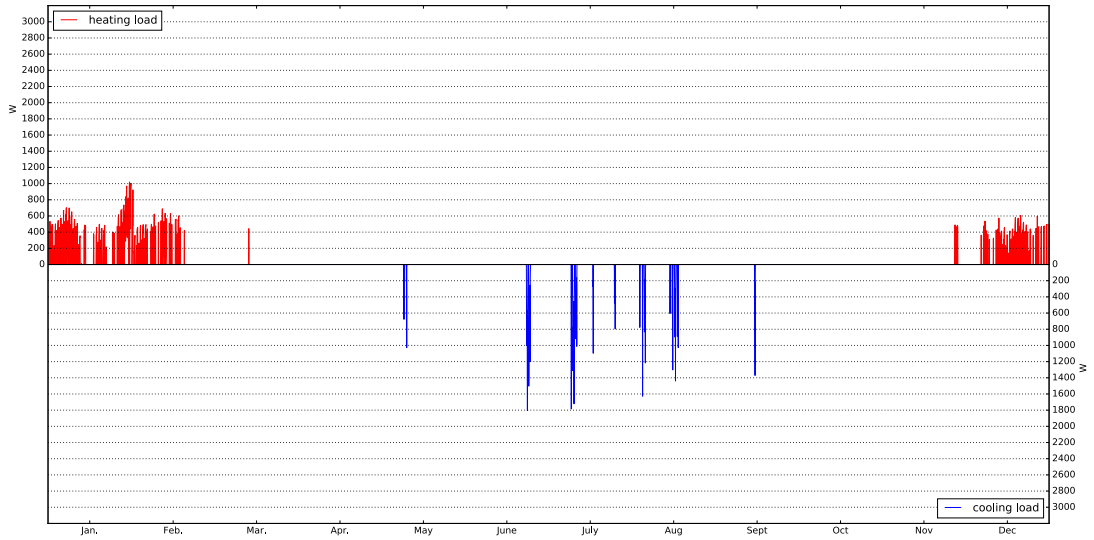


Figure 101 Heating and cooling loads for Scenario 4B in Hradec 2070 - 2100

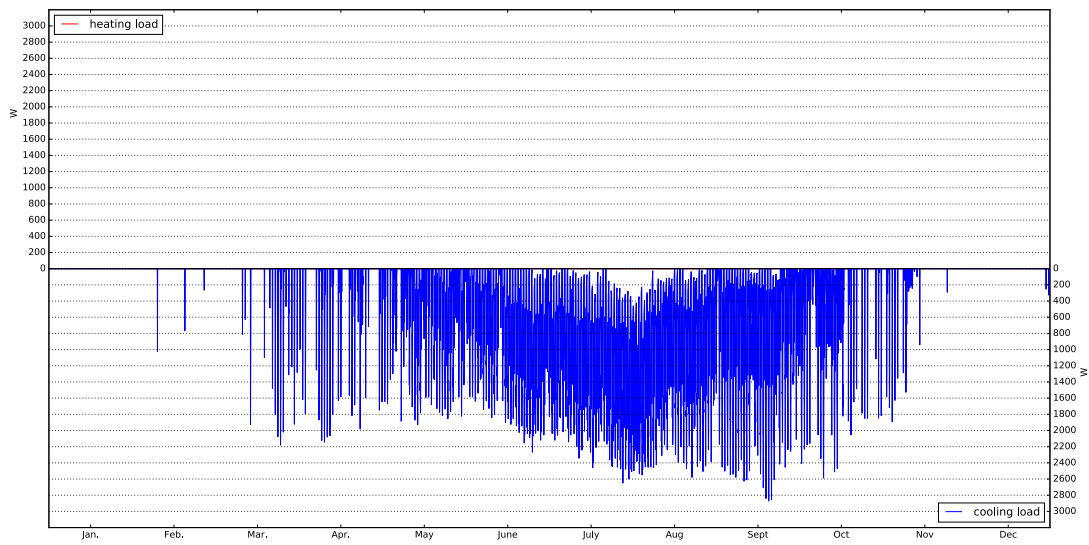


Figure 102 Heating and cooling loads for Scenario 2B in Marseille 2070 - 2100

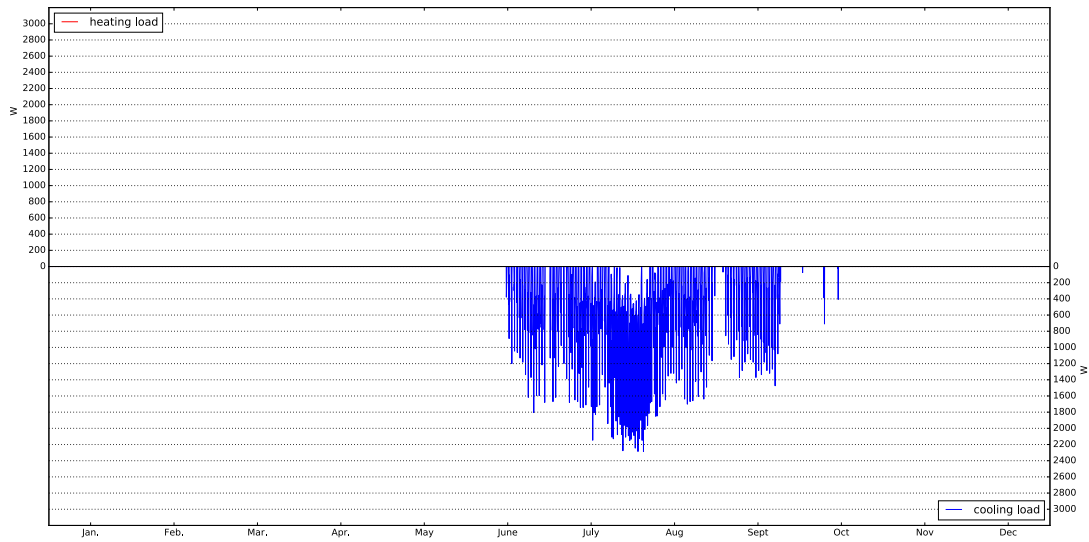


Figure 103 Heating and cooling loads for Scenario 4B in Marseille 2070 - 2100

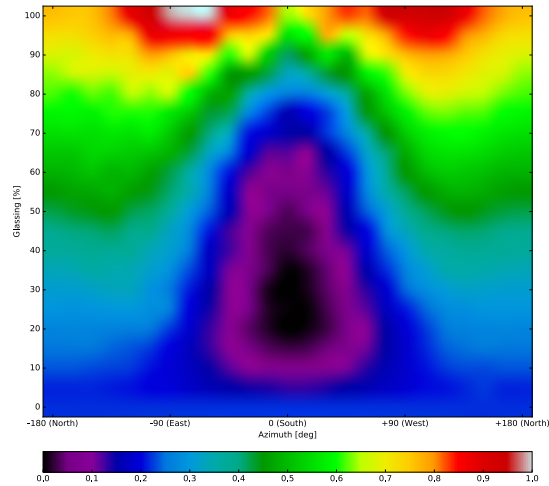


Figure 104 Parameter optimization results for Scenario 4B in Prague 1960 - 1990 with 0.1 weight for heating and 0.9 weight for cooling that represents original model house design (aim for no cooling energy demand, with heating from renewable source)

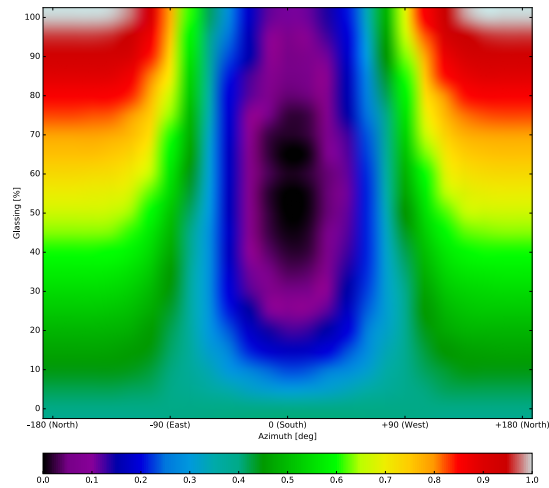


Figure 105 Parameter optimization results for Scenario 4B in Prague 2070 - 2100 with 1.0 weight for heating and 0.0 weight for cooling

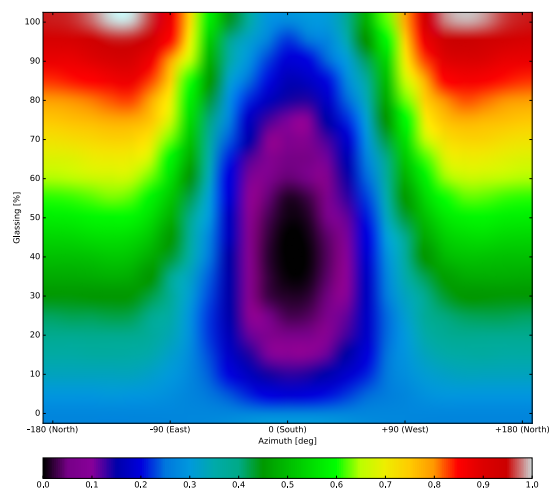


Figure 106 Parameter optimization results for Scenario 4B in Prague 2070 - 2100 with 0.7 weight for heating and 0.3 weight for cooling

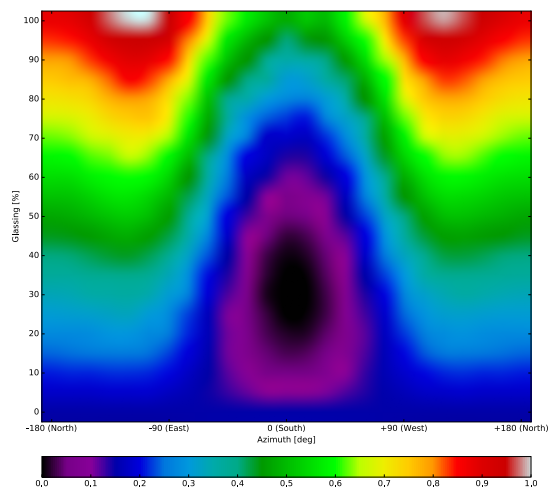


Figure 107 Parameter optimization results for Scenario 4B in Prague 2070 - 2100 with 0.5 weight for heating and 0.5 weight for cooling

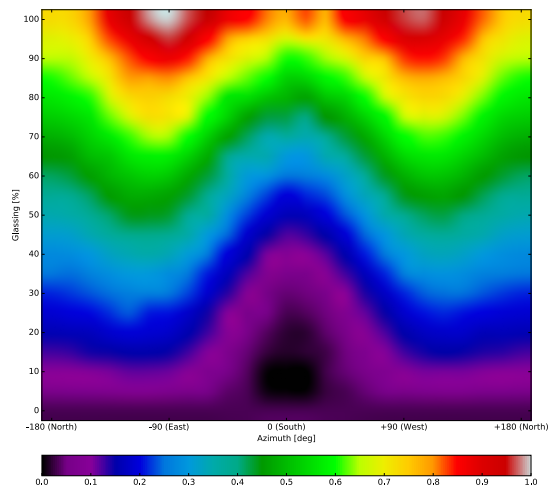


Figure 108 Parameter optimization results for Scenario 4B in Prague 2070 - 2100 with 0.3 weight for heating and 0.7 weight for cooling

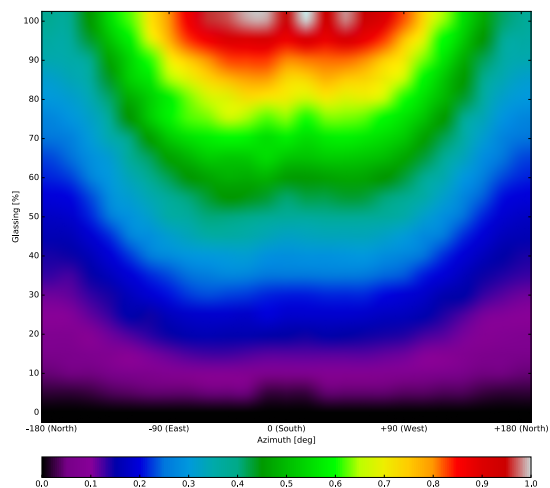


Figure 109 Parameter optimization results for Scenario 4B in Prague 2070 - 2100 with 0.0 weight for heating and 1.0 weight for cooling

Appendix C

Model House Documentation



Figure 110 Model house - 3D model



Figure 111 Model house - visualization 1



Figure 112 Model house - visualization 2



Figure 113 Model house - visualization 3

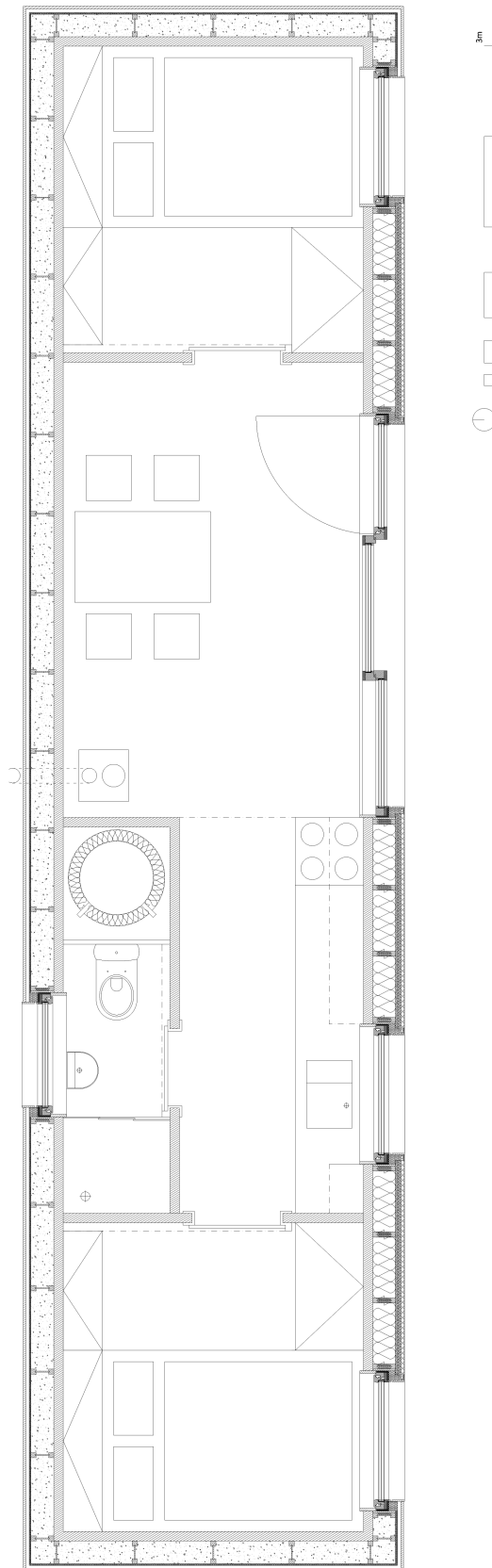


Figure 114 Model house - floor plan

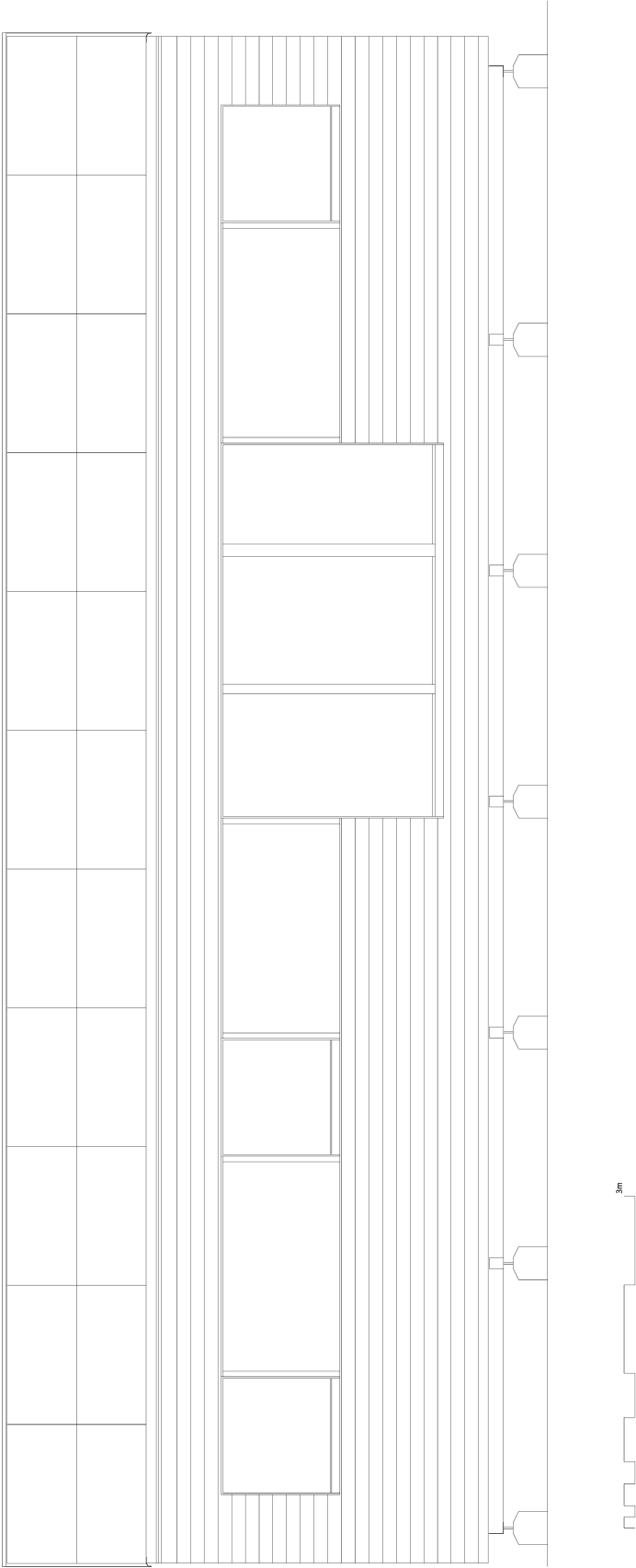


Figure 115 Model house - front view

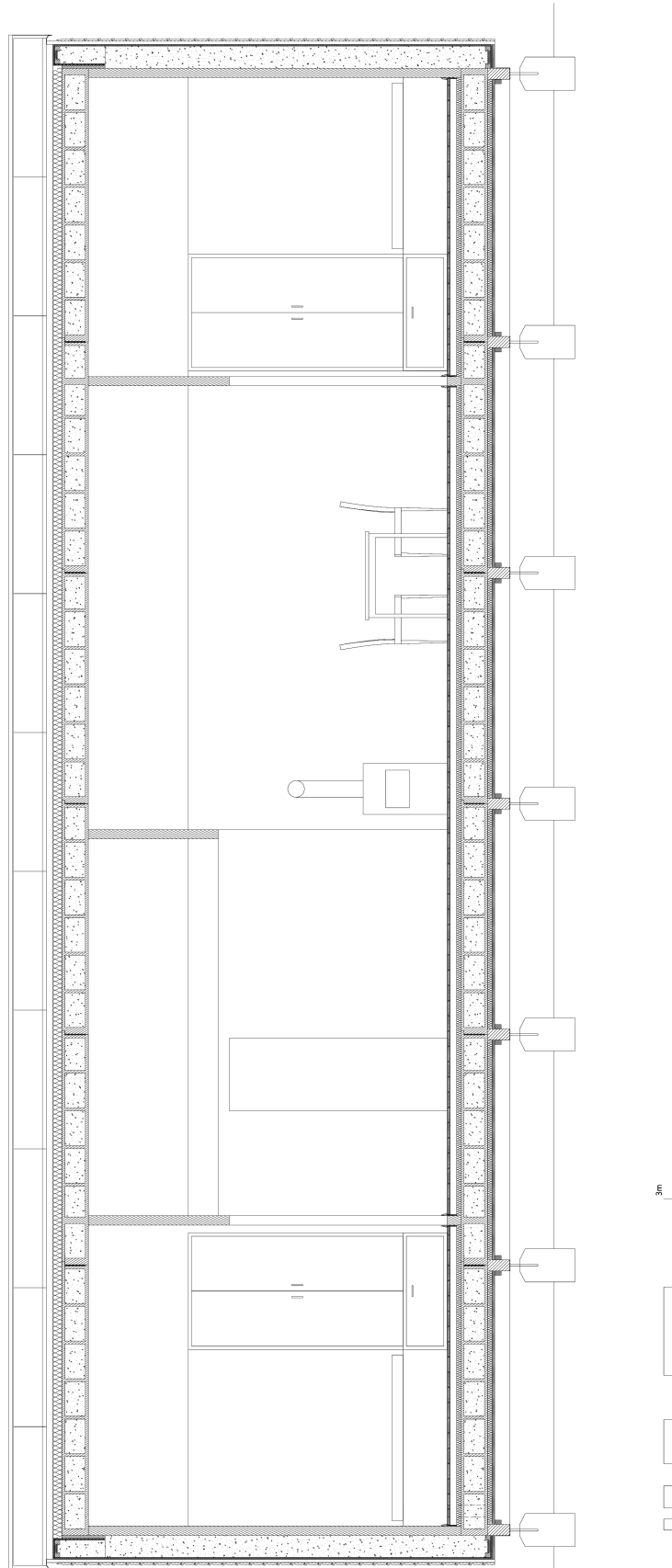


Figure 116 Model house - longitudinal section

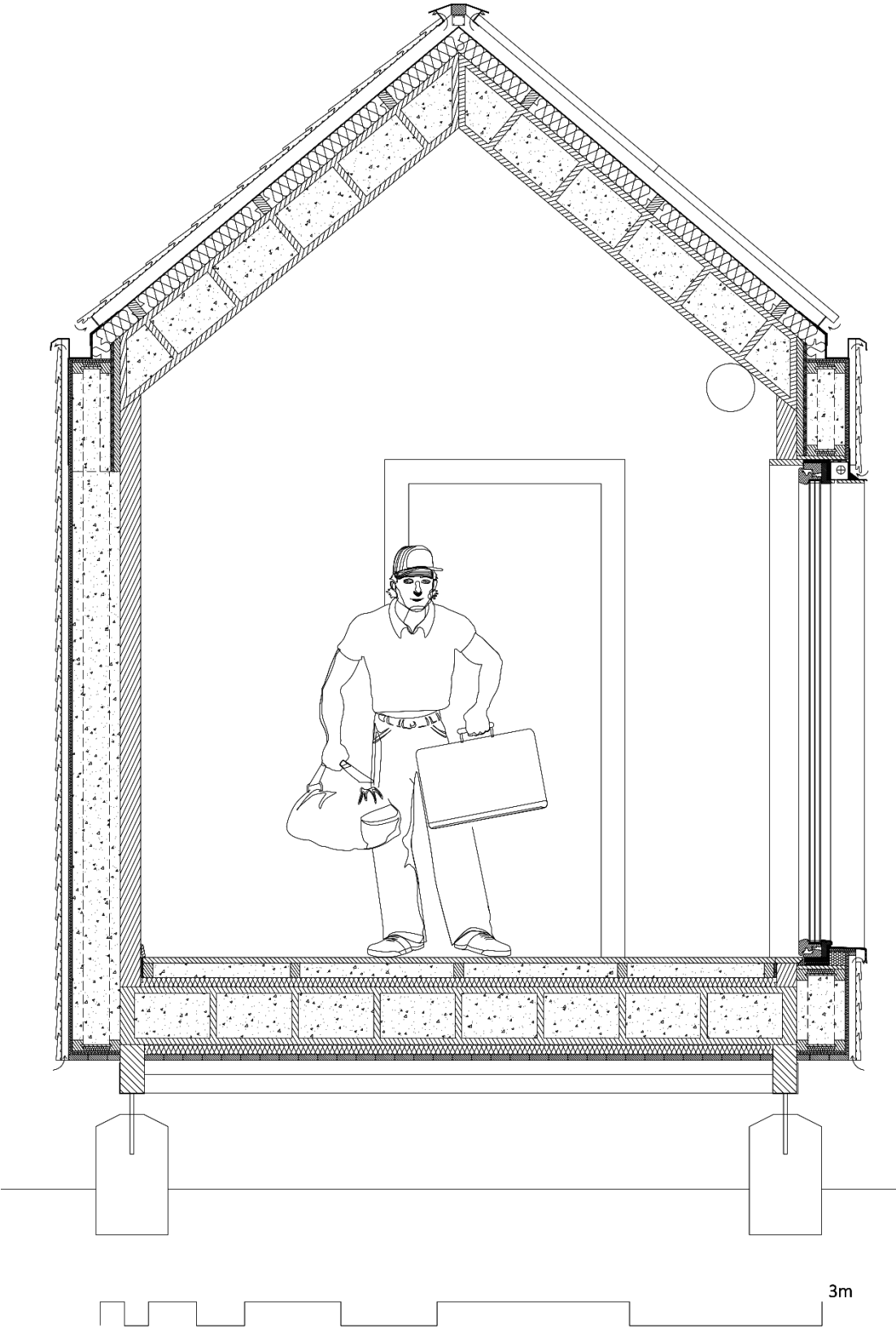


Figure 117 Model house - cross section

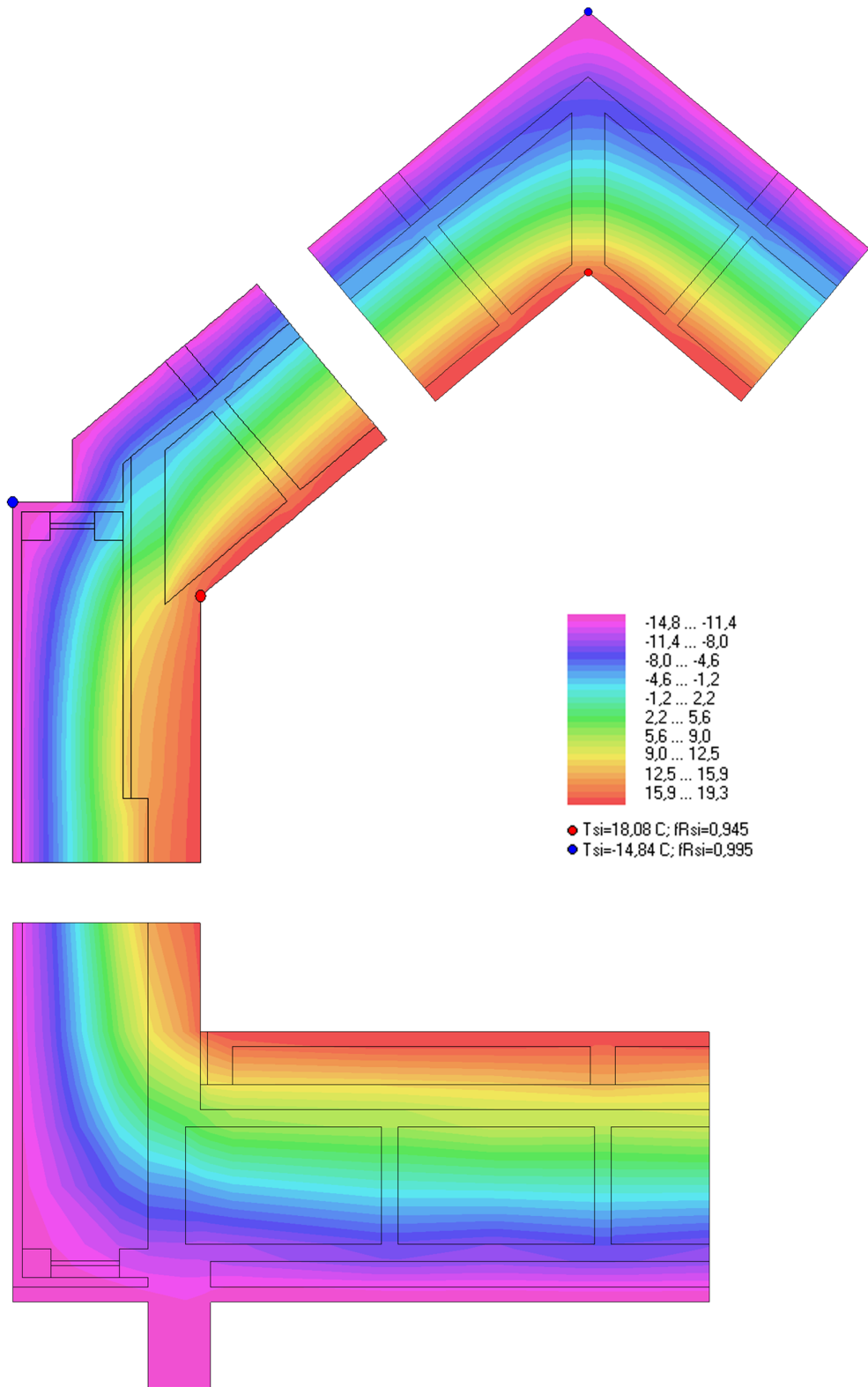


Figure 118 Model house - detail of heat transmission